



Food and Agriculture  
Organization of the  
United Nations



IHE  
DELFT

## REMOTE SENSING FOR WATER PRODUCTIVITY



W A T E R   A C C O U N T I N G   S E R I E S

# Water Accounting in the Jordan River Basin

# Water accounting in the Jordan River Basin

REMOTE SENSING FOR WATER PRODUCTIVITY

WaPOR water accounting series

Published by  
the Food and Agriculture Organization of the United Nations  
and  
IHE Delft Institute for Water Education

**Required citation:**

**FAO and IHE Delft.** 2020. *Water Accounting in the Jordan River Basin*. FAO WaPOR water accounting reports. Rome, <https://doi.org/10.4060/ca9181en>

The designations employed and the presentation of material in this information product do not imply the expression of any opinion whatsoever on the part of the Food and Agriculture Organization of the United Nations (FAO) or –IHE Delft Institute for Water Education (IHE DELFT) concerning the legal or development status of any country, territory, city or area or of its authorities, or concerning the delimitation of its frontiers or boundaries. The mention of specific companies or products of manufacturers, whether or not these have been patented, does not imply that these have been endorsed or recommended by FAO or IHE DELFT in preference to others of a similar nature that are not mentioned. The views expressed in this information product are those of the author(s) and do not necessarily reflect the views or policies of FAO or IHE DELFT.

FAO encourages the use, reproduction and dissemination of material in this information product. Except where otherwise indicated, material may be copied, downloaded and printed for private study, research and teaching purposes, or for use in non-commercial products or services, provided that appropriate acknowledgement of FAO and IHE DELFT as the source and copyright holders is given and that FAO/IHE DELFT's endorsement of users' views, products or services is not implied in any way.

All requests for translation and adaptation rights, and for resale and other commercial use rights should be made via [www.fao.org/contact-us/licence-request](http://www.fao.org/contact-us/licence-request) or addressed to [copyright@fao.org](mailto:copyright@fao.org).

FAO information products are available on the FAO website ([www.fao.org/publications](http://www.fao.org/publications)) and can be purchased through [publications-sales@fao.org](mailto:publications-sales@fao.org)"

© FAO and IHE Delft, 2020

ISBN 978-92-5-132661-9 [FAO]

Cover photograph: [Michael Loadenthal](#)

# Contents

Acknowledgements	viii
Executive summary	ix
1. Introduction	1
1.1. Case study description	1
1.2. Water resources developments and challenges in Jordan River Basin	3
1.2.1. Overview of water resources developments	3
1.2.2. Water resources management challenges	3
1.3. Objective of water accounts	4
2. Materials and Methods	7
2.1. WaPOR datasets	7
2.1.1. Precipitation	7
2.1.2. Actual Evapotranspiration and Interception	7
2.1.3. Land Cover Classes	8
2.2. Preliminary assessments	9
2.2.1. Comparison with in situ observations	9
2.2.2. Water generation and consumption analysis	12
2.2.3. Basin scale water balance	14
2.2.3.1. Observed inter-basin flows	15
2.2.3.2. GRACE Total Water Storage Change	15
2.2.3.3. Assessment of errors in water balance	18
2.2.4. Conclusion	20
2.3. WA+ methodology	21
2.3.1. WA+ Land Use categorization	21
2.3.2. Pixel scale analysis – Monthly soil moisture balance	22
2.3.2.1. Method	22
2.3.2.2. Results	27
2.3.3. WaPOR-based WA+ Sheet 1: Resource Base	28

<b>3. Water Accounting+ Results</b>	<b>32</b>
3.1. WA+ Sheet 1: Resource Base	32
3.2. WA+ Key indicators	34
<b>4. Conclusions</b>	<b>37</b>
 <b>References</b>	 <b>39</b>
 <b>Annexes</b>	 <b>42</b>
Annex I. Total annual Precipitation (P) of hydrological years	42
Annex II. Total annual actual evapotranspiration (ET <sub>a</sub> ) of hydrological years	43
Annex III. Yearly WaPOR Land cover classification maps	44
Annex IV. Total annual P - ET <sub>a</sub> of hydrological years	46
Annex V. Yearly WA+ Land use classification maps	47
Annex VI. Total annual reference evapotranspiration (ET <sub>ref</sub> ) of hydrological years	48
Annex VII. Total annual estimated Incremental ET (ET <sub>incr</sub> ) of hydrological years	49
Annex VIII. Total annual estimated Rainfall ET (ET <sub>rain</sub> ) of hydrological years	50
Annex IX. Yearly WA+ Sheet 1 Resource Base	51
Annex X. Supplementary WA+ Sheet 1 results	55
Annex XI. Comparison of Remote Sensing products	56
Annex XI.1 Introduction	56
Annex XI.2 Datasets	57
Precipitation products	57
Evapotranspiration products	57
GRACE Solutions	58
Annex XI.3 Data comparison	58
Precipitation products	58
ET <sub>a</sub> products	60
GRACE solutions	64
Annex XI.4 Comparison of runoff and storage change	67
Annex XI.5 Spatial comparison of ET <sub>a</sub> products	69
Annex XI.6 Conclusion	70
Annex XI.7 Additional references	70

# Figures

<b>Figure 1</b>	The geography of the Jordan River Basin. Basin	2
<b>Figure 2</b>	Transboundary aquifers delineation and depletion rate	4
<b>Figure 3</b>	WA+ Sheet 1 Resource Base template	6
<b>Figure 4</b>	Spatial variation of WaPOR P and $ET_a$ in Jordan River Basin	8
<b>Figure 5</b>	Monthly variation (left) and yearly variation (right) of precipitation and actual evapotranspiration in the Jordan River Basin (JRB)	8
<b>Figure 6</b>	Temporal variation from 2010-2018 (A) and spatial variation in 2018 (B) of land cover area in the Jordan River Basin	9
<b>Figure 7</b>	Monthly precipitation derived from WaPOR data compared with measurements from GHCN stations in the Jordan River Basin between 2009 and 2019	10
<b>Figure 8</b>	Monthly precipitation derived from WaPOR data compared with measurements from GHCN stations Beer Sheva, Beer Sheeva city, and Ben Gurion between 2009 and 2019	11
<b>Figure 9</b>	Monthly precipitation derived from WaPOR data compared with measurements from GHCN stations Bet Dagan and Elat between 2009 and 2019	12
<b>Figure 10</b>	Yearly average of difference between total Precipitation and total Actual Evapotranspiration and Interception ( $P - ET_a$ ) from hydrological years 2010 to 2018	13
<b>Figure 11</b>	Contribution of the land cover classes to mean annual precipitation (P) and actual evapotranspiration ( $ET_a$ ) of the JRB	14
<b>Figure 12</b>	Yearly and monthly values of volume water pumped from Lake Tiberias to the National Water Carrier for the hydrological years from 2009 to 2019	15
<b>Figure 13</b>	Monthly Total Water Storage solved from GRACE measurements for the JRB in equivalent water height from 2009 to mid-2016	17
<b>Figure 14</b>	The total water storage change derived from WaPOR data and GRACE TWSA for 2 selected sub-catchments of the Jordan River Basin: Zarqa and Yarmouk for the hydrological years from 2010 to 2015	18
<b>Figure 15</b>	Cumulative monthly difference of WaPOR $P - ET_a - Q_{out}$ and GRACE TWSA for JRB	18
<b>Figure 17</b>	WA+ Land Use category map of Jordan River Basin in 2009 based on WaPOR Level 2 Land cover (LCC) layers and global dataset of protected area and reservoirs	22
<b>Figure 16</b>	Flowchart of steps in WaPOR-based WA+ process	23
<b>Figure 18</b>	Main schematization of the flows and fluxes in the WaterPix model	24
<b>Figure 19</b>	The yearly average map of $ET_{rain}$ and $ET_{incr}$ estimated from WaPOR data in JRB of hydrological years from 2010 to 2018	29
<b>Figure 21</b>	The WA+ Sheet 1 of Jordan River Basin with average values of hydrological years 2010 - 2018	30

<b>Figure 20</b>	The area percentage (left) and yearly average Precipitation, $ET_{rain}$ and $ET_{inc}$ , (right) of each land cover class for the hydrological years 2010-2018	31
<b>Figure 22</b>	Yearly variability of Sheet 1 fluxes. Total storage change ( $\Delta S$ ) was estimated as the difference $P - ET_a - Q_{sw}^{out}$ to close the water balance	32
<b>Figure 23</b>	Variability of rainfall ET and incremental ET in Jordan River Basin from 2010 to 2018	34
<b>Figure XI - 1</b> Precipitation values from GPM, TRMM and CHIRPS for Jordan River Basin		59
<b>Figure XI - 2</b> Monthly mean precipitation for Jordan River Basin from CHIRPS, TRMM and GPM		59
<b>Figure XI - 3</b> Annual Precipitation for Jordan River Basin from CHIRPS, TRMM and GPM		60
<b>Figure XI - 4</b> Correlation of the three precipitations data for Jordan River Basin		60
<b>Figure XI - 5</b> Annual Evapotranspiration for 2009 of JRB from SEBS, ALEXI and MODIS		61
<b>Figure XI - 6</b> Evapotranspiration values from WaPOR, SSEBop, GLEAM and CMRSET for JRB		61
<b>Figure XI - 7</b> Monthly $ET_a$ for Jordan River Basin from CMRSET, GLEAM, SSEBop and WaPOR		62
<b>Figure XI - 8</b> Annual $ET_a$ for Jordan River Basin from CMRSET, GLEAM, SSEBop and WaPOR		62
<b>Figure XI - 9</b> Mean Annual $ET_a$ of Jordan River Basin from CMRSET, GLEAM, SSEBop and WaPOR		63
<b>Figure XI - 10</b> Correlation of CMRSET, GLEAM, SSEBop and WaPOR $ET_a$ for Jordan River Basin		64
<b>Figure XI - 11</b> Storage changes from CSR, GFZ, JPL and GSFC for Jordan River Basin		64
<b>Figure XI - 12</b> Mean monthly change in storage for JRB as computed from four different GRACE solutions		65
<b>Figure XI - 13</b> Mean annual change in storage for JRB as computed from four different GRACE solutions		65
<b>Figure XI - 14</b> Correlation of the four different GRACE solutions for JRB		66
<b>Figure XI - 16</b> Runoff generation map for the best (left) and worst (right) performer in terms of coefficient of determination		67
<b>Figure XI - 17</b> Runoff generation map for the best (left) and worst (right) performer in terms of error in change of storage as percentage of precipitation		67
<b>Figure XI - 15</b> Performance of different combinations of the remote sensing products to calculate the runoff generated from JRB		68
<b>Figure XI - 18</b> $P - ET_a$ per land cover classes for CHIRPS P compared to CMRSET, GLEAM, SSEBop and WaPOR		69

# Tables

<b>Table 1</b>	The total annual precipitation ( $P$ ) and actual evapotranspiration and interception ( $ET_a$ ) from WaPOR data for the Jordan River Basin for hydrological years from 2010 to 2018	13
<b>Table 2</b>	The average $P - ET_a$ for each land cover class for the hydrological years from 2010 to 2018 in the JRB	16
<b>Table 3</b>	Estimation of Error in Water Balance of Jordan River Basin based on GRACE Total Water Storage from 2010 to 2018	19
<b>Table 4</b>	Inputs of WaterPix	24
<b>Table 5</b>	Outputs of the water balance model at pixel level	24
<b>Table 6</b>	Root depth look-up table	25
<b>Table 7</b>	Consumed fraction per land use class	26
<b>Table 8</b>	Data and estimation methods used for fluxes in WA+ Sheet 1	33
<b>Table 9</b>	WA+ Sheet 1 key indicators of JRB for the hydrological years from 2010 to 2018 based on water balance derived from WaPOR datasets	35
<b>Table 10</b>	Contribution of irrigated crop's $ET_{incr}$ to Managed Water	35
<b>Table 11</b>	Estimation of Error in WaPOR-based WA+ of JRB based on GRACE Total Water Storage from 2010 to 2015	36
<b>Table X-1</b>	WA+ Sheet 1 key indicators of Jordan River Basin for the hydrological years from 2010 to 2018 based on WaPOR Precipitation and Actual evapotranspiration datasets and $\Delta S$ from GRACE TWSA solution	55
<b>Table XI - 1</b>	Data sets considered for Water Balance Computation	56
<b>Table XI - 2</b>	Annual $ET_a$ from CMRSET, GLEAM, SSEBop and WaPOR in mm/year	62
<b>Table XI - 3</b>	$P - ET_a$ (Mm <sup>3</sup> /year) per land cover classes for CHIRPS $P$ compared to CMRSET, GLEAM, SSEBop and WaPOR	69

# Acknowledgements

This report was prepared by Bich Tran, Solomon Seyoum and Marloes Mul through a collaboration between IHE-Delft Institute for Water Education and the Food and Agriculture Organization of the United Nations, with contributions from Claire Michailovsky, Bert Coerver, Quan Pan, Elga Salvadore, and Abebe Chukalla. The report is an output of the project “Using remote sensing in support of solutions to reduce agricultural water productivity gaps” (<http://www.fao.org/in-action/remote-sensing-for-water-productivity/en/>), funded by the Government of The Netherlands.

FAO is also leading the project “Implementing the 2030 Agenda for water efficiency/productivity and water sustainability in NENA countries” through its Regional Office in Cairo. As part of this project, additional and complemental water accounting activities are being undertaken in the region, including in Jordan.

Water Accounting Plus (WA+) is an approach which is based on open access data sets and information. The validation of the water accounts for the Jordan River Basin depends on observed data. We are therefore grateful for the following institutions: the Governmental Authority for Water and Sewage of Israel for providing us the measurements of the National Water Carrier pump of the study period; the Global Runoff Data Centre (GRDC) for providing us the river discharge data at the two tributaries Yarmouk and Zarqa. Though not having direct contact, we also appreciated all the institutions that publish their database openly, which are all valuable for this water accounts study. These institutions/ research groups include, but not limited to, the National Oceanic and Atmospheric Administration, the World Protected Area Database, NASA’s Goddard Space Flight Center (GSFC), the International Groundwater Resources Assessment Centre (IGRAC), and FutureWater. In addition, we are also grateful to Prof. Dr. Graham Jewitt for editing the manuscript and providing valuable comments on the results interpretation.

# Executive summary

The Jordan River Basin is the most important water resource shared between the Middle East countries: Israel, Lebanon, Syria, and Jordan. Its surface water and groundwater have been highly exploited and fought over throughout history. The diverse climate over its area results in spatially variable precipitation and evapotranspiration, thus, variability of water generation and consumption. The basin is considered a closed one with no outlet except for an inter-basin transfer from Lake Tiberias through the National Water Carrier to Israel. To be able to manage the water resources in a sustainable manner, it is important to understand the current state of the water resources. However with limited up-to-date ground observations, in terms of duration, completeness and quality of the hydro-meteorological records it is difficult to draw an appropriate picture of the water resources conditions. A simplified Water Accounting Plus (WA+) system was designed by IHE Delft with its partners FAO and IWMI using open access spatial data. This framework has been applied to gain insights as far as possible into the state of the water resources in the basin.

This report describes the rapid water accounting study for the Jordan River Basin using the Water Productivity (WaPOR) database of the Food and Agricultural Organization (FAO). For this study, we used the WaPOR datasets for the period 2009 to 2018. The WaPOR version 2.0 level 1 with 5km resolution data for precipitation and level 2 with 100m resolution data for actual evapotranspiration, reference evapotranspiration, interception and land cover classification layers were used for WA+ analyses. Additional open access data was used to assess changes in storage (the Gravity Recovery and Climate Experiment (GRACE) data). In addition, the WaPOR land cover classification layer was reclassified to WA+ classes using the World Database on Protected Areas and the Global Reservoir and Dam Database.

The initial data analysis showed a considerable discrepancy in the water balance using WaPOR data (29% of precipitation). A comparison using other remote sensing precipitation and actual evaporation products showed that none of the combinations were able to close the water balance, with a best error of 16% of precipitation, however the quality of the different datasets in representing accurately the spatial variability varies a lot. There is insufficient information on inter-basin transfers and groundwater outflows which could be an additional reason for the discrepancies, besides the uncertainties of the remote sensing data. It is therefore important to review the WaPOR precipitation and evapotranspiration data before drawing any final conclusions on the state of the water resources in the Jordan River Basin.

Sustainable management of the water resources in the Jordan River Basin is critical not only for water-dependent sectors but also geopolitical stability among the riparian countries. Open access remote sensing derived data can provide useful information about the status of water resources in the basin. However, for better management of these resources in the basin, collaboration and sharing information about water availability, abstraction, and reuse among the riparian states are the way forward to a sustainable development.



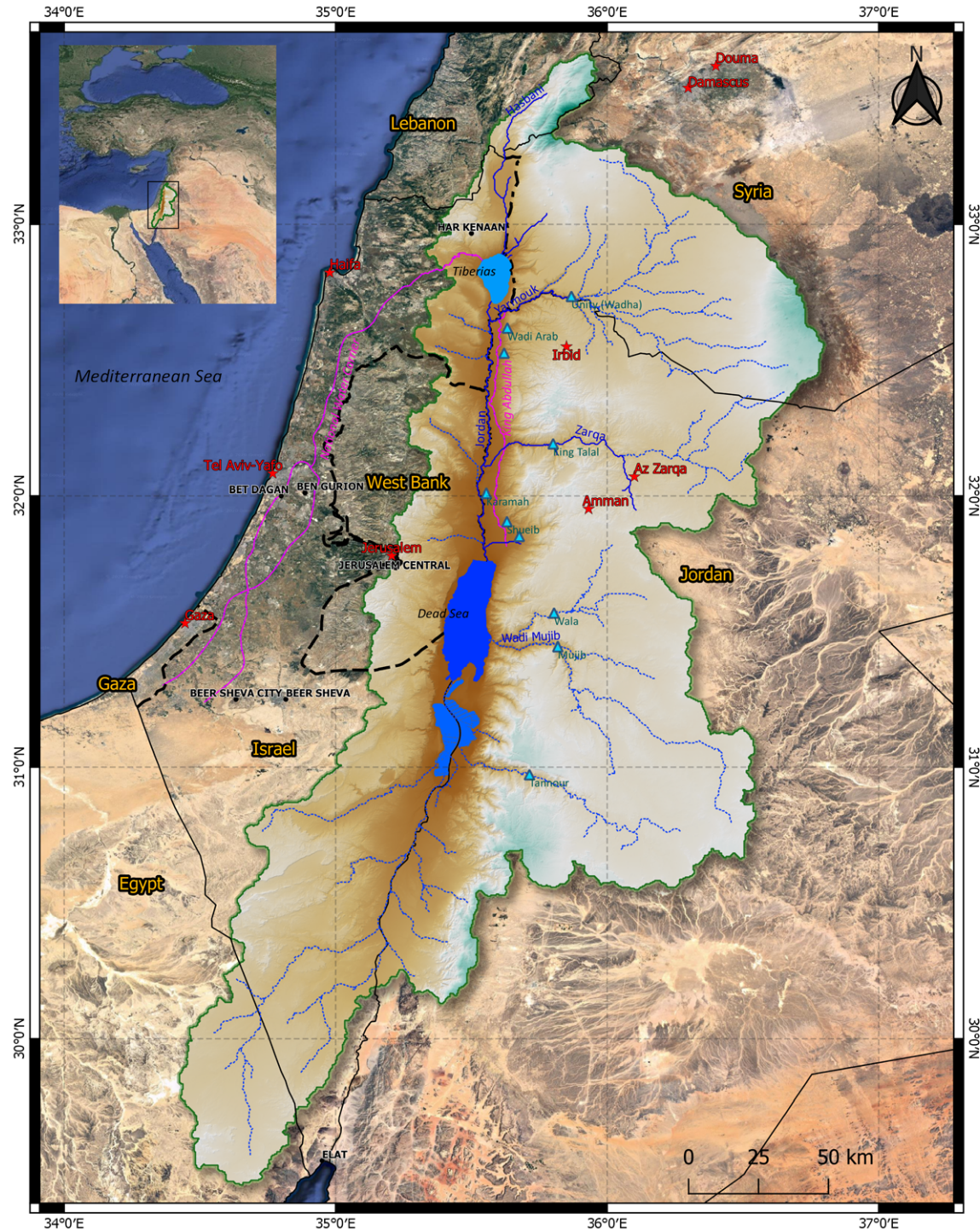
# 1. Introduction

## 1.1. Case study description

The Jordan River Basin is one of the selected pilot basins for Rapid Water Accounting using the WaPOR database. It covers an area of 43,200 km<sup>2</sup> (between 34°02'E 29°02'N and 36°04'E 33°04'N), which is shared by Jordan, Israel, West Bank, Lebanon, Syria, and Egypt (Figure 1). It is an endorheic basin, whose generated water converges into the Dead Sea. The perennial rivers run North-South to the Dead Sea, while from the opposite direction, there are many intermittent wadis draining into the Dead Sea. The headwater of the Jordan River originates from three rivers, the Hasbani, the Banias, and the Dan, which flow into Lake Tiberias (or Sea of Galilee, total area of about 166 km<sup>2</sup>). The outflow of Lake Tiberias receives water from the main tributaries of the Jordan River: Yarmouk and Zarqa and continues flowing southwards to the Dead Sea. The Jordan River Basin is the main source of fresh water supply to many agricultural zones, industrial sectors, and domestic use of populated cities (e.g. Amman, Tel Aviv-Yafo) mainly in Israel, Jordan, and Syria.

The Jordan River Basin is characterized by very diverse ecosystems, especially in the north of the basin, with climate ranging from sub-humid Mediterranean to arid in a very short distance (FAO, 2016a). The hydrological year typically starts in September before the rainy season starts and ends in August of the following year after a prolonged dry season. The average annual precipitation varies greatly across the basin, from more than 1,200 mm/year in the north of Lake Tiberias to less than 100 mm/year in the south. The major area of fertile land (suitable for agricultural development) of the Jordan River Basin is located to the north of the Dead Sea, along the eastern and western banks of the Jordan River, tributaries, and wadis. This area is also the most populated part of the basin with approximately 7.18 million residents (UN-ESCWA and BGR, 2013).

The Dead Sea, the terminal sink of the Jordan River Basin, is one of the saltiest water bodies in the world and is the lowest point on earth (about 420 m below sea level). Its current surface area is approximately 615 km<sup>2</sup> with 255 km<sup>2</sup> of the southern open water surface being exploited as evaporation ponds for potash and magnesium chloride production. Since the 1960s, the water level of Dead Sea has been decreasing at an alarming rate (-1 m/year) due to diversion of its natural water sources (Salameh and El Naser, 2000). The major problem caused by the decline of Dead Sea level are sink holes and shrinking sea shores (UN-ESCWA and BGR, 2013). Therefore, more efforts have been made to conserve its natural level such as reducing the amount of diverted water and conveying water through the Red Sea – Dead Sea pipeline which was initiated in 2018 and expected to be completed by 2021 (Al-Omari et al., 2009).



#### Legends

- ▲ Dam
- ★ Cities
- GHCN rainfall stations
- Evaporation ponds
- Freshwater lake

#### Saltwater

..... Intermittent river, wadi

#### River

— Canal, irrigation tunnel

□ Jordan Basin

□ Countries

#### Digital Elevation Model (m a.s.l.)

■ -400

■ 300

■ 1000

■ 1700

■ 2400

Figure 1: The geography of the Jordan River Basin. Basin boundary and stream network data were collected from HydroSHED database. Digital Elevation Model (DEM) was achieved from SRTM 1sec. Location of main dams was collected from FAO GeoNetwork database. Location of populated cities was collected from NaturalEarth database.

## 1.2. Water resources developments and challenges in Jordan River Basin

### 1.2.1. Overview of water resources developments

The Jordan River Basin is highly developed with extensive water infrastructure to exploit available water resources, with more than 45 dams (maximum storage capacity of 390 Mm<sup>3</sup>) to the north of the Dead Sea (UN-ESCWA and BGR, 2013). The main dams in Jordan are the Al-Wadha (Unity) Dam shared between Jordan and Syria (Capacity: 110 Mm<sup>3</sup>) which, as claimed by Jordan's Ministry of Water and Irrigation (2016), mostly diverts Yarmouk water to Syria and the King Talal Dam on Zarqa River (Capacity: 80 Mm<sup>3</sup>). The Yarmouk River is also the main water source of the King Abdullah Canal, which carries water to irrigation area in Jordan Valley. In Israel, Lake Tiberias and the Jordan River headwaters are the main surface water sources. The National Water Carrier of Israel, a system of about 130 kilometres of open canals and tunnels with maximum capacity of 1.1 Mm<sup>3</sup>/day conveys this water from Lake Tiberias across Israel for domestic supply and irrigation (Israel Water Authority, 2019).

Groundwater resources are also highly exploited in the Jordan River Basin. In Israel, groundwater accounts for about 65% of the total internal renewable water resources (FAO, 2016a). The main groundwater aquifers are the Coastal Aquifer and the Mountain Aquifer (Figure 2), which, as with many other aquifers in the Jordan River Basin, are transboundary aquifers. In Jordan, the major groundwater resources are concentrated mainly in the Yarmouk, Amman-Zarqa and Dead Sea basins. Half of the groundwater basins in Jordan are being overexploited (FAO, 2016b). The recent project to pump groundwater from the Disi Aquifer in the south of Jordan to Amman was started in 2009 and expected to reach full capacity of 100 Mm<sup>3</sup> by 2025, but is limited to water supply for domestic use in Amman (Salameh et al., 2014).

In addition to conventional water resources (surface and groundwater), non-conventional water resources including treated wastewater, desalinated sea water and brackish water, and harvested precipitation are also utilized in the Jordan River Basin. Treated wastewater is an important resources in Jordan and mostly used in irrigation. For example, in the Greater Amman municipality, almost 90% of treated wastewater is being reused in irrigation (FAO, 2016b). Desalinated water is often produced in small- and medium- facilities, and of quality adequate for irrigation. According to FAO AQUASTAT, the total non-conventional water resources accounts for about 20% of Israel's water withdrawal, 10% in Jordan, and 16% in Syria (FAO, 2016b, 2016a, 2016c), which suggests that these can be important fluxes in the Jordan River Basin.

### 1.2.2. Water resources management challenges

As the main water resources which are shared by Jordan, Israel, Palestine and Syria, the most challenging issues that the Jordan River Basin faces are water scarcity and adequate water allocation among the riparian countries and different sectors within them (Abu-Sharar and Battikhi, 2002; Al-Kharabsheh and Ta'any, 2005; Phillips et al., 2009). Existing physical water scarcity in the Jordan River Basin is likely to be exacerbated by climate change, deteriorating water quality, and fast-growing demands from overpopulation. The recent 15 year drought (1998-2012), which was the driest in the Levant (Easter Mediterranean countries including Turkey, Syria, Occupied Palestinian Territory, Lebanon, Israel, and Jordan) over the past 900 years (Cook et al., 2016) is an example of the Jordan River Basin vulnerability to extreme climate anomalies.

The Jordan River and tributaries have been the subject of conflicts between the riparian countries for many decades largely due to the relatively small amount of available water compared to high demands (Abu-Sharar and Battikhi, 2002; Borthwick, 2003; FAO, 2016a; Shuval, 2000; UN-ESCWA and BGR, 2013; Wolf, 1995).

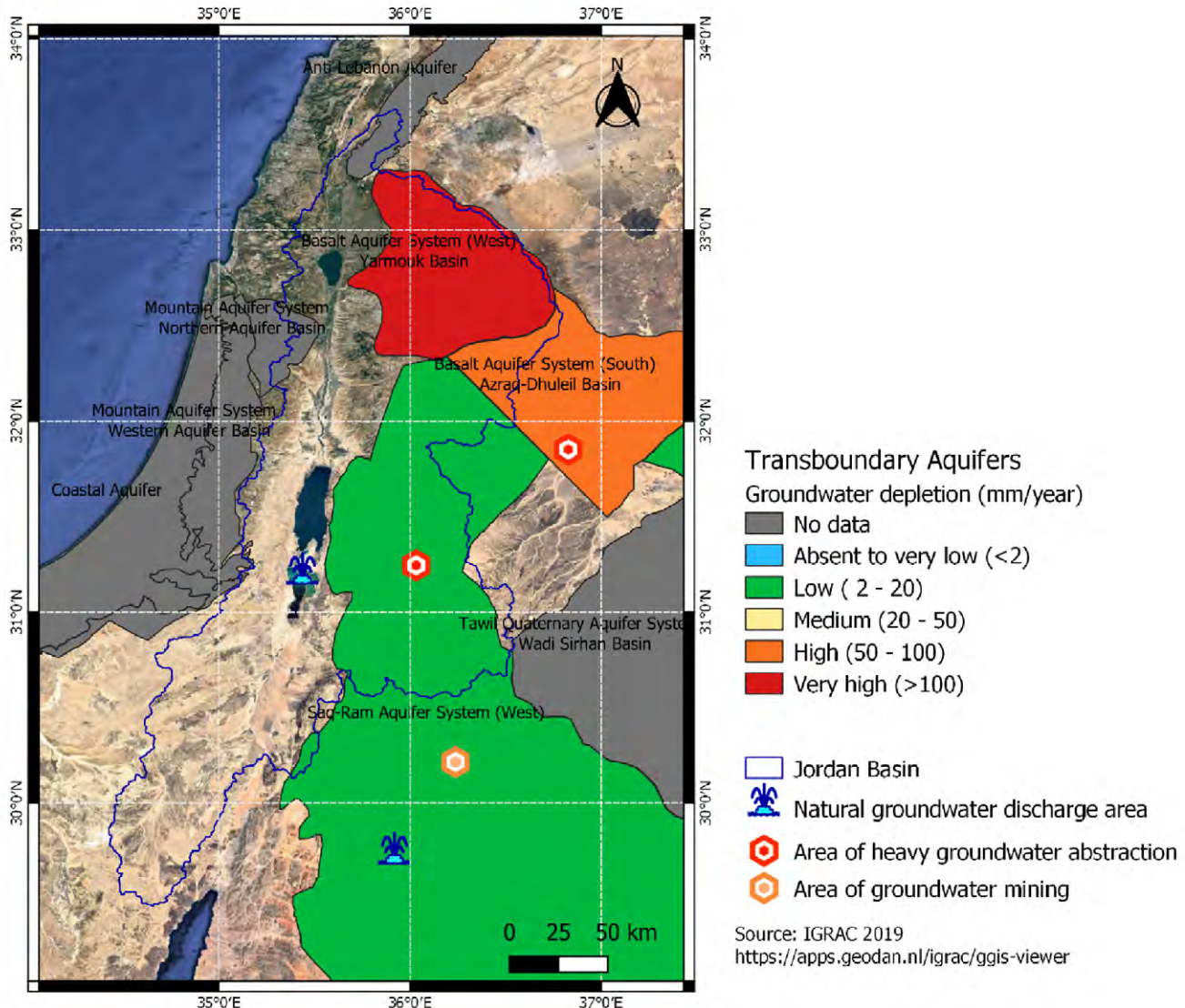


Figure 2: Transboundary aquifers delineation and depletion rate. The major groundwater discharge and abstraction area are also located. Source of data is from the International Groundwater Resources Assessment Center (IGRAC).

Therefore, sharing information about water availability is important not only to support integrated water resources management, but also geopolitical stability of the basin. However, different sources report different values and often at sub-basin level (Al-Omari et al., 2009; Comair et al., 2012; Courcier et al., 2005; Gunkel and Lange, 2012; Klein, 1998; UN-ESCWA and BGR, 2013) or administrative level (Abu-Sharar and Battikhi, 2002; FAO, 2016a), which makes it difficult to develop water accounts of the whole basin.

### 1.3. Objective of water accounts

The purpose of this study is to assess water availability, consumptive use, and non-consumptive use in the Jordan River Basin using remote sensing derived data from FAO WaPOR database in conjunction with other open-access data sources. In particular, the study seeks to investigate:

- What is the current water resources availability in the Jordan River Basin?
- How much water is being consumed by irrigated agriculture in the Jordan River Basin?
- What are the safe caps of water withdrawals for the agricultural sector in the Jordan River Basin?

A system referred to as Water Accounting Plus (WA+) has been designed by IHE Delft with its partners FAO and IWMI using spatial data from earth observations and various other open-access databases. It aims to complement the lack of routine water resources data collection and incorporates spatially distributed water consumption. The WA+ framework is a reporting mechanism that summarizes the state of the water resources conditions by means of customized sheets. While the WaPOR database does not contain all the input data required for fully implementing the WA+ framework, key data is provided, such as precipitation, actual evapotranspiration, the breakdown between transpiration, evaporation and interception (FAO, 2018).

Thus, the present study implements a rapid WaPOR-based WA+ framework, which used WaPOR v2.0 level 2 data (100m resolution), for the Jordan River Basin which is available between 2009 and 2018. It focusses on the basin-wide analyses (WA+ Resource Base, see example Figure 3) as an initial analysis of the state of the water resources utilisation in a river basin. Finally, this report reflects on the quality of the WaPOR v2.0 data for WA+.

## Sheet 1: Resource Base (NaN)

Basin: NaN  
Period: NaN

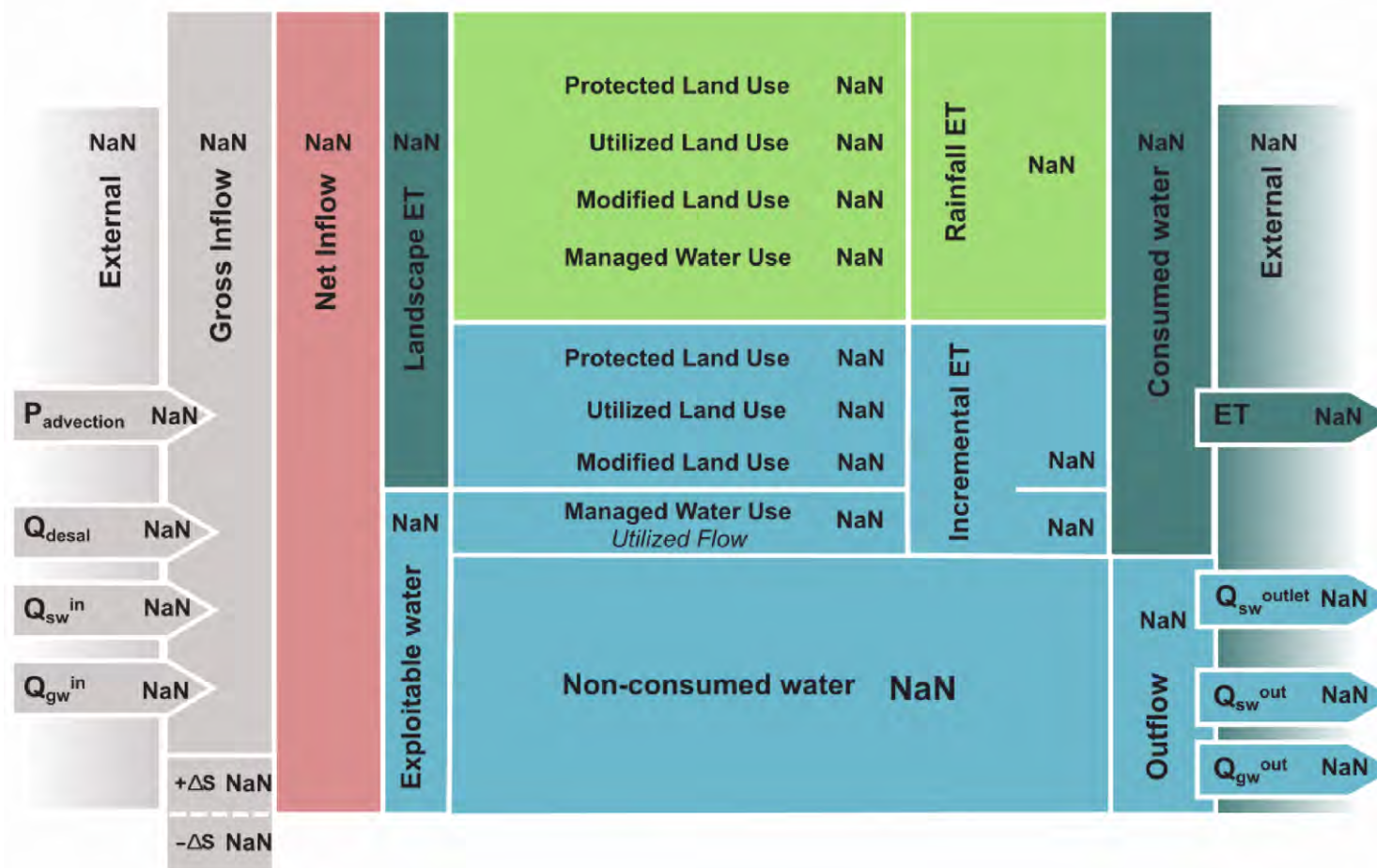


Figure 3: WA+ Sheet 1 Resource Base template. Description of WA+ Sheet 1 is given in Section 2.3

## 2. Materials and Methods

In this chapter, we describe: [2.1] key datasets from WaPOR database used for WA+; [2.2] preliminary assessment of WaPOR data using other global datasets and available observations; and [2.3] the rapid assessment procedure for WA+ Sheet 1 Resource Base.

### 2.1. WaPOR datasets

The WaPOR v2.0 database contains information at three different spatial resolutions. At continental level, data is available at 250m resolution (Level 1). For selected countries and basins, data is available at 100m resolution (Level 2). For detailed crop water productivity analyses for selected irrigation systems, 30m resolution data is available (Level 3). In this study, we used the Level 1 Precipitation data (5 km resolution) and Level 2 Land Cover Classification (LCC) and Actual Evapotranspiration and Interception (AETI) data (100m resolution). The AETI data is further indicated as  $ET_a$  in this report.

#### 2.1.1. Precipitation

WaPOR precipitation data is based on the CHIRPS database created by the United States Geological Survey (FAO, 2018; Funk et al., 2015). Temporal variation of precipitation in WaPOR data can be seen in Figure 5. The monthly-average precipitation shows that hydrological year typically starts in September at the end of the dry season. Therefore, for annual values aggregation, the hydrological year period was used and indicated as the year in which it ends. The annual precipitation over the Jordan River Basin varied between 210 to 260 mm/year during the period of 2010-2018. Figure 4 shows the spatial variability of the mean annual WaPOR precipitation ( $P$ ) in the Jordan River Basin for the hydrological years 2010-2018. It can be seen clearly in the precipitation map that most of the precipitation falls north of the Dead Sea while the biggest land area of the Jordan River Basin receives less than 200 mm/year.

#### 2.1.2. Actual Evapotranspiration and Interception

The WaPOR evapotranspiration ( $ET_a$ ) layer estimates the total evapotranspiration, including interception. Figure 4 also shows the spatial variability of  $ET_a$  in comparison with precipitation in the Jordan River Basin. The highest  $ET_a$  value is observed in water bodies while the vast bare land has  $ET_a$  much lower than 200 mm/year. It can be seen from this map that the agriculture development along the Jordan River and King Abdullah Canal has relatively high  $ET_a$ . The inter-annual variation of basin average  $ET_a$  follows similar trend with precipitation but in a lower range between 150 to 185 mm/year, which means in total, the basin has net water generated from precipitation (Figure 5). In contrast, the monthly variation of  $ET_a$  follows different pattern from precipitation. During the driest month when there is no precipitation, the average  $ET_a$  of the Jordan River Basin is relatively high (about 16mm/month) which means evaporated water is mostly sourced from stored water of the previous months.

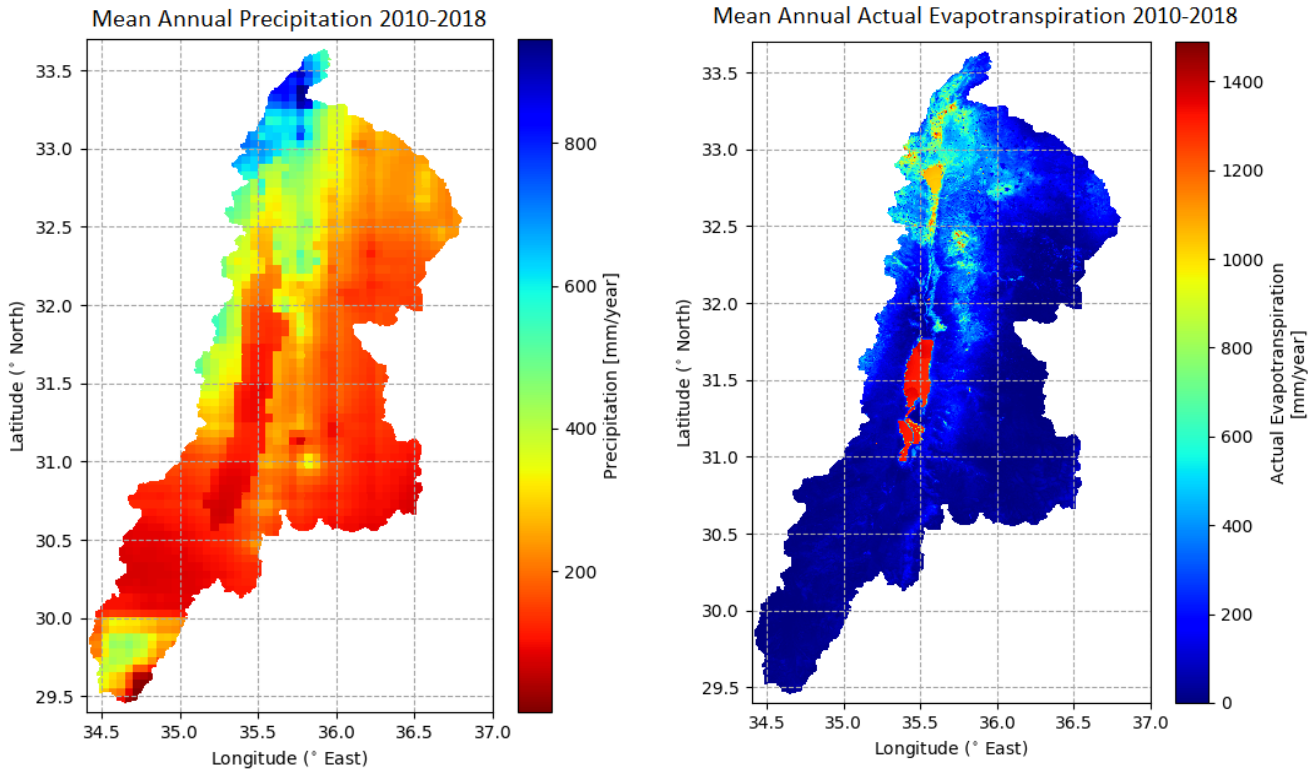


Figure 4: Spatial variation of WaPOR  $P$  and  $ET_a$  in Jordan River Basin based on WaPOR average annual data of hydrological years from 2010 to 2018 (maps of the individual years are provided in Annex I and Annex II)

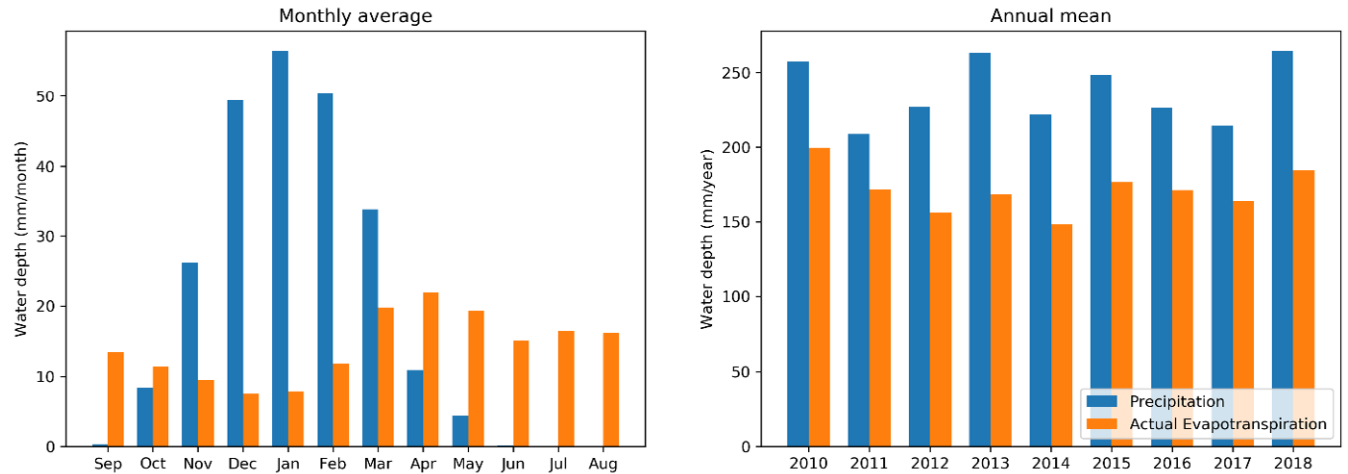


Figure 5: Monthly variation (left) and yearly variation (right) of precipitation and actual evapotranspiration in the Jordan River Basin (JRB) based on WaPOR data of hydrological years from 2010 to 2018. A hydrological year in the JRB starts in September

### 2.1.3. Land Cover Classes

The WaPOR database provides a yearly land cover maps (LCC) for the Jordan River Basin, which is based on the Copernicus land cover product (FAO, 2019). The land cover map of the year 2018 from the WaPOR database is presented in Figure 6B. The land cover map provides 23 land use classes, with 11 different land cover classes for trees. The major land cover classes in the Jordan River Basin are bare/sparse vegetation, grass land, and crop land. Throughout the study period, there were no significant changes in the area of natural land cover classes based on WAPOR data (Figure 6A).

The land cover area of cropland classes varies between 2011 and 2015; total area of rainfed cropland decreased while that of irrigated cropland increased (Figure 6A). It should be noted that the irrigated cropland class in WaPOR's LCC layers is identified by applying a water deficit index that takes into consideration seasonal cumulated values of precipitation and actual evapotranspiration (FAO, 2019). The total change in cropland area is due to two major changes in the basin: the growing area of irrigated cropland in the Jordan Valley, and the decreasing area of cropland (both irrigated and rainfed) in the Syrian territory of Yarmouk sub-catchment (Annex VI), which might be an impact of the conflict since 2011 (ESA, 2017).

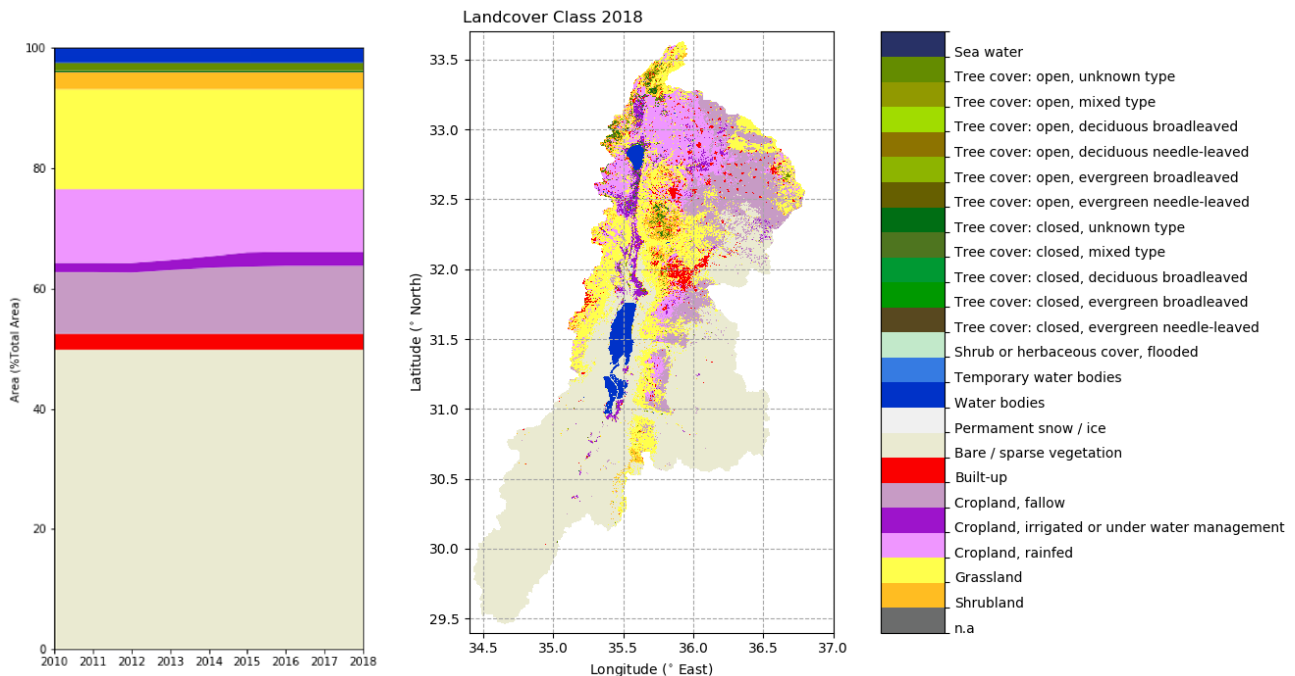


Figure 6: Temporal variation from 2010-2018 (A) and spatial variation in 2018 (B) of land cover area in the Jordan River Basin based on WaPOR L2\_LCC\_A layers. Maps of the individual years are provided in Annex III.

## 2.2. Preliminary assessments

Before using the data for the Water Accounting Plus, several checks were performed including (1) comparing WaPOR data with in situ observations, (2) mapping net water generation and consumption and identifying net consumer land cover class, and (3) assessing WaPOR-derived basin scale water balance using remotely sensed total water storage.

### 2.2.1. Comparison with in situ observations

In situ precipitation measurements were collected from the Global Historical Climatology Network (GHCN) open-access database by the National Oceanic and Atmospheric Administration (NOAA) (Menne et al., 2012). The location of GHCN stations with data available for the study period are shown in Figure 1. Unfortunately, most stations are located outside of the basin, with only Har Kenaan and Jerusalem central are located in the basin. The monthly precipitation measured from these two stations are compared with monthly precipitation derived from WaPOR datasets at the location of the station in Figure 7. The data was available from 2009 to 2015.

Overall, WaPOR precipitation data shows adequate agreement with in situ observations at these locations except in the highest precipitation months. However, comparison with only two stations is insufficient to validate the precipitation map of the whole large area of the Jordan River Basin, thus, stations within the range of latitude and longitude were also selected for comparison with WaPOR monthly precipitation.

As can be seen from Figure 7 and 8, stations that are close to the coast (Bet Dagan, Ben Gurion, Beer Sheva City and Elat) show high overestimation of precipitation (from +23 up to +75% bias) while the more inland stations (Beer Sheva) show stronger agreement with WaPOR data (only +5% bias). Unfortunately, there were no records at locations in the bare land area in the west and south of the Jordan River Basin, thus, a large part of the precipitation map was not validated.

There are no actual evapotranspiration measurements in the Jordan River Basin to validate the WaPOR  $ET_a$  map. However, compared to reported evaporation in natural lakes, WaPOR  $ET_a$  over open water bodies seems to be underestimated. Courcier et al. (2005) has consolidated several secondary data sources and reported that evaporation over Lake Tiberias is about 285 Mm<sup>3</sup>/year, which is divided by the average surface area to be about 1,700 mm/year. This is about 55% higher than the average  $ET_a$  of Lake Tiberias (1,100 mm/year) from WaPOR data-set as seen from Figure 4.

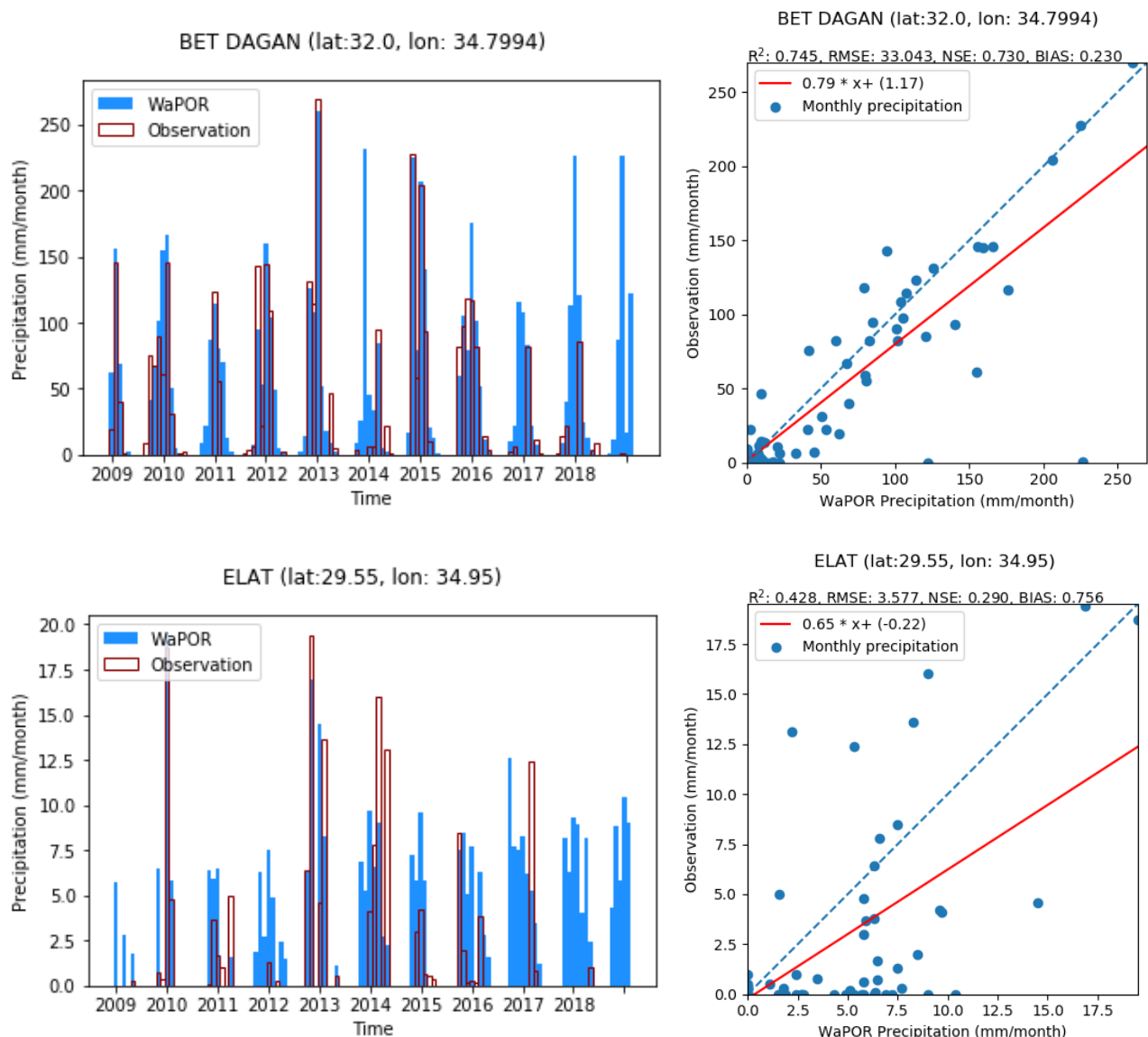


Figure 7: Monthly precipitation derived from WaPOR data compared with measurements from GHCN stations in the Jordan River Basin between 2009 and 2019.

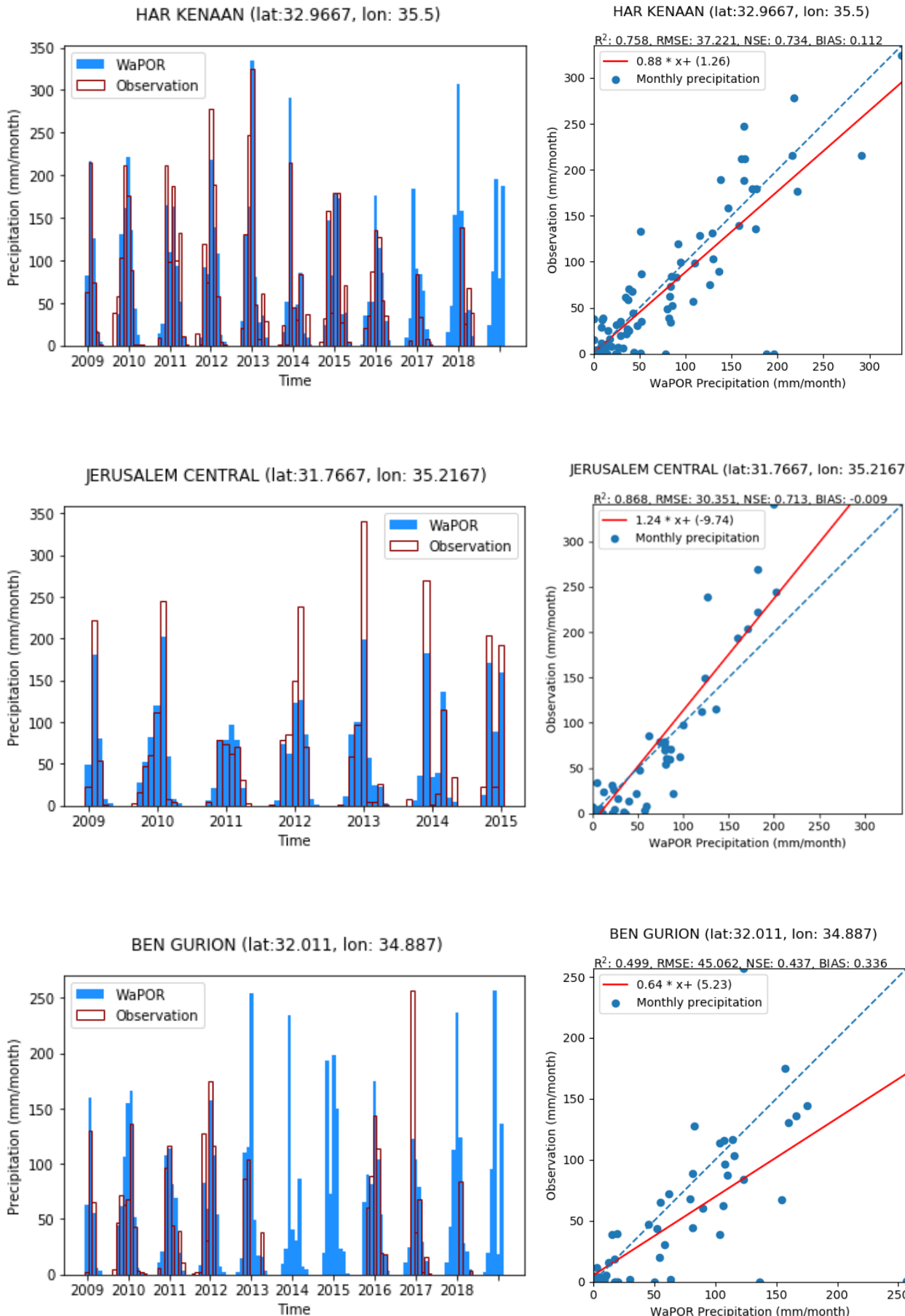


Figure 8: Monthly precipitation derived from WaPOR data compared with measurements from GHCN stations Beer Sheva, Beer Sheeva city, and Ben Gurion between 2009 and 2019

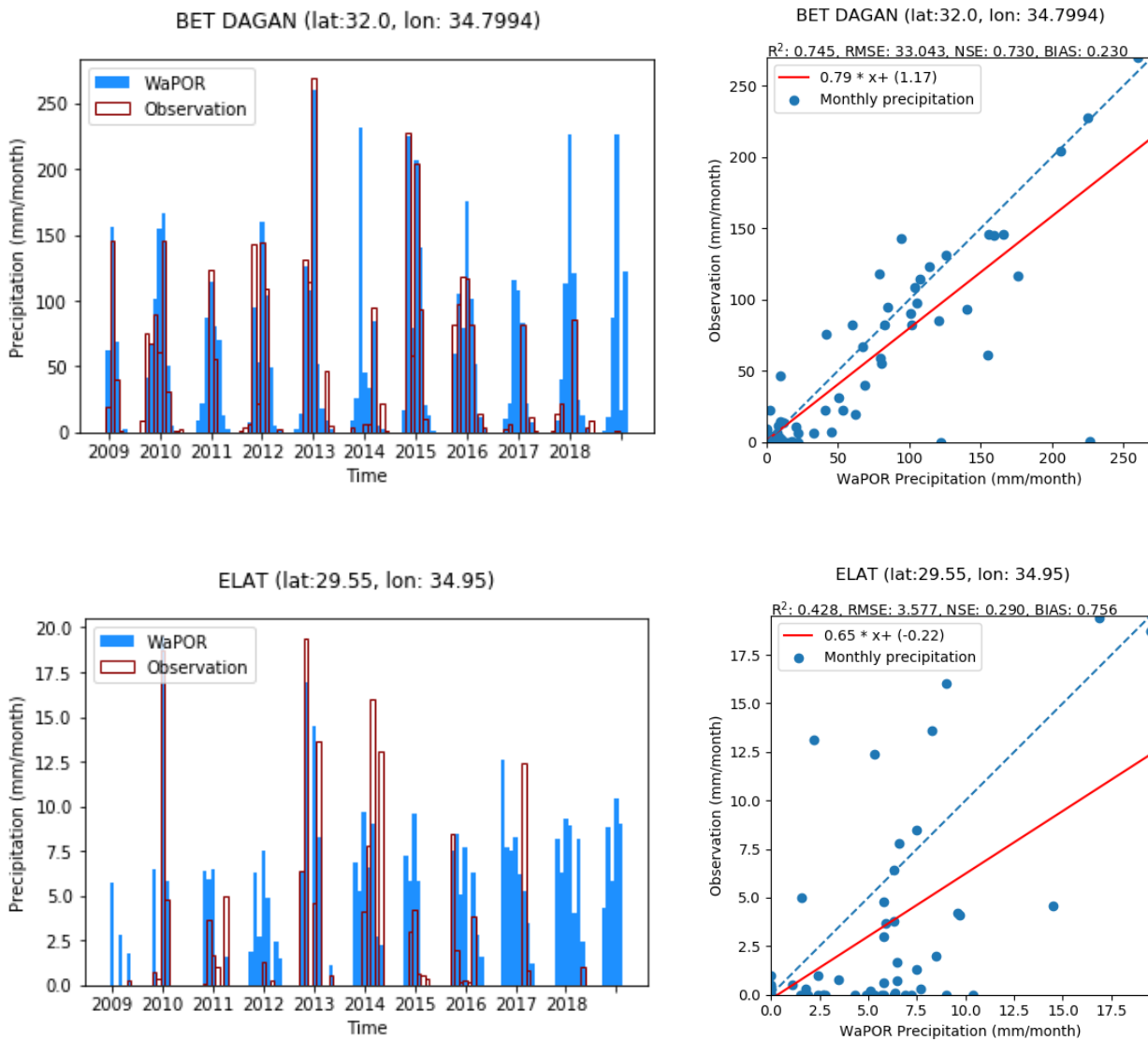


Figure 9: Monthly precipitation derived from WaPOR data compared with measurements from GHCN stations Bet Dagan and Elat between 2009 and 2019

## 2.2.2. Water generation and consumption analysis

The WaPOR datasets for precipitation, actual evapotranspiration and interception, and land cover class were used to describe precipitation excess (water generation), and thus, lateral transport of water from water surplus to net water consumption per land cover class. Land cover classes that satisfy  $P > ET_a$  are considered water generating areas while those fulfil  $ET_a > P$  are net consumers of water (Bastiaanssen et al., 2014). The yearly average precipitation excess or deficit ( $P - ET_a$ ) for the hydrological years from 2010 to 2018 is mapped in Figure 10. As can be seen in this map, the net water consumers are water bodies and croplands. Most parts of the Jordan River Basin are net water generating areas yielding between 0 and 200 mm/year. However, the total area of these parts is large so even a small excess can accumulate into a large amount of water. The western area adjacent to the Red Sea and in the highland area to the south-west of the Dead Sea have relatively high precipitation excess (between 250 and 500 mm/year). The total  $P - ET_a$  of the whole basin and each land cover class are reported in Table 1 and Table 2.

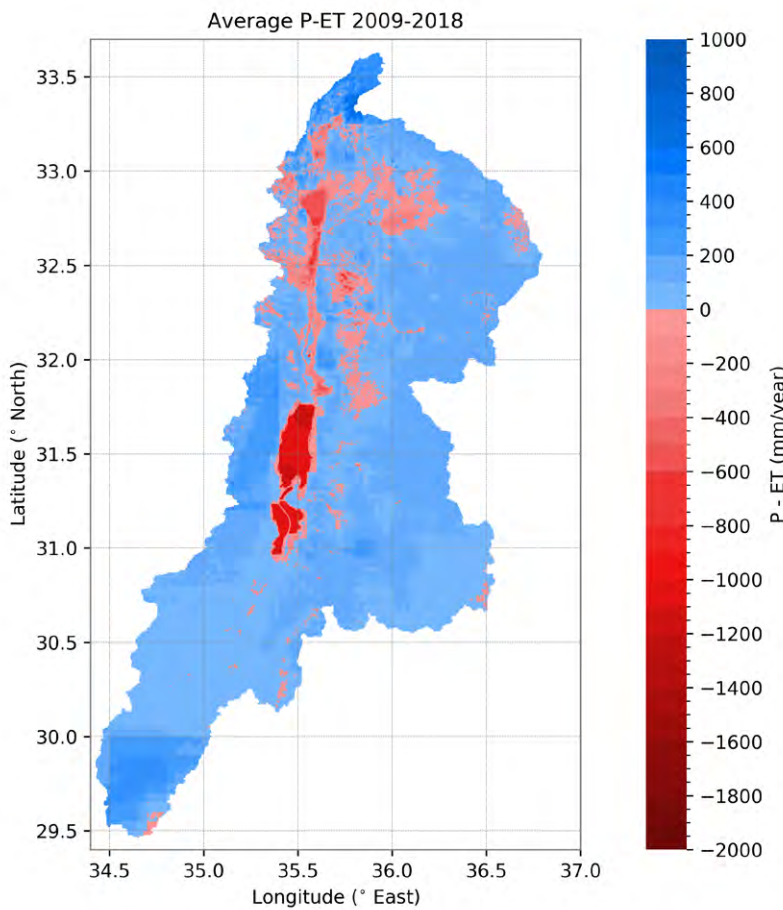


Figure 10: Yearly average of difference between total Precipitation and total Actual Evapotranspiration and Interception ( $P - ET_a$ ) from hydrological years 2010 to 2018. The blue to light blue color represents the net water producers and the red to light orange color represents the net consumers. Maps of the individual years are presented in Annex IV.

The basin wide long-term precipitation excess is 66 mm/year with positive value reported for all years between 2010 and 2018 (Table 1). If values from WaPOR data are accurate, it implies that, as a whole, the Jordan River Basin generates water. Excess precipitation that is not consumed via evapotranspiration can generate surface runoff, interflow, drainage, groundwater recharge, seepage, and baseflow (Bastiaanssen et al., 2014). Since the Jordan River Basin is an endorheic basin, which means there is no surface water outlet, excess water can only exit the basin through groundwater outflow, man-made inter-basin transfers or in the form of recharge to deep groundwater storage which is no longer accessible in the basin.

**Table 1:** The total annual precipitation ( $P$ ) and actual evapotranspiration and interception ( $ET_a$ ) from WaPOR data for the Jordan River Basin for hydrological years from 2010 to 2018

Year	P (mm/year)	ET <sub>a</sub> (mm/year)	P - ET <sub>a</sub> (mm/year)	P (mm <sup>3</sup> /year)	ET <sub>a</sub> (mm <sup>3</sup> /year)	P - ET <sub>a</sub> (mm <sup>3</sup> /year)
2010	256	198	58	11,071	8,570	2,501
2011	208	170	38	8,978	7,340	1,638
2012	225	155	71	9,746	6,689	3,057
2013	262	167	95	11,330	7,208	4,122
2014	221	147	74	9,550	6,369	3,181
2015	247	176	72	10,694	7,602	3,092
2016	226	170	56	9,759	7,356	2,404
2017	214	163	51	9,240	7,046	2,194
2018	263	184	80	11,376	7,938	3,439
Average	236	170	66	10,194	7,346	2,848

The same calculation was done for each land cover class to identify net water generating and consuming land cover classes (Table 2). It can be seen here that 50% of the Jordan River Basin area is made up of the bare/sparse vegetation class, which is the biggest net water generator (+2,536 Mm<sup>3</sup>/year). This class receives 32.7% of total precipitation, while only contributing 10.9% of the total  $ET_a$  (Figure 11). The excess precipitation ( $P - ET_a$ ) of this class is 77% of its precipitation (3,332 Mm<sup>3</sup>/year), which means the runoff coefficient is very high. Grassland and fallow are the second and third largest net water producers, and generated +934 and +568 Mm<sup>3</sup>/year respectively. Table 2 also clearly shows that the rainfed croplands are net water generators, which might not be easily seen from Figure 10 due to these small areas being scattered across the landscape. Though having the largest contribution to total  $ET_a$  (25.3%), the rainfed crop also receives significant share from total precipitation (18.7%) (Figure 11), which resulted in a net water generation. The built-up (urban) class yields the highest average  $P - ET_a$  (+147 mm/year), which is due to high runoff coefficient of the impermeable surfaces.

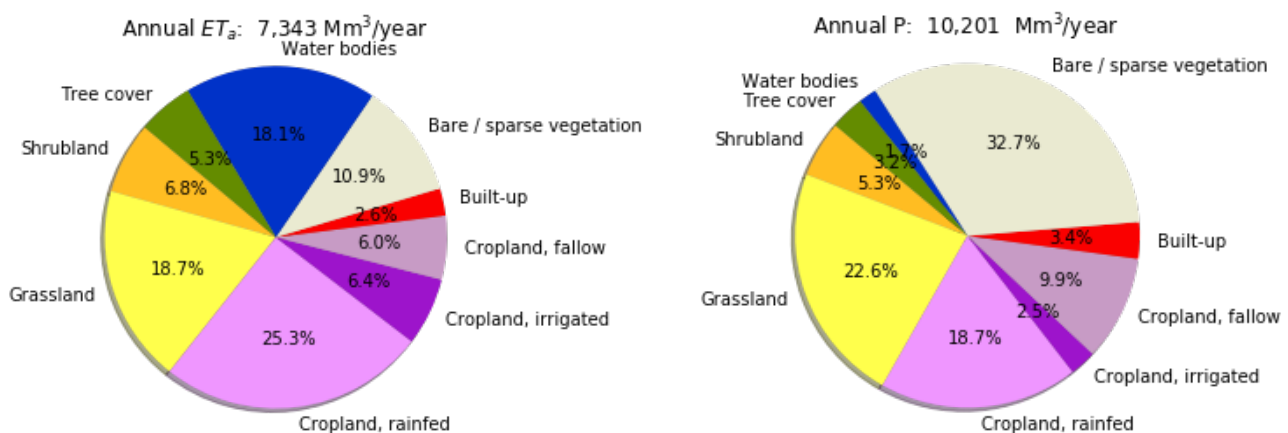


Figure 11: Contribution of the land cover classes to mean annual precipitation (P) and actual evapotranspiration ( $ET_a$ ) of the Jordan River Basin for the hydrological years from 2010 to 2018. The land cover classes that contribute less than 0.1% are not presented in the graphs. Contribution from all tree cover classes are summed together.

The biggest net water consumers are water bodies (-1,157 Mm<sup>3</sup>/year), followed by the irrigated croplands class (-217 Mm<sup>3</sup>/year). Figure 11 shows that ‘water bodies’ class receives only 1.2% of total precipitation, while it contributes to 18.1% of total  $ET_a$ . Though all tree cover classes are net water consumers, they account for very small area (less than 2% of the Jordan River Basin), thus, the total volume of net water consumption is relatively insignificant. It can also be seen here that needle-leaved tree consumes much less water (-15 to -50 mm/year) than broadleaved trees (-380 to -430 mm/year).

### 2.2.3. Basin scale water balance

Some components of the catchment water balance in the Jordan River Basin, such as inter-basin transfer, groundwater outflow, cannot be directly derived from WaPOR datasets. Therefore, to check whether WaPOR data can close the water balance, additional data sources must be utilised

### 2.2.3.1. Observed inter-basin flows

There are several water diversion projects intra-basin and inter-basin. The exact amount of these human-induced fluxes are not well reported. In this analysis, we were only able to obtain the volume of water pumped to the Nation Water Carrier (NWC) from Lake Tiberias to Israel between 2009 and 2019 (Figure 12).

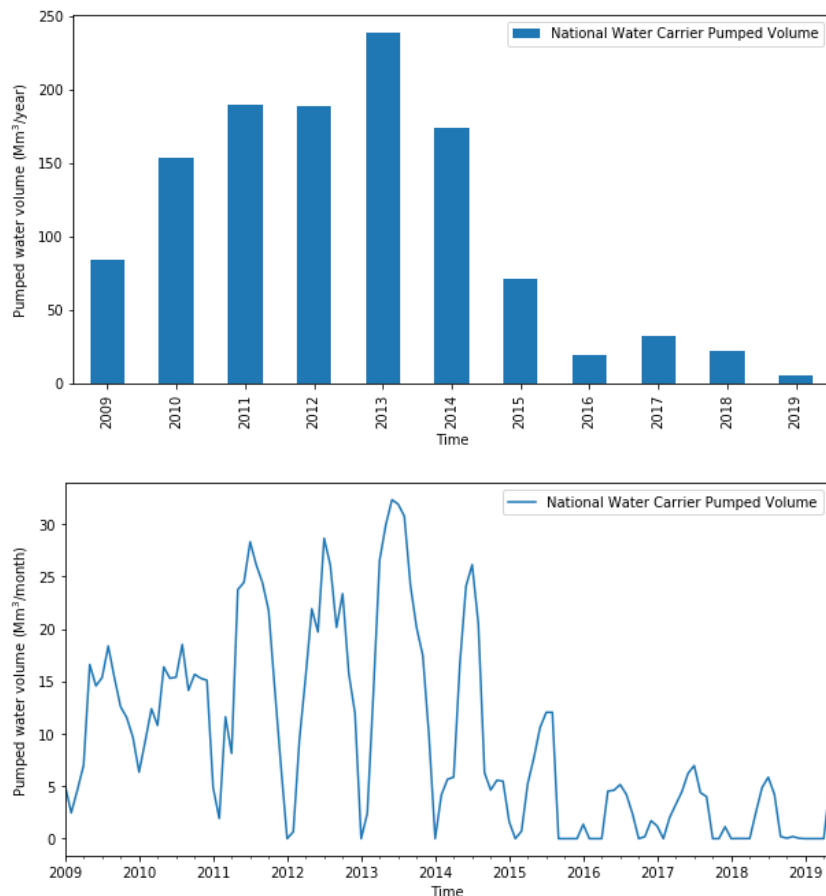


Figure 12: Yearly and monthly values of volume water pumped from Lake Tiberias to the National Water Carrier for the hydrological years from 2009 to 2019 (Source: The Governmental Authority for Water and Sewage of Israel).

The measurements show that the annual total volume of pumped water in NWC has decreased from above 150 Mm<sup>3</sup>/year before 2015 to less than 50 Mm<sup>3</sup>/year for the subsequent years. Two processes could attribute to this decline, 1) the area around Lake Tiberias observed below average precipitation during the period after 2015 (see also Annex I) and 2) Israel is increasing its capacity of desalination, thereby reducing its dependency on the NWC. Even during the year with highest value, it is much lower than the maximum capacity of the NWC. The peak month for the transfer is typically around mid-year, i.e. during the dry season. On average, each year in the period 2009-2019, the NWC pumped 107 Mm<sup>3</sup>/year from Lake Tiberias, which is only a quarter of the value before 2005 (440 Mm<sup>3</sup>/year as reported by Courcier et al., 2005). This amount is only about 3.75% of the total excess precipitation  $P - ET_a$  each year, which suggests that there could be other unaccounted inter-basin transfers or groundwater outflows.

### 2.2.3.2. GRACE Total Water Storage Change

To assess how much of the difference between  $P$  and  $ET_a$  is due to change in total water storage, we used data from the Gravity Recovery and Climate Experiment (GRACE), a dual-satellite mission continuously

**Table 2:** The average  $P - ET_a$  for each land cover class for the hydrological years from 2010 to 2018 in the Jordan River Basin.

Land Cover Class Description	Area (km <sup>2</sup> )	Area percentage (%)	P (mm/year)	P (mm <sup>3</sup> /year)	ET <sub>a</sub> (mm/year)	ET <sub>a</sub> (mm <sup>3</sup> /year)	P - ET <sub>a</sub> mm/year)	P - ET <sub>a</sub> (mm <sup>3</sup> /year)
Bare / sparse vegetation	21,586	50.0%	154	3,332	37	796	118	2,536
Grassland	7,191	16.6%	320	2,302	190	1,368	130	934
Cropland, fallow	4,686	10.8%	215	1,010	94	441	121	569
Built-up	1,092	2.5%	320	350	173	189	147	161
Cropland, rainfed	4,883	11.3%	389	1,900	379	1,850	10	50
Shrub land	1,207	2.8%	447	540	411	496	37	44
Tree cover: open, evergreen needle-leaved	1	< 0.1%	635	1	649	1	-15	< -1
Shrub or herbaceous cover, flooded	2	< 0.1%	438	1	459	1	-21	< -1
Tree cover: closed, deciduous broadleaved	< 1	< 0.1%	640	< 1	1,029	< 1	-389	< -1
Tree cover: open, deciduous broadleaved	< 1	< 0.1%	641	< 1	1,072	1	-430	< -1
Tree cover: closed, evergreen needle-leaved	24	0.1%	690	17	742	18	-53	-1
Tree cover: closed, mixed type	4	< 0.1%	718	2	1,137	4	-419	-1
Tree cover: open, unknown type	558	1.3%	481	268	519	289	-38	-21
Tree cover: closed, unknown type	101	0.2%	529	53	911	92	-382	-38
Cropland, irrigated or under water management	847	2.0%	299	253	555	470	-257	-217
Water bodies	1,057	2.4%	163	172	1,258	1,329	-1,095	-1,157
<b>Total</b>	<b>43,238</b>	<b>100.0%</b>	-	<b>10,201</b>	-	<b>7,343</b>	-	<b>2,848</b>

monitoring and mapping Earth's changing gravity field to estimate the total water storage anomalies (TWSA). There are several GRACE solutions for TWSA estimation from gravity anomalies, which covers the whole globe from 2003 till end of 2015. The GSFC-v02.4-ICE6G solution (Luthcke et al., 2013) was used to validate the storage change in the water balance calculated using WaPOR data. Since GRACE solution provides mean monthly TWSA not the exact TWSA of the first and last day of the month, change of storage ( $\Delta S/\Delta t$ ) in a time period was approximated using a second order central difference as proposed by Biancamaria et al. (2019). After that, the residual ( $P - ET_a - Q_{out}$ ) should be equal to the change of storage (JS/Jt) following the simplified water balance equation:

$$\frac{\Delta S}{\Delta t} = P - ET_a - Q_{out}$$

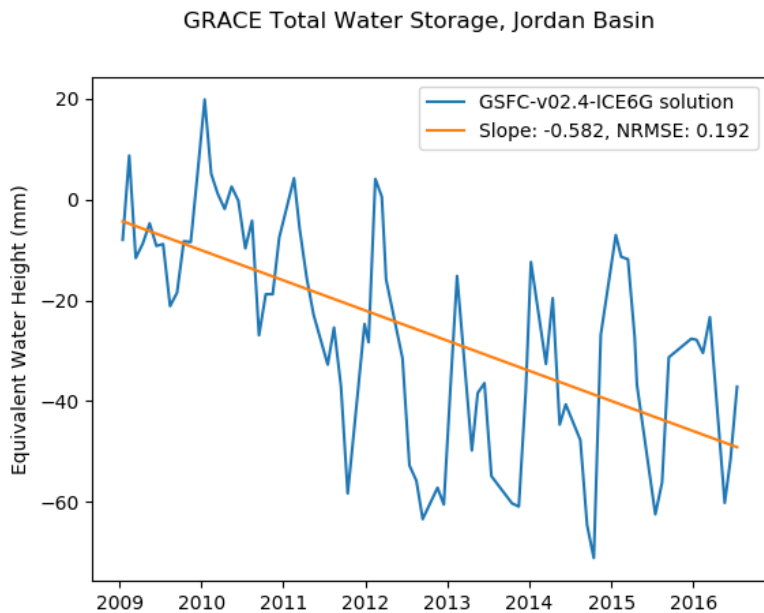


Figure 13: Monthly Total Water Storage solved from GRACE measurements for the Jordan River Basin in equivalent water height from 2009 to mid-2016

The longer term trend in storage change ( $\Delta S$ ) as observed by GRACE is negative (Figure 13). The trend of total water storage in equivalent water height for a number of GRACE solution grids, or mass concentration (also called mascons), that cover the Jordan River Basin from 2009 to 2016 is  $-0.582 \text{ mm/month}$ , which is translated into about  $-300 \text{ Mm}^3/\text{year}$ . This amount represents only about 10.5% of the yearly difference between WaPOR  $P$  and  $ET_a$ . In combination with the NWC measurements, the available data can only explain for 14.3% of the average WaPOR  $P - ET_a$  gap over the study period. This implies that up to 85.7% of excess precipitation, is not accounted for. Part of this could be groundwater outflow and other inter-basin transfers, however this is not quantified and the significant amount indicates it is probably more likely an issue with the quality of the WaPOR  $P$  and  $ET_a$  data.

### 2.2.3.3. Assessment of errors in water balance

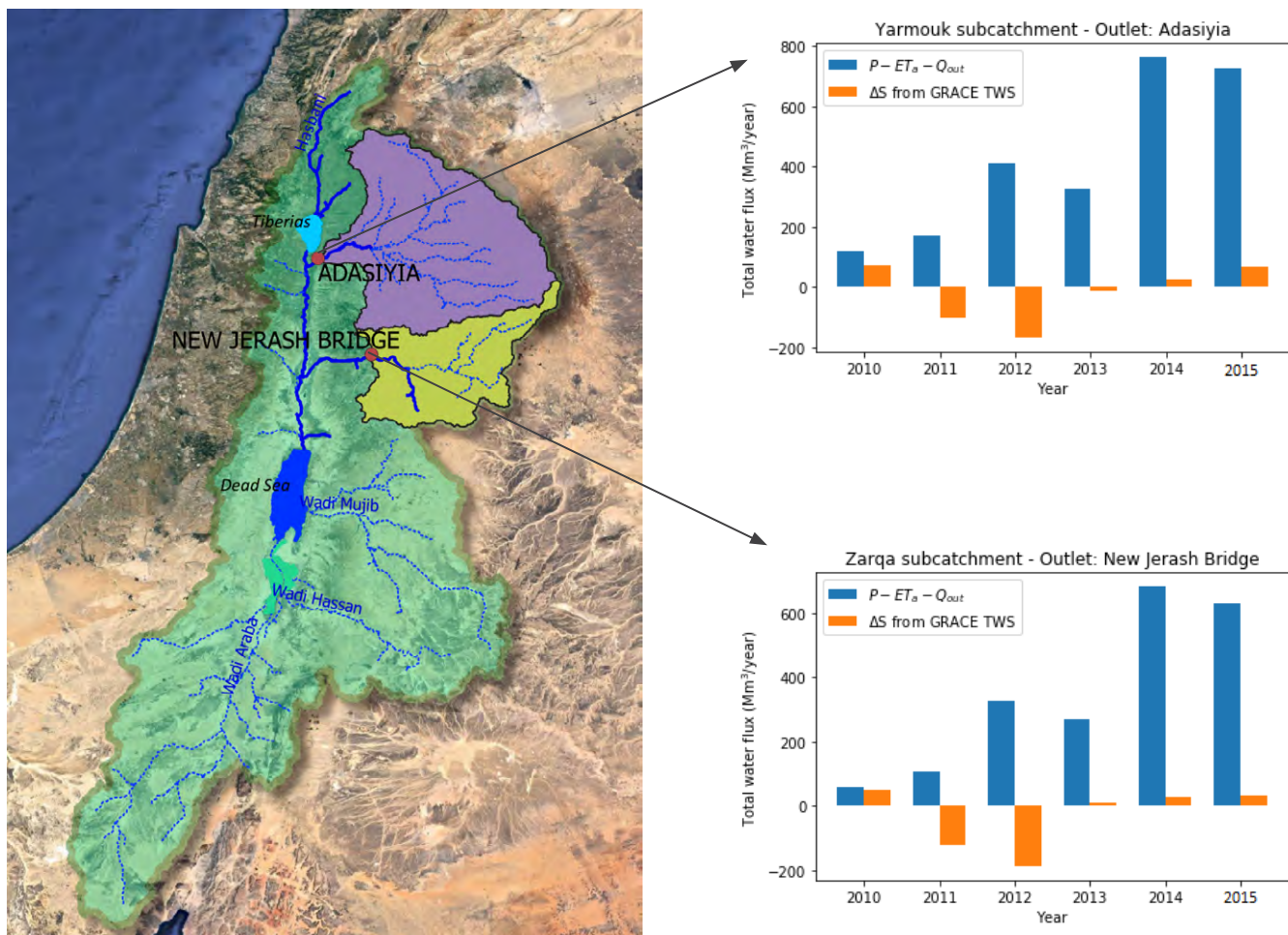


Figure 14: The total water storage change derived from WaPOR data and GRACE TWSA for 2 selected sub-catchments of the Jordan River Basin: Zarqa and Yarmouk for the hydrological years from 2010 to 2015.

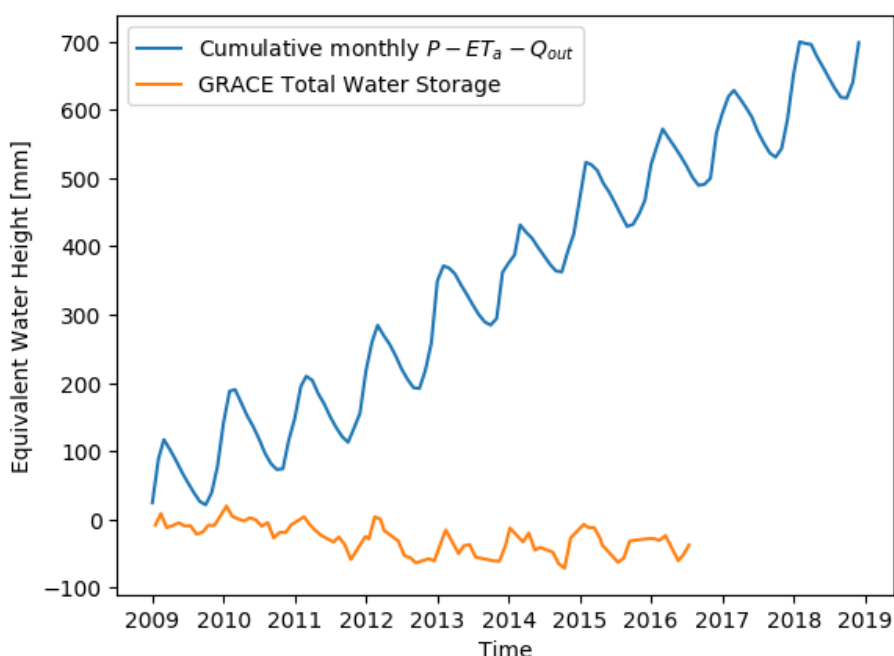


Figure 15: Cumulative monthly difference of WaPOR  $P - ET_a - Q_{out}$  and GRACE TWSA for Jordan River Basin.

Since groundwater flows data in Jordan River Basin from both in situ measurements and remote sensing or hydrogeological modelling are not well reported, the gap between computed  $P - ET_a - Q_{out}$  and GRACE TWSA can be used as a proxy of error in water balance derived from available datasets. This error can be due to uncertainty in WaPOR  $P$  and  $ET_a$ , total inter-basin transfers data, from unquantified groundwater flows and/or from GRACE TWSA solution. Two sub-catchments with available outlet discharge data was selected to assess the difference between WaPOR  $P - ET_a - Q_{out}$ . As can be seen in Figure 14, there was a huge difference between WaPOR  $P - ET_a - Q_{out}$  and the estimated total water storage change in both sub-catchments, especially from the hydrological year 2011, in terms of both trend and magnitude.

At the basin scale, Figure 15 shows the plot of cumulative storage based on GRACE data compared to WaPOR  $P - ET_a - Q_{out}$  in equivalent water height. On average, the error compared to GRACE TWSA change is 29.4% of total precipitation (Table 3). Based on results reported in the available literature regarding the water scarce conditions in the Jordan River Basin, this amount of excess precipitation is questionable. When compared to reported values, WaPOR  $ET_a$  over water bodies seems to be underestimated. Ultimately, this results in a significant error in water balance of the whole basin, since water bodies are the largest net water consumers in the Jordan River Basin (Table 2). Moreover, WaPOR  $P$  exceed in situ measurements at many locations adjacent to the Jordan River Basin (Figure 8 and Figure 9). Karimi and Bastiaanssen (2015) also reported that precipitation estimates from remote sensing have higher mean absolute error percentage (ranging from 0 to 70%) than actual evapotranspiration (ranging from 0 to 20%), which implies that overestimation of precipitation could be a source of error in water balance.

**Table 3:** Estimation of Error in Water Balance of Jordan River Basin based on GRACE Total Water Storage from 2010 to 2018.  $\Delta S$  from GRACE was calculated from the GRACE TWSA solution and  $\Delta S$  from Water Balance was calculated as  $P - ET_a - Q_{out}$ , where  $P$  and  $ET_a$  were aggregated from WaPOR data and  $Q_{out}$  was the outflow to the National Water Carrier.

	<b><math>\Delta S</math> from GRACE (mm<sup>3</sup>/year)</b>	<b><math>\Delta S</math> from Water Balance (mm<sup>3</sup>/year)</b>	<b><math>\Delta S</math> difference (mm<sup>3</sup>/year)</b>	<b>Error percentage (% Precipitation)</b>
<b>Year</b>				
2010	256	2,347	2,091	18.9
2011	-810	1,449	2,258	25.2
2012	-1,159	2,868	4,028	41.3
2013	22	3,883	3,861	34.1
2014	230	3,007	2,776	29.1
2015	36	3,020	2,984	27.9
<b>Average</b>	<b>-237</b>	<b>2,762</b>	<b>3,000</b>	<b>29.4</b>

The error in the water balance for the Jordan River Basin using WaPOR precipitation and evapotranspiration data is significant. Besides the WaPOR data there are other uncertainties in the data used, for example the storage change, which can be computed using different GRACE solutions, and the reliability of the observed outflow in the form of the inter-basin transfer through the National Water Carrier. The assumption that there are no other in- or outflows from the basin has also not been validated.

We therefore wanted to assess if other remote sensing products for precipitation and evapotranspiration were better able to close the water balance. In addition we evaluated four different GRACE solutions. For this purpose, the water balance of Jordan River Basin was computed using three precipitation, four evapotranspiration remote sensing products and four different GRACE solutions. These data provide forty-eight combination for computing the outflow from the basin and the change in storage in the basin. Performance of the different

combinations was evaluated in two ways. The first evaluation was by computing the coefficient of determination from the runoff generated using the water balance and the observed runoff in the form of inter-basin transfer. The second one is by computing the error in change in storage from the water balance computation and the change of storage estimated from GRACE solutions as percentage of the precipitation (similar to Table 3). The details of this analysis are presented in Annex XI.

The analyses show that though some combination of different products are better in reducing the gap, none of the product combinations were able to close the water balance. The gap for the best combination is 16% of the precipitation. Because the Jordan River basin receives low amount of precipitation, small errors in the data could lead to significant errors at basin scale. There is also a large variation between the products in being able to accurately represent the spatial variability. For example GLEAM has a much lower resolution compared to the other products and the  $P - ET_a$  comparison for the different land use classes does not show the variance as expected.

## 2.2.4. Conclusion

The preliminary data quality assessments shows that WaPOR 2.0 Level 2 data can be useful to map and show spatial patterns of net water generation and water consumption in the basin. In general, spatial variation of  $P$  and  $ET_a$  are consistent with the characteristics of the basin. However, when compared with the GRACE TWSA dataset, it appears that the absolute value aggregated from the WaPOR data might have errors up to 40% of total precipitation (Table 3). This error could be a consequence of uncertainty in  $P$  and  $ET_a$  estimates, and/or from unquantified groundwater flows and inter-basin transfers. In summary, the following aspects of the WaPOR datasets are highlighted:

Precipitation is often overestimated relative to available observations. However, the number of observation points is not sufficient for spatial bias correction (only 2 stations within the basin). Therefore, WaPOR precipitation maps were used without modification.

Evapotranspiration ( $ET$ ) is lower than Precipitation every year, more so for the large areas of bare soil, where more water is generated than the consumption via evapotranspiration. Evaporation over water bodies (Lake Tiberias) is also underestimated compared to information available from literature. Therefore in the following WA+ analysis, WaPOR  $ET$  reference will be used instead of WaPOR actual  $ET$  for water bodies.

Land cover maps from WaPOR include some essential Land cover classes (rainfed and irrigated croplands) but lack many Land and Water use classes in the current WA+ methodology. For example, WaPOR does not differentiate between natural and dammed water bodies and built-up areas of different sectors (residential, industry, greenhouses, etc.). In WaPOR, the differentiation between rainfed and irrigated croplands is based on a water deficit index, which does not necessarily replicate the actual irrigated crop area. Therefore, for this rapid assessment, land use maps with only four categories were derived and used in WA+ Sheet 1. For full WA+ sheets, more detailed land use maps will be required.

Error in Water balance: For the WaPOR-based Water Accounts of 2010-2018, the total storage change estimated from water balance will be used as GRACE data is not available for the whole period. However, the error estimated for years 2010-2015 should be kept in consideration when interpreting the rapid WA+ outputs. To improve the water accounts of the Jordan River Basin, it is highly recommended that groundwater flows are quantitatively estimated either by groundwater monitoring or modelling. It is also recommended that the quality of WaPOR  $P$  and  $ET_a$  data should be further validate and improved for this area.

## 2.3. WA+ methodology

The longer term planning process of water and environmental resources in river basins requires that a measurement – reporting – monitoring system is in place. The Water Accounting Plus (WA+) framework is based on the early WA work of Molden (1997) focussing on agriculture and irrigation systems. WA+ was further developed by Karimi (2014) and Karimi and Bastiaanssen (2015) for river basin analyses to incorporate all water use sectors. Further developments include more hydrological and water management processes and focus on specific land uses.

A key element of WA is that it separates ET into rainfall ( $ET_{rain}$ ) and incremental ET (ETinc), thereby clearly identifying managed water flows. WA+ includes the hydrology of natural watersheds that provide the mains generation of water in streams and aquifers, as well as quantifying water consumption. The current study utilises the WaPOR v2.0 Level 2 data (100 m resolution) for the analyses. As such, it provides a rapid WaPOR-based water accounting framework.

The output of WA+ is presented a number of sheets and supporting spatial maps. Remote sensing, GIS and spatial models form the core methodology, so all data has a spatial context. The accounts are reported on an annual basis, as WA+ is meant for longer term planning. Software tools have been developed that automatically collect and download data from WaPOR database as well as for the calculations. The models and scripts for the creation of the water accounts and the elaboration of the reports are available on GitHub under the Water Accounting account . The WA+ framework is public and open for all users.

Figure 16 shows the flow chart of the rapid WA+ process and the data used, where  $ET_a$  is Evapotranspiration,  $P$  is Precipitation,  $I$  is Interception, TWS is Total Water Storage, LUWA is WA+ Land Use maps,  $ET_{incr}$  is ET incremental,  $ET_{rain}$  is ET from rainfall. L1\_PCP\_E, L1\_PCP\_M, L1\_RET\_M, L2\_I\_M and L2\_AETI\_M are WaPOR data cubes (Level 1 daily and monthly precipitation, monthly reference evapotranspiration, Level 2 monthly actual evapotranspiration and interception respectively). The rapid WA+ mainly uses WaPOR data such as the level 1 monthly precipitation and level 2 annual time series of land cover classification, interception and actual evapotranspiration and interception. Based on the preliminary assessment, WaPOR  $ET_a$  is replaced with ET reference (Annex VI) for water bodies to reduce the error in  $ET_a$  estimation. External data sources used include GRACE satellite data for estimating the change in storage in the basin, Global Reservoir and Dam Database (GRanD) to identify dam locations and extents, the World Database on Protected Areas to identify the protected land uses, and the map of top soil saturated water content (de Boer, 2016).

### 2.3.1. WA+ Land Use categorization

The WaPOR land cover map forms the basis for dividing the basin landscape into the four main categories (PLU, ULU, MLU, and MWU). Four main categories of land and water uses are distinguished:

- **Protected Land Use (PLU);** areas that have a special nature status and are protected by National Governments or Internationals NGO's
- **Utilized Land Use (ULU);** areas that have a light utilization with a minimum anthropogenic influence. The water flow is essentially natural
- **Modified Land Use (MLU);** areas where the land use has been modified. Water is not diverted but

land use affects all unsaturated zone physical process such as infiltration, storage, percolation and water uptake by roots; this affects the vertical soil water balance

- **Managed Water Use (MWU)**; areas where water flows are regulated by humans via irrigation canals, pumps, hydraulic structures, utilities, drainage systems, ponds etc.

The underlying reason for framing these four land use categories is that their management options widely differ from keeping them pristine to planning hourly water flows.

The land use categories map (Figure 17) is based on the land cover layer (LCC) from WaPOR database, but needed to be reclassified into the Water Accounting classes. Protected Land Use (PLU) class was updated using the protected area profile from the World Database on Protected Areas (UNEP-WCMC, 2019a, 2019b, 2019c, 2019d). The areas which are designated as IUCN categories I and II are reclassified as PLU. The Managed Water Use class was reclassified from the ‘Cropland, irrigated or under water management’ and ‘Built-up’ classes in WaPOR LCC layer and updated with the area of constructed reservoirs from the Global Reservoir and Dam Database (GRanD) (Lehner et al., 2011). WaPOR Water bodies class except for natural lakes were also reclassified as Managed Water Use class to include irrigation and evaporation ponds. The Modified Land Use was reclassified from the class ‘Cropland, fallow’ and ‘Cropland, rainfed’ in the WaPOR LCC layer. Thereafter, the rest of the area was reclassified as Utilized Land Use class.

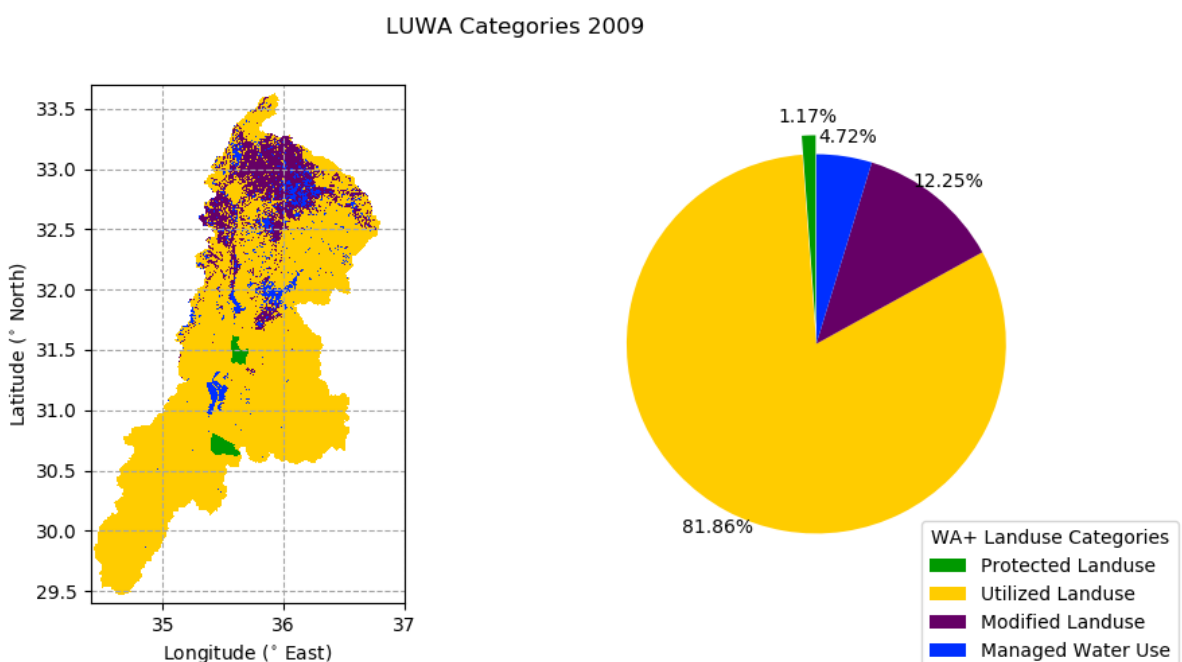


Figure 17: WA+ Land Use category map of Jordan River Basin in 2009 based on WaPOR Level 2 Land cover (LCC) layers and global dataset of protected area and reservoirs. Maps of the individual years are provided in Annex V.

### 2.3.2. Pixel scale analysis – Monthly soil moisture balance

#### 2.3.2.1. Method

The water accounting framework distinguishes between a vertical and horizontal water balance. A vertical water balance is made for the unsaturated root zone of every pixel and describes the exchanges between land and atmosphere (i.e. precipitation and evapotranspiration) as well as the partitioning into infiltration and surface runoff. Percolation and water supply are also computed for every pixel, to facilitate attributing water supply and consumption to each land use class.

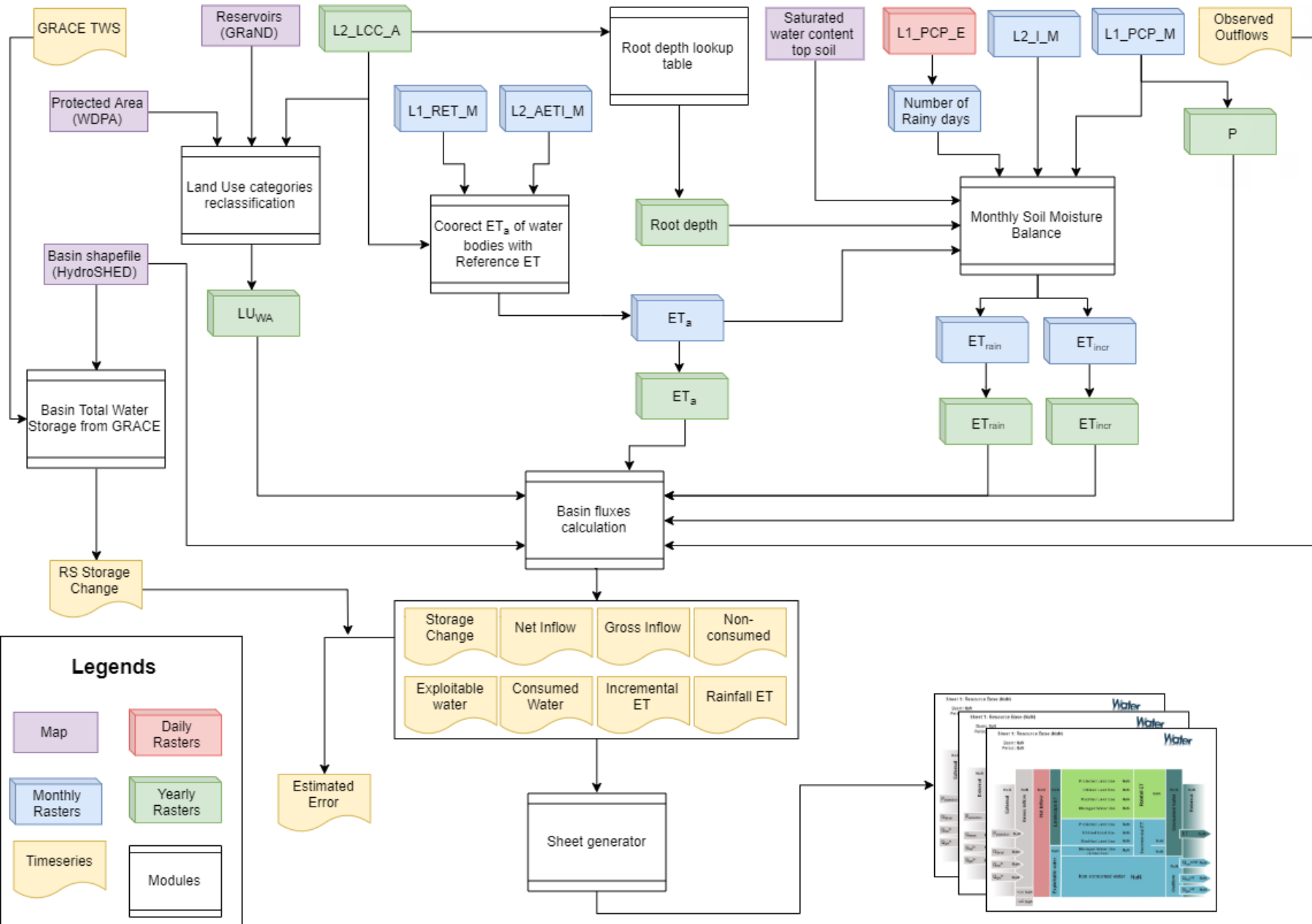


Figure 16: Flowchart of steps in WaPOR-based WA+ process

The WaterPix model calculates for each pixel the vertical soil water balance (See Figure 18 and described below). Rainfall ET ( $ET_{rain}$ ) and incremental ET ( $ET_{incr}$ ) are separated by keeping track of the soil moisture balance and determining if ET is satisfied only from precipitation or stored in the soil moisture or additional source (supply) is required. The main inputs into WaterPix are provided in Table 4 and the outputs are provided in Table 5. Each parameter is calculated at the model resolution of 100m and available for monthly and annual time steps.

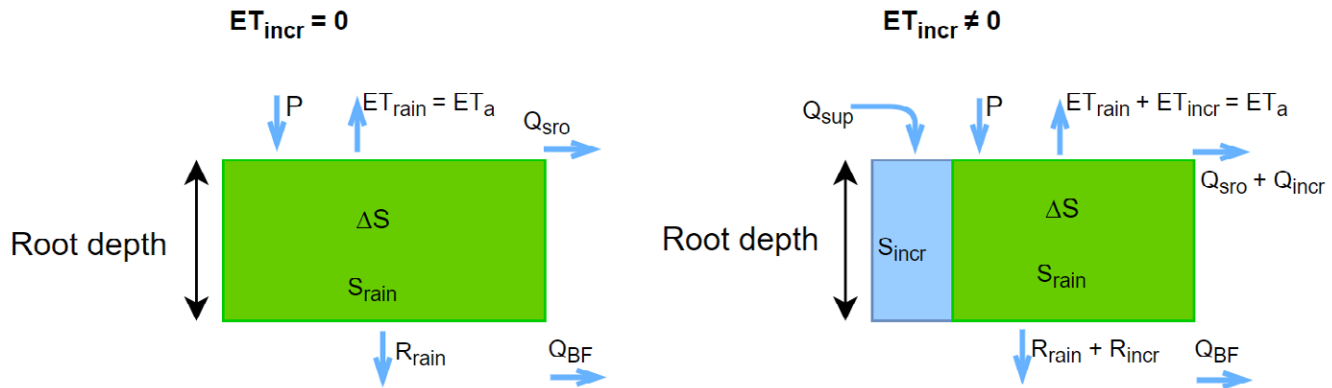


Figure 18: Main schematization of the flows and fluxes in the WaterPix model

**Table 4:** Inputs of WaterPix

Variable	Parameter	Source	Spatial Resolution	Temporal resolution
Precipitation	P	WaPOR	5,000 m	Daily
Actual Evapotranspiration	$ET_a$	WaPOR	100 m	Monthly
Interception	I	WaPOR	100m	Monthly
Land cover map	LULC	WaPOR	100 m	Yearly
Saturated Water Content		HiHydroSoil	0.008333 degree (about 900m at the equator)	Static

**Table 5:** Outputs of the water balance model at pixel level

Variable	Calculation step	Definition
S	1	Soil Moisture
$Q_{sro}$	1,4	Surface Runoff
R	1,4	Recharge
ET	2	ET
$Q_{sup}$	3	Supply

### Step 1: Compute soil moisture

The soil moisture ( $S_{rain,t}$ ) is computed as the soil moisture storage at the end of the previous timestep ( $S_{rain,t-1}$ ) plus the effective precipitation ( $P - I$ ) minus recharge ( $R_{rain}$ ) and surface runoff ( $Q_s$ ) (eq 1):

$$S_{rain,t} = S_{rain,t-1} + P - I - R_{rain} - Q_{sro,rain} \quad (\text{eq 1})$$

Where the surface runoff ( $Q_{sro,rain}$ ) is calculated using an adjusted version of the Soil Conservation Service runoff method. The adjusted version replaces the classical Curve Numbers by a dynamic soil moisture defi-

cit term that better reflects the dry and wet season infiltration versus runoff behaviour (see Schaake et al., 1996; Choudhury & DiGirolamo, 1998). As the Curve Number method is developed for event based runoff, we calculated  $Q_{sro,rain}$  on daily basis, dividing the effective precipitation by the number of rainy days (n) and a calibration parameter to account for the soil moisture variation due to drying up and filling with in a month. The total surface runoff for a month is then multiplied by n:

$$Q_{sro,rain} = \begin{cases} 0 \text{ if } P = 0 \\ \frac{\left( \frac{P-I}{n} \right)^2}{\frac{P-I}{n} + f(S_{sat} - S_{rain,t-1})} * n \text{ if } P \neq 0 \end{cases}$$

Where the saturated soil moisture ( $S_{sat}$ ) is calculated by multiplying the Saturated Water Content ( $\theta_{SAT}$ ) by the effective root depth (RD) for each land cover class estimated based on the effective root depth by Yang et al. (2016) (Table 6).

**Table 6:** Root depth look-up table. The values of root depth for each land cover class is based on study by Yang et al. (2016)

WaPOR Land cover class	Root depth (mm)
Shrubland	370
Grassland	510
Cropland, rainfed	550
Cropland, irrigated or under water management	550
Fallow cropland	550
Built-up	370
Bare/sparse vegetation	370
Permanent snow/ice	0
Water bodies	0
Temporary water bodies	0
Shrub or herbaceous cover, flooded	0
Tree cover: closed, evergreen needle-leaved	1,800
Tree cover: closed, evergreen broad-leaved	3,140
Tree cover: closed, deciduous broad-leaved	1,070
Tree cover: closed, mixed type	2,000
Tree cover: closed, unknown type	2,000
Tree cover: open, evergreen needle-leaved	1,800
Tree cover: open, evergreen broad-leaved	3,140
Tree cover: open, deciduous needle-leaved	1,070
Tree cover: open, deciduous broad-leaved	1,070
Tree cover: open, mixed type	2,000
Tree cover: open, unknown type	2,000
Seawater	0

## Step 2: Separate $ET_a$ into $ET_{rain}$ and $ET_{incr}$ and update S

To compute the precipitation and incremental component of ET,  $ET_a$  is subtracted from  $S_{rain,t}$ . When  $S_{rain}$ , this is insufficient for  $ET_a$ , the difference will be supplied by surface or groundwater uptake. The rainfall ET ( $ET_{rain}$ ) becomes the amount which can be supplied by the soil moisture, whereas the difference will become incremental ET ( $ET_{incr}$ ):

$$ET_{rain} = \text{if } (S_{rain,av} > ET_a, ET_a, S_{rain,av})$$

$$ET_{incr} = ET_a - ET_{rain}$$

The new soil moisture storage then becomes:

$$S_{rain,t} = S_{rain,av} - ET_{rain}$$

## Step 3: Estimation of Water Supply

The amount of water supplied to each pixel is a function of  $ET_{incr}$  and the so called consumed fraction (fc):

$$Q_{sup} = f(ET_{incr}, LU) = \frac{ET_{incr}}{f_c}$$

fc is dependent on the land use class and was suggested to replace the classical irrigation efficiencies (Molden, 1997; Simons et al., 2016). The consumed fractions applied in this study are specified in Table 7.

**Table 7:** Consumed fraction per land use class

Land use class	Consumed fraction ( $f_c$ )
Natural land use classes	1.00
Rainfed crops	1.00
Irrigated crops	0.80

## Step 4: Estimating incremental soil moisture

A separate soil moisture storage (blue area in Figure 18) is added to store  $Q_{sup}$  and calculate incremental recharge and runoff as follows:

$$S_{incr,t} = S_{incr,t-1} + Q_{supply} - ET_{incr} - R_{incr} - Q_{sro,incr}$$

And total soil moisture storage (St) becomes:

$$S_t = S_{rain,t} + S_{incr,t}$$

Then total recharge ( $R_t$ ) is calculated as exponential function of the soil moisture. If the soil moisture is above a certain percentage (calibration parameter) of the saturated content, the percolation will be computed using the following simple exponential function:

$$R_t = S_t * \exp\left(-\frac{1}{S_t}\right)$$

And the incremental recharge ( $R_{incr}$ ) and the recharge from rainfall ( $R_{rain}$ ) are computed as proportions of the incremental and rain soil moisture values.

The surface runoff is updated to account the increase due to incremental surface runoff from the supply

$$Q_{sro,rain} = \begin{cases} 0 & \text{if } P = 0 \\ \frac{\left(\frac{P+Q_{sup}-I}{n}\right)^2}{\frac{P+Q_{sup}-I}{n} + f(S_{sat} - (S_{rain,t} + S_{incr}))} * n & \text{if } P \neq 0 \text{ or } Q_{sup} \neq 0 \end{cases}$$

The incremental surface runoff ( $Q_{sro,incr}$ ) is then computed as:

$$Q_{sro,incr} = Q_{sro,tot} - Q_{sro,rain}$$

### 2.3.2.2. Results

The maps of estimated annual  $ET_{rain}$  and  $ET_{incr}$  averaged over the study period are shown in Figure 19. The upstream area has high  $ET_{rain}$  while water bodies, irrigated cropland show high  $ET_{incr}$ , and are aligned with the  $P-ET_a$  maps. In most areas of bare land and grassland,  $ET_{rain}$  and  $ET_{incr}$  are of the same range. Figure 20 describes the partition of  $ET_{rain}$  and  $ET_{incr}$  of each land cover class and the ratio of each component relative to total precipitation.  $ET_{incr}$  over water bodies is about 10 times total precipitation.  $ET_{incr}$  of irrigated cropland is 103% of total precipitation (Figure 20), which shows that supplied blue water is an important source for these crop areas.  $ET_{rain}$  in tree cover classes, which includes interception is estimated to be about 70% to 80% of total precipitation (Figure 20), which means 20 to 30 % percolates or forms runoff. The mean annual  $ET_a$  of the bare/sparse vegetation land cover class is only 23% of the total precipitation it receives, with more than 80% of that is  $ET_{rain}$ .

### 2.3.3. WaPOR-based WA+ Sheet 1: Resource Base

The WA+ sheet 1 Resource Base provides an overview of the water resources and its current utilisation per different land use categories. The rapid WaPOR-based WA+ approach estimates gross inflow, precipitation and incremental evapotranspiration for each of the WA+ land use categories. Therefore, it provides an overview of the current utilisation of precipitation for each land use for the study period. Details of how each flux in the WA+ Sheet 1 was estimated is given in Table 8.

Based on the WA+ sheet 1, a number of key performance indicators, which were developed by Dost et al. (2013) in consultation with the Land and Water Division of FAO, can be calculated to describe the entire system. These indicators help the basin planners to understand the key information on water management in the basin (Karimi, 2014).

The first set of indicators can be related to the Resource Base Sheet:

- ET Fraction = 
$$\frac{ET_{tot}}{(P+Q_{in})}$$

ET fraction indicates which portion of the total inflow of water is consumed and which part is converted into renewable resources. A value higher than 100% indicates over-exploitation or a dependency on external resources.

- Stationarity Index = 
$$\frac{\Delta Storage}{ET_{tot}} \quad (\%)$$

Stationarity Index is an indication of the depletion of water resources. Positive values indicate that water is added to the groundwater and/or surface water storage. Negative values indicate a depletion of the storage.

- Basin Closure = 
$$\frac{1 - \text{outflow}}{(P+Q_{in})} \quad (\%)$$

Basin Closure defines the percentage of total available water resources (Precipitation + basin inflow) that is consumed and/or stored within the basin. A value of 100% indicates that all available water is consumed and/or stored in the basin.

The second set of indicators focuses on the actual amount of water that is currently managed, or is available to be managed:

- Available Water (AW) = Gross Inflow – Landscape ET – Reserved flow ( $\text{km}^3/\text{year}$ )

Total amount of water that is available to be managed.

- Managed Water (MW) = Incremental ET of Managed Water Use ( $\text{km}^3/\text{year}$ )

Total amount of water that is abstracted for Managed Water Use.

- Managed Fraction = 
$$\frac{\text{Managed water}}{\text{Available water}} \quad (\%)$$

Percentage of water that is actually managed from the total amount of water that is available.

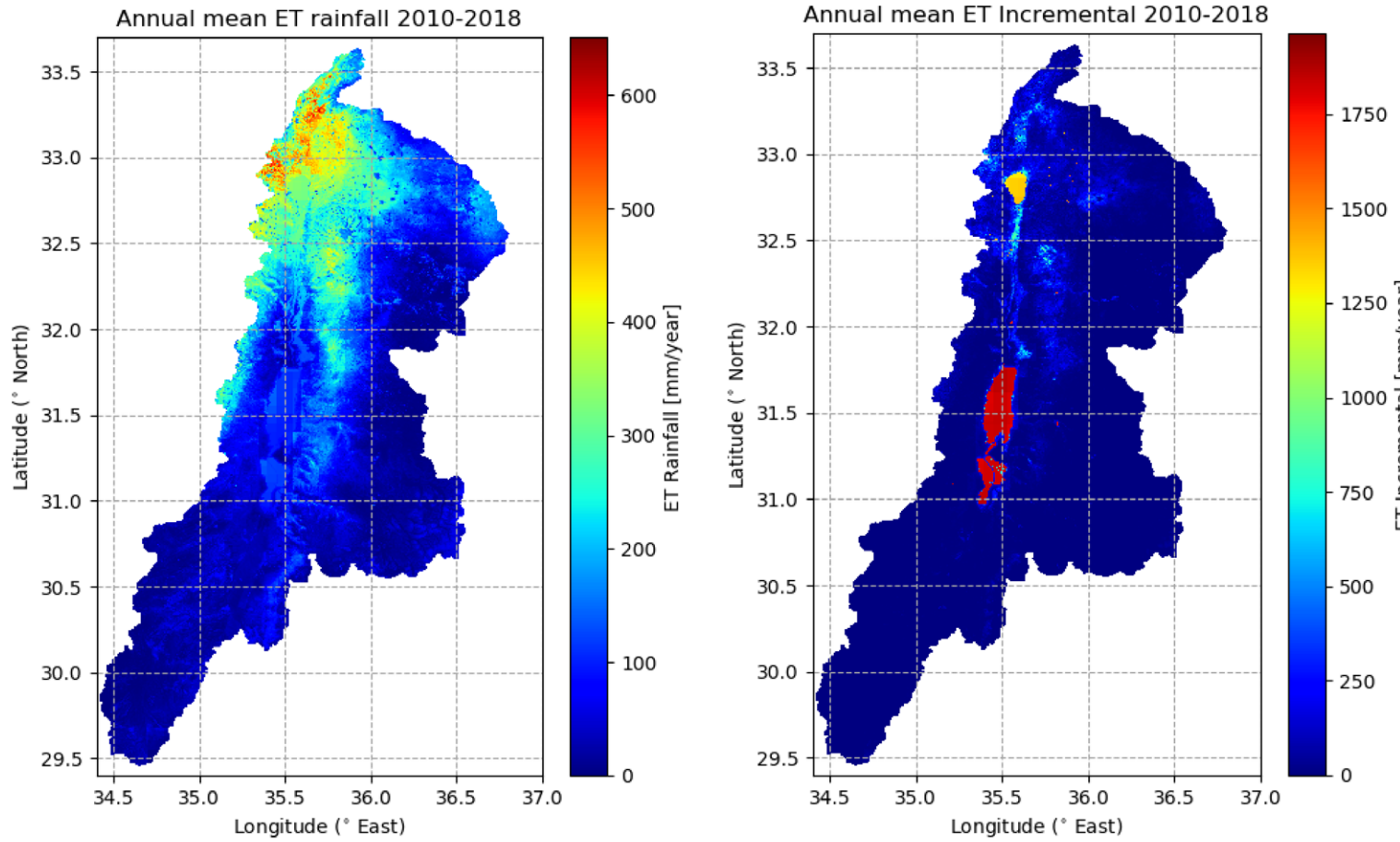


Figure 19: The yearly average map of  $ET_{rain}$  and  $ET_{incr}$  estimated from WaPOR data in Jordan River Basin of hydrological years from 2010 to 2018. Maps of the individual years are provided in Annex VII and Annex VIII

**Sheet 1: Resource Base**

Basin: Jordan

Period: 2010-2018

Unit: km<sup>3</sup>/year (cubic kilometers per year)

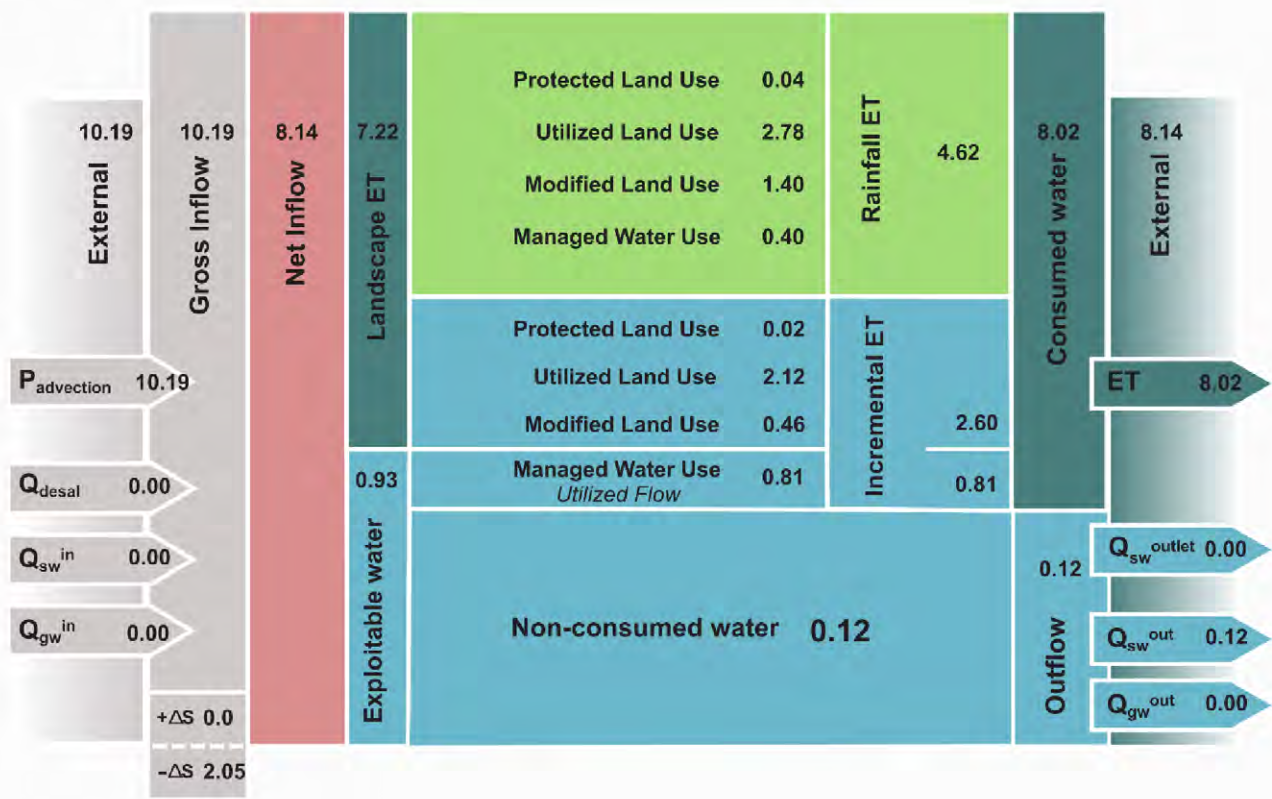


Figure 21: The WA+ Sheet 1 of Jordan River Basin with average values of hydrological years from 2010 to 2018

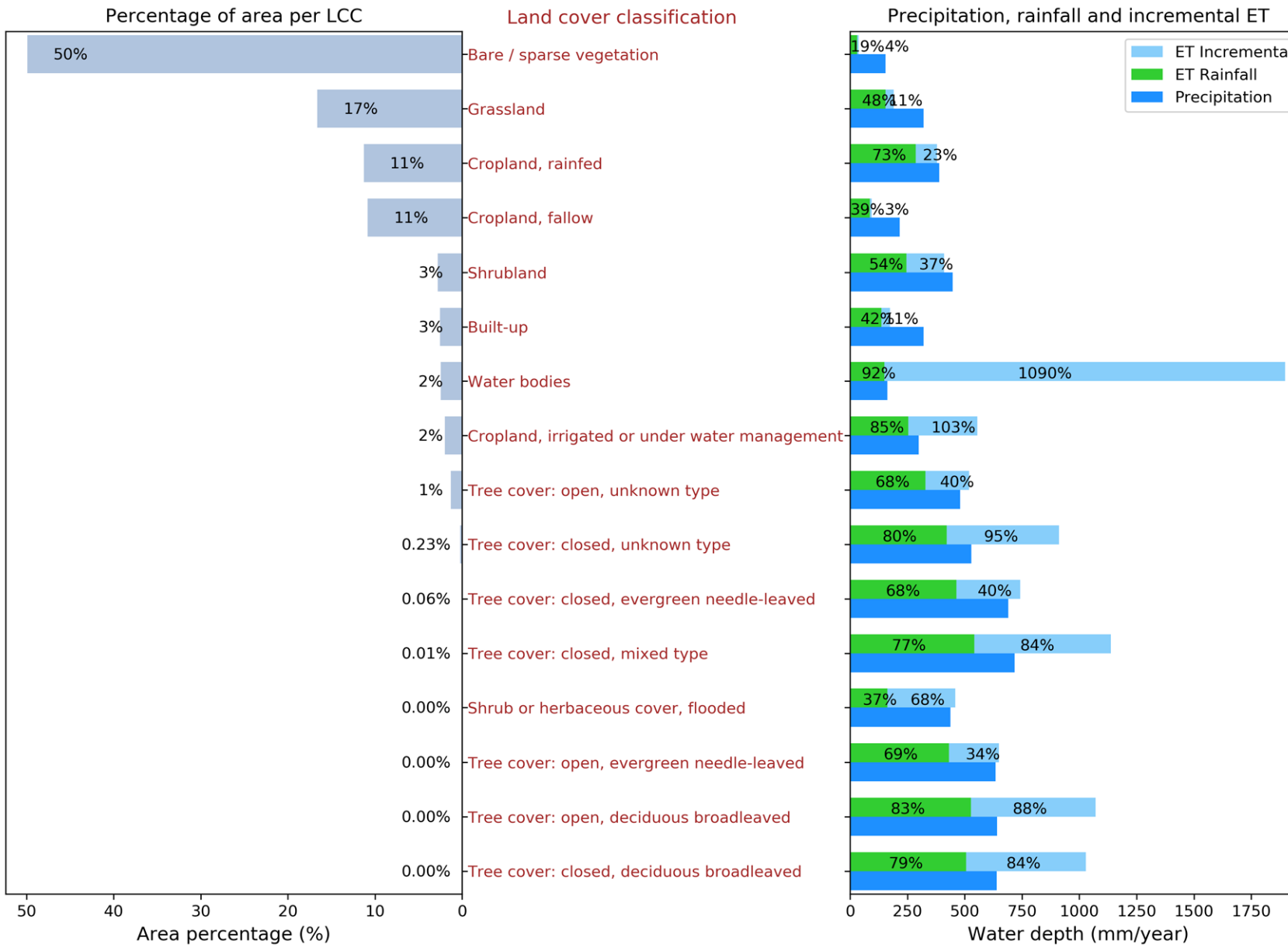


Figure 20: The area percentage (left) and yearly average Precipitation,  $ET_{rain}$  and  $ET_{incr}$ , (right) of each land cover class for the hydrological years 2010-2018. The percentages in the right indicate the proportion of  $ET_{rain}$  and  $ET_{incr}$  to Precipitation

### 3. Water Accounting+ Results

#### 3.1. WA+ Sheet 1: Resource Base

Figure 21 shows the summary of water resources in the Jordan River Basin of the WA+ framework for Sheet 1 only and depicts average values for the 2010-2018 hydrological years (Annex VIII shows the WA+ sheet 1 for the individual years). The gross inflow is  $10.19 \text{ km}^3/\text{year}$  and the total outflow and consumed water is  $8.02 \text{ km}^3/\text{year}$ , which results in  $2.05 \text{ km}^3/\text{year}$  remaining as total water storage change. The basin has no natural outlet, however, surface water that is transferred out of basin through canals and tunnels accounts for about  $0.12 \text{ km}^3/\text{year}$  on average. The utilized land use has the highest water consumption ( $2.78 \text{ km}^3/\text{year}$  from  $ET_{rain}$  and  $2.12 \text{ km}^3/\text{year}$   $ET_{incr}$ ). Protected land use consumes the least water ( $0.06 \text{ km}^3/\text{year}$ ). The modified land use category consumes about  $1.86 \text{ km}^3/\text{year}$  with about 75% from  $ET_{rain}$ . The managed water use category water consumption is mainly  $ET_{incr}$  (67%).

The variation of the main fluxes in these sheets is shown in Figure 22 and Figure 23. Overall, the proportion of each component compared to gross inflow is stable over the study period. Landscape ET, which is sum of  $ET_{rain}$  and  $ET_{incr}$  of non-managed water use, is the largest component. Surface water outflow ( $Q_{sw}^{out}$ ) or inter-basin transfer is relatively small.

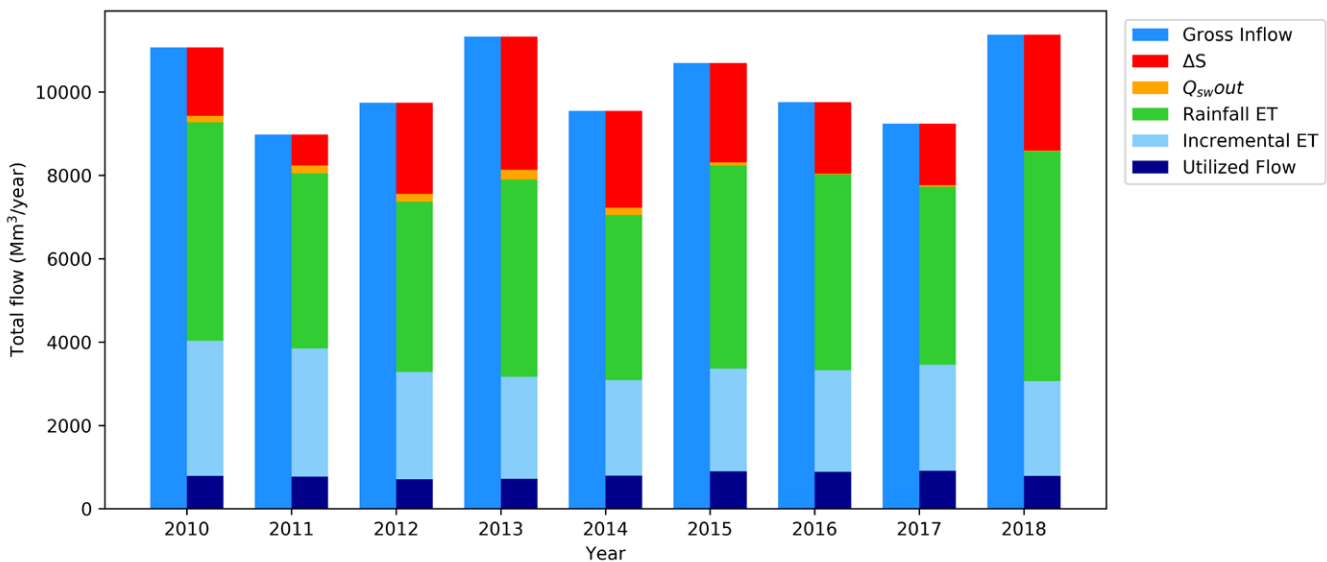


Figure 22: Yearly variability of Sheet 1 fluxes. Total storage change ( $\Delta S$ ) was estimated as the difference  $P - ET_a - Q_{sw}^{out}$  to close the water balance.  $ET_a$  in water bodies was corrected using WaPOR ET reference.

**Table 8:** Data and estimation methods used for fluxes in WA+ Sheet 1. N/A stands for Not Available.

WA+ Sheet 1 Flux	Description	Data used	Calculation approach
$P_{advection}$	Precipitation	WaPOR's L1_PCP_M	Aggregate by hydrological year
$Q_{desal}$	The inflow from desalinated water	N/A	-
$Q_{sw}^{in}$	The inflow from surface water (i.e. interbasin surface water inflow)	N/A	-
$Q_{gw}^{in}$	The inflow from groundwater (i.e. interbasin groundwater inflow)	N/A	-
Gross Inflow	Total inflow from all sources	-	$P_{advection} + Q_{desal} + Q_{sw}^{in} + Q_{gw}^{in}$
Net Inflow	The gross inflow and the storage change	-	Consumed water + Outflow
$\Delta S$	Change in total water storage	-	Net Inflow – Gross Inflow
Rainfall ET - PLU - ULU - MLU - MWU	ET that occurs from effective precipitation and canopy interception. Effective precipitation is the part of the rain water that does not percolate below the root zone, flows away over the soil surface as run-off, or evaporates from canopy interception, thus, available in the root zone and can be used by the plants.	WaPOR-derived ET rainfall; WA+ Landuse maps	Aggregate by hydrological year and LU classes
Incremental ET - PLU - ULU - MLU - MWU	ET that occurs from other sources except effective precipitation and interception. For example, evaporation of irrigation water, evaporation of groundwater through deep rooted vegetation, water evaporation from a lake or other water surface that exceeds the precipitation on the water body itself.	WaPOR-derived ET incremental; WA+ Landuse maps	Aggregate by hydrological year and LU classes
Landscape ET	ET that occurs naturally, not due to water management (i.e. evaporation on natural land cover classes, rainfall ET from Managed Water Use).	-	Rainfall ET + Total Incremental ET of PLU, ULU, MLU
Consumed water/ ET	ET occurs as interception, evaporation, soil evaporation, water evaporation, canopy transpiration/ The total Evapotranspiration is evapotranspiration from non-manageable, manageable and managed land uses.	WaPOR's L2_AETI_M	Aggregate by hydrological year
Utilized flow	ET from managed water use (i.e. irrigated crops, managed reservoirs)	-	MWU Incremental ET
Exploitable water	The net inflow minus Landscape ET	-	Utilized flow + Outflow
$Q_{sw}^{outlet}$	The river outflow at the outlet of the basin	N/A	o.o (Endorheic basin)
$Q_{sw}^{out}$	The outflow as surface water (i.e. interbasin surface water outflow)	NWC's monthly flow records	Aggregate by hydrological year
$Q_{gw}^{out}$	The outflow as groundwater (i.e. interbasin groundwater outflow)	N/A	-
Non-consumed water/ Outflow	Total outflow	-	$Q_{sw}^{outlet} + Q_{sw}^{out} + Q_{gw}^{out}$

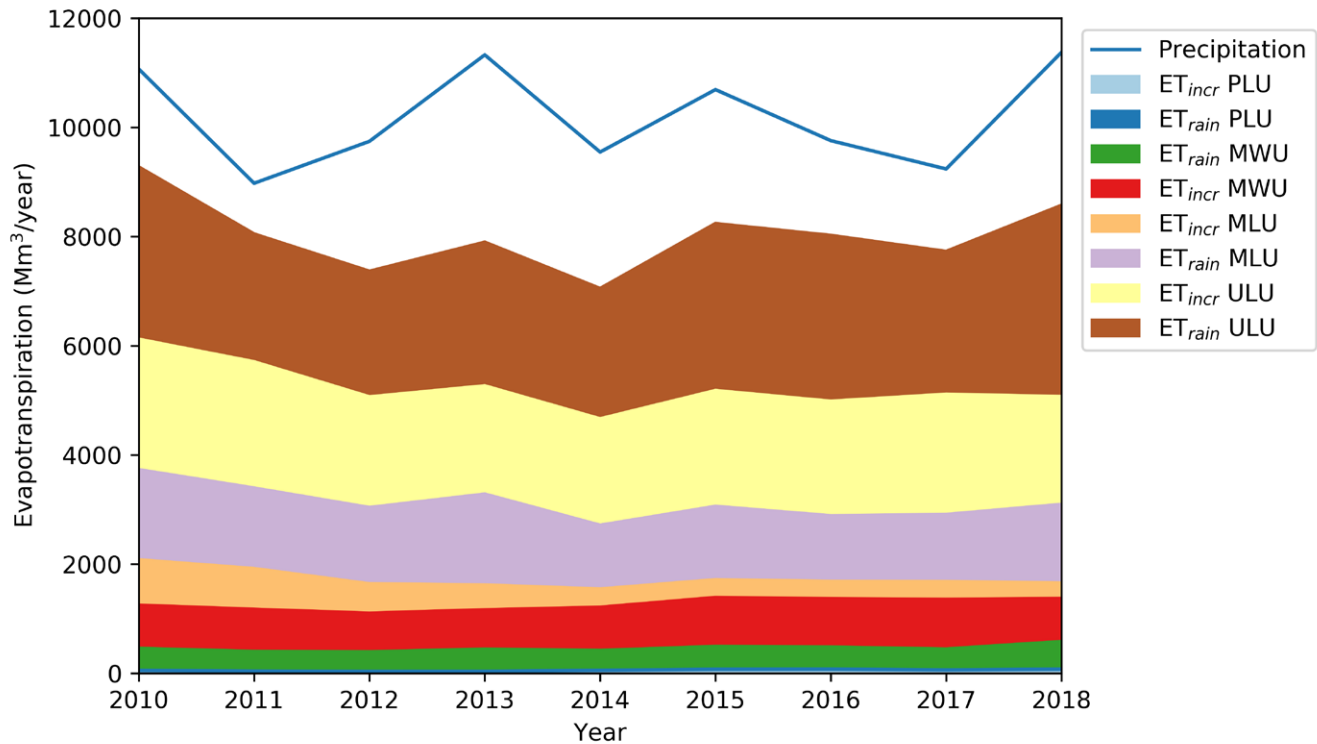


Figure 23: Variability of rainfall ET and incremental ET in Jordan River Basin from 2010 to 2018

### 3.2. WA+ Key indicators

The key performance indicators are presented in Table 9. From 2010 to 2018, the average ET fraction of the Jordan River Basin is ranging from 69.7 to 89.6 %, which indicates that not all precipitation is consumed. The excess precipitation is either contribute to increase storage and/or generate outflow from the basin. Since the Jordan River Basin has no outlet except for the inter-basin transfer in the NWC, this surplus water was added to the groundwater storage. Therefore, the estimated average stationarity index is 25.8%. Based on the preliminary assessments, this index value might be overestimated due to errors in the WaPOR data, unaccounted groundwater outflows and/or inter-basin transfers.

The average basin closure index is 98.8%, which shows that almost all water resources is consumed and/or stored in the basin. About 1.2% of the gross inflow become outflow through the Israel's National Water Carrier. The average available water is 2.98 km<sup>3</sup>/year, out of which approximately 28.9% is currently managed. The Managed Water, which is  $ET_{incr}$  of Managed Water Use is on average 0.81 km<sup>3</sup>/year, which is 87% of the total exploitable water. Managed Water Use includes irrigated crops, dammed water bodies, built-up area, and evaporation ponds. Among these, irrigated crops  $ET_{incr}$  consumed 31.5% of total managed water (Table 10) which shows the importance of agriculture development in managed water.  $ET_{incr}$  for irrigated crops therefore accounts for 28% of exploitable water.

The difference between the water storage changes derived from WaPOR-based WA+ and GRACE TWSA is 2.3 km<sup>3</sup>/year on average (Table 11), which is 23% of the mean annual precipitation. Compared to Table 3, the difference magnitude was reduced by 6% of mean annual precipitation thanks to the correction of actual evapotranspiration on water bodies with reference ET. This difference was used as a proxy of error in water balance derived from WaPOR data, which indicates that the estimated available water is unreliable, thus, the safe caps of water withdrawals for the agricultural sector could not be determined with any confidence. Moreover, this error in storage change derived from water balance significantly influenced the results of stationarity index, basin

**Table 9:** WA+ Sheet 1 key indicators of Jordan River Basin for the hydrological years from 2010 to 2018 based on water balance derived from WaPOR datasets.

	ET fraction	Stationarity index	Basin Closure	Available water	Managed water	Managed fraction
Year	(%)	(%)	(%)	(km <sup>3</sup> /year)	(km <sup>3</sup> /year)	(%)
2010	83.8	17.7	98.6	2.58	0.79	30.5
2011	89.6	9.2	97.9	1.70	0.77	45.4
2012	75.6	29.7	98.1	3.09	0.71	22.9
2013	69.7	40.4	97.9	4.15	0.72	17.3
2014	73.8	33.0	98.2	3.29	0.79	24.0
2015	77.1	28.9	99.3	3.35	0.90	26.7
2016	82.2	21.4	99.8	2.62	0.88	33.7
2017	83.7	19.1	99.6	2.42	0.91	37.6
2018	75.4	32.4	99.8	3.59	0.79	21.9
<b>Average</b>	<b>79.0</b>	<b>25.8</b>	<b>98.8</b>	<b>2.98</b>	<b>0.81</b>	<b>28.9</b>

**Table 10:** Contribution of irrigated crop's  $ET_{incr}$  to Managed Water

	ET <sub>incr</sub> of irrigated crops	Managed water	ET <sub>incr</sub> of irrigated crops/Managed water
Year	(km <sup>3</sup> /year)	(km <sup>3</sup> /year)	(%)
2010	0.22	0.79	27.4
2011	0.20	0.77	26.1
2012	0.18	0.71	24.9
2013	0.18	0.72	25.2
2014	0.24	0.79	30.8
2015	0.34	0.90	37.9
2016	0.33	0.88	37.6
2017	0.35	0.91	38.1
2018	0.28	0.79	35.9
<b>Average</b>	<b>0.26</b>	<b>0.81</b>	<b>31.6</b>

A part of the available water amount can be contaminated by anthropogenic pollution loads to the extent that exceeds the basin's assimilation capacity. The water pollution level of the Jordan River Basin related to anthropogenic Nitrogen and Phosphorus loads from diffuse and point sources from 2002 to 2010 was estimated to be 5.5 (Mekonnen and Hoekstra, 2015) and more than 10 (Mekonnen and Hoekstra, 2018) respectively. In these studies, the water pollution levels were calculated as the ratio of Gray Water Footprint over the annual actual runoff of the basin. These values indicate that it would take more than 10 times of actual runoff of the basin to dilute the pollution related to anthropogenic Nitrogen and Phosphorus loads. As a result, the estimated available water might not be suitable for some uses (irrigation, drinking water, etc.). It should be noted that the uncertainty range of the global GWF is of -33% to +60% (Mekonnen and Hoekstra, 2015).

**Table 11:** Estimation of Error in WaPOR-based WA+ of Jordan River Basin based on GRACE Total Water Storage from 2010 to 2015\*.

	<b>ΔS from GRACE</b> (mm <sup>3</sup> /year)	<b>ΔS from WaPOR-based WA+</b> (mm <sup>3</sup> /year)	<b>ΔS difference</b> (mm <sup>3</sup> /year)	<b>Error percentage</b> (%Precipitation)
<b>Year</b>				
2010	256	1,642	1,386	13
2011	-810	740	1,550	17
2012	-1,159	2,191	3,350	34
2013	22	3,192	3,170	28
2014	230	2,326	2,096	22
2015	36	2,382	2,346	22
<b>Average</b>	<b>-237</b>	<b>2,079</b>	<b>2,316</b>	<b>23</b>

\*ΔS from GRACE was calculated from the GRACE TWSA solution and ΔS from Water Balance was calculated as  $P - ET_a - Q_{out}$ , where  $P$  and  $ET_a$  were aggregated from monthly WaPOR data and  $Q_{out}$  was the outflow to the National Water Carrier.  $ET_a$  in water bodies was corrected using WaPOR ET reference.

## 4. Conclusions

The rapid water accounts are valuable in terms of demonstrating the suitability of the WaPOR datasets for applying the WA+ framework and closing the water balance. The results of this study highlights that the WaPOR datasets can provide a spatial overview of where in the basin water is generated and consumed via ET, the largest water sink in the Jordan River Basin. The WaPOR  $P - ET_a$  analysis showed that, on average, the whole Jordan River Basin is a net water generator as precipitation is always higher than total evapotranspiration for the study period 2010-2018. The largest water consumers in the basin are water bodies and irrigated crops. Bare land class (50% of the basin area) shows the highest contribution to water availability and an unrealistic runoff coefficient of 77%. Overall, the water balance analysis showed a large discrepancy in total storage change estimated from WaPOR and NWC data from the GRACE TWSA solution. Although there is high uncertainty in the measurements of the interbasin transfer and GRACE TWSA, the trend in GRACE TWSA is in line with the current water scarce conditions in the basin (e.g. a decline in the Dead Sea level and groundwater aquifer). This observation is not in-line with the quality assessment report of the WaPOR v1.0 data (FAO and IHE Delft, 2019), which shows very high correlation at basin level between WaPOR  $ET_a$  and  $P - Q$  in various river basins in Africa. The arid conditions of the Jordan River Basin were not included in the analyses, and the results of this study showing significant surplus at basin level should be further investigated.

The main weakness of this study is lack of data for several fluxes that cannot be obtained from remote sensing data. For a basin such as this, where the water balance is highly influenced by interbasin transfer activities, and groundwater depletion like the Jordan River Basin, the simplified water balance ( $P - ET - \Delta S = Q_{out}$ ) cannot be closed in absence of this information. The WA+ results of the study, therefore, cannot be used to estimate the safe caps of water withdrawals in the basin as the error of the WaPOR water balance is in the same range as the estimated available water. For a detailed water accounts, more information of groundwater, interbasin transfer, utilized and return flows is needed. At the moment, these data cannot be directly derived from remote sensing, thus, in situ measurements still play important roles in the water accounts. In case these data are not available, assimilation of available data with comprehensive hydrological modelling results are recommended.



# References

- Abu-Sharar, T.M., Battikhi, A.M. 2002.** Water Resources Management under Competitive Sectoral Demand A Case Study from Jordan. *Water International*. 27, 364–378. <https://doi.org/10.1080/02508060208687016>
- Al-Kharabsheh, A., Ta'any, R. 2005.** Challenges of Water Demand Management in Jordan. *Water International*. 30, 210–219. <https://doi.org/10.1080/02508060508691861>
- Al-Omari, A., Al-Quraan, S., Al-Salihi, A., Abdulla, F. 2009.** A Water Management Support System for Amman Zarqa Basin in Jordan. *Water Resources Management*. 23, 3165. <https://doi.org/10.1007/s11269-009-9428-z>
- Bastiaanssen, W.G.M., Karimi, P., Rebelo, L.-M., Duan, Z., Senay, G., Muthuwatte, L., Smakhtin, V. 2014.** Earth observation based assessment of the water production and water consumption of Nile Basin agro-ecosystems. *Remote Sensing*. 6, 1030610334. <https://doi.org/10.3390/rs61110306>
- Biancamaria, S., Mballo, M., Le Moigne, P., Sánchez Pérez, J.M., Espitalier-Noël, G., Grusson, Y., Cakir, R., Häfliger, V., Barathieu, F., Trasmonte, M., Boone, A., Martin, E., Sauvage, S. 2019.** Total water storage variability from GRACE mission and hydrological models for a 50,000 km<sup>2</sup> temperate watershed: the Garonne River basin (France). *Journal of Hydrology: Regional Studies*. 24, 100609. <https://doi.org/10.1016/j.ejrh.2019.100609>
- Borthwick, B. 2003.** Water in Israeli-Jordanian Relations: From Conflict to the Danger of Ecological Disaster. *Israel Affairs*. 9, 165–186. <https://doi.org/10.1080/714003523>
- Comair, G.F., McKinney, D.C., Siegel, D. 2012.** Hydrology of the Jordan River Basin: Watershed Delineation, Precipitation and Evapotranspiration. *Water Resources Management*. 26, 4281–4293. <https://doi.org/10.1007/s11269-012-0144-8>
- Cook, B.I., Anchukaitis, K.J., Touchan, R., Meko, D.M., Cook, E.R. 2016.** Spatiotemporal drought variability in the Mediterranean over the last 900 years. *Journal of Geophysical Research Atmospheres*. 121, 2060–2074. <https://doi.org/10.1002/2015JD023929>
- Courcier, R., Venot, J.-P., Molle, F. 2005.** *Historical Transformations of the Lower Jordan River Basin (in Jordan): Changes in Water Use and Projections (1950-2025) (Research Report No. 9)*, Comprehensive Assessment of water management in agriculture. International Water Management Institute.
- de Boer, F. 2016.** *HiHydroSoil: A High Resolution Soil Map of Hydraulic Properties (Version 1.2)*, Report FutureWater: 134.
- Dost, R., Obando, E.B., Bastiaanssen, W., Hoogeveen, J. 2013.** Water Accounting Plus (WA+) in the Awash River Basin. Coping with Water Scarcity – Developing National Water Audits Africa. [https://www.wateraccounting.org/files/projects/awash\\_basin.pdf](https://www.wateraccounting.org/files/projects/awash_basin.pdf) (accessed 1.8.19).
- ESA. 2017.** Satellite-derived information to assess the consequences of armed conflict on the agriculture sector. Project: “Agriculture and Rural Development Cluster - Syria,” ESA’s Earth Observation for Sustainable Development (EO-4SD) Initiative. European Space Agency.
- FAO. 2019.** FAO Water Productivity - Catalog - Land Cover Classification. [https://wapor.apps.fao.org/catalog/2/L2\\_LC-C\\_A](https://wapor.apps.fao.org/catalog/2/L2_LC-C_A) (accessed 9.20.19).
- FAO. 2018.** WaPOR Database Methodology: Level 1. Remote Sensing for Water Productivity (Technical Report). Food and Agriculture Organization of the United Nations, Rome.

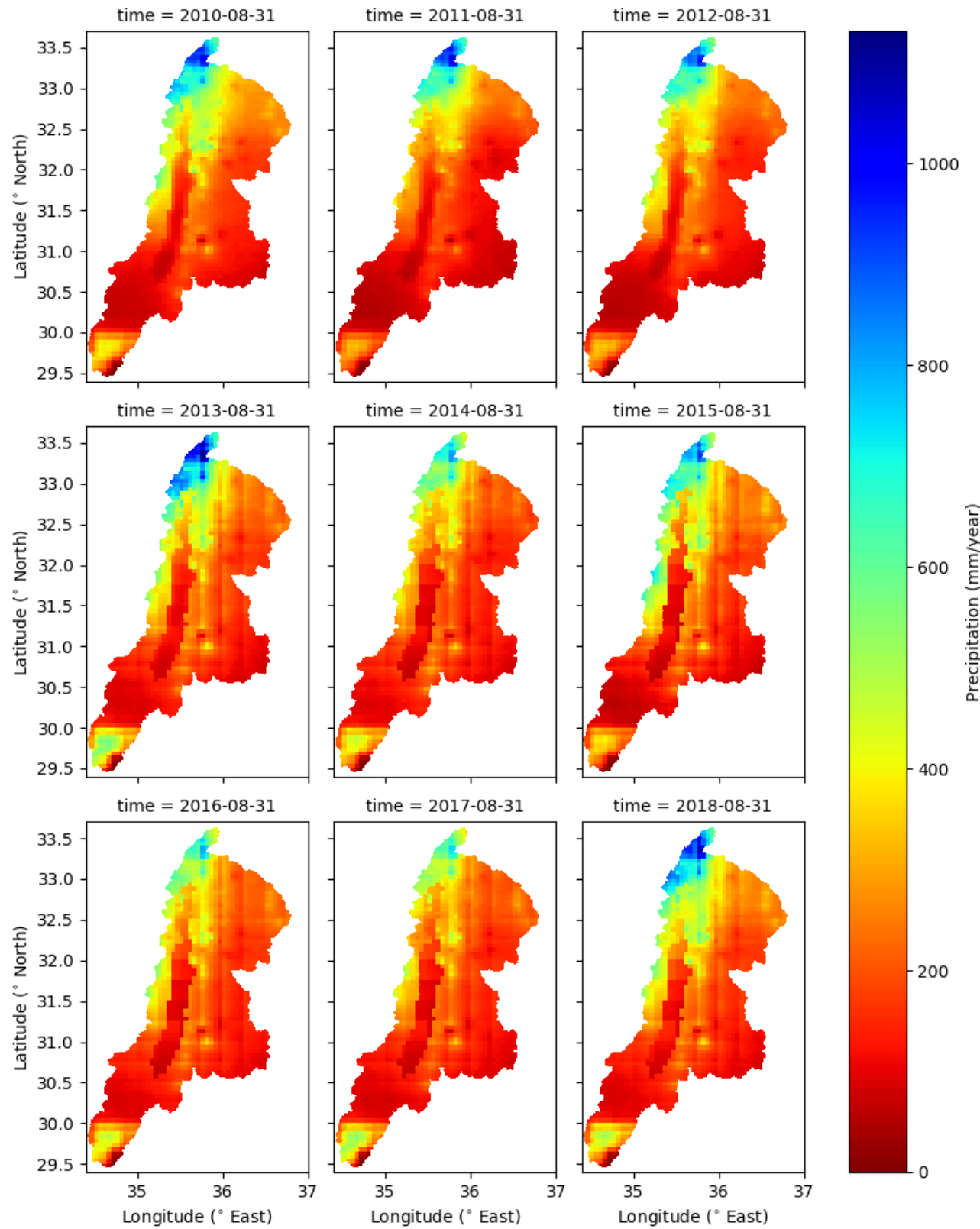
- FAO. 2016a.** AQUASTAT Website. Food and Agriculture Organization of the United Nations (FAO). Israel. [http://www.fao.org/nr/water/aquastat/countries\\_regions/ISR/index.stm](http://www.fao.org/nr/water/aquastat/countries_regions/ISR/index.stm) (accessed 3.21.19).
- FAO. 2016b.** AQUASTAT Website. Food and Agriculture Organization of the United Nations (FAO) . Jordan. [http://www.fao.org/nr/water/aquastat/countries\\_regions/JOR/index.stm](http://www.fao.org/nr/water/aquastat/countries_regions/JOR/index.stm) (accessed 6.19.19).
- FAO. 2016c.** AQUASTAT Website. Food and Agriculture Organization of the United Nations (FAO). Syria. [http://www.fao.org/nr/water/aquastat/countries\\_regions/SYR/index.stm](http://www.fao.org/nr/water/aquastat/countries_regions/SYR/index.stm) (accessed 8.19.19).
- Funk, C., Peterson, P., Landsfeld, M., Pedreros, D., Verdin, J., Shukla, S., Husak, G., Rowland, J., Harrison, L., Hoell, A., Michaelsen, J. 2015.** The climate hazards infrared precipitation with stations—a new environmental record for monitoring extremes. *Scientific Data*. 2, 1–21. <https://doi.org/10.1038/sdata.2015.66>
- Gunkel, A., Lange, J, 2012.** New Insights Into The Natural Variability of Water Resources in The Lower Jordan River Basin. *Water Resources Management*. 26, 963–980. <https://doi.org/10.1007/s11269-011-9903-1>
- Israel Water Authority. 2019.** *The national water system*. <http://www.water.gov.il/Hebrew/Planning-and-Development/Pages/National-water-system.aspx> (accessed 9.16.19).
- Karimi, P. 2014.** *Water Accounting Plus for Water Resources Reporting and River Basin Planning* (PhD thesis). TU Delft, Delft, The Netherlands.
- Karimi, P., Bastiaanssen, W.G.M. 2015.** Spatial evapotranspiration, rainfall and land use data in water accounting; Part 1: Review of the accuracy of the remote sensing data. *Hydrology and Earth System Sciences*. 19, 507–532. <https://doi.org/10.5194/hess-19-507-2015>
- Klein, M., 1998.** Water Balance of the Upper Jordan River Basin. *Water International*. 23, 244–248. <https://doi.org/10.1080/02508069808686778>
- Lehner, B., Liermann, C.R., Revenga, C., Vörösmarty, C., Fekete, B., Crouzet, P., Döll, P., Endejan, M., Frenken, K., Magome, J., Nilsson, C., Robertson, J.C., Rödel, R., Sindorf, N., Wisser, D. 2011.** High-resolution mapping of the world's reservoirs and dams for sustainable river-flow management. *Frontiers in Ecology and the Environment*. 9, 494–502. <https://doi.org/10.1890/100125>
- Luthcke, S.B., Sabaka, T.J., Loomis, B.D., Arendt, A.A., McCarthy, J.J., Camp, J. 2013.** Antarctica, Greenland and Gulf of Alaska land-ice evolution from an iterated GRACE global mascon solution. *Journal of Glaciology*. 59, 613–631. <https://doi.org/10.3189/2013JoG12J147>
- Mekonnen, M.M., Hoekstra, A.Y. 2018.** Global Anthropogenic Phosphorus Loads to Freshwater and Associated Grey Water Footprints and Water Pollution Levels: A High-Resolution Global Study. *Water Resources Research*. 54, 345–358. <https://doi.org/10.1002/2017WR020448>
- Mekonnen, M.M., Hoekstra, A.Y. 2015.** Global Gray Water Footprint and Water Pollution Levels Related to Anthropogenic Nitrogen Loads to Fresh Water. *Environmental Science & Technology*. 49, 12860–12868. <https://doi.org/10.1021/acs.est.5b03191>
- Menne, M.J., Durre, I., Vose, R.S., Gleason, B.E., Houston, T.G. 2012.** An Overview of the Global Historical Climatology Network-Daily Database. *Journal of Atmospheric and Oceanic Technology*. 29, 897–910. <https://doi.org/10.1175/JTECH-D-11-00103.1>
- Ministry of Water and Irrigation. 2016.** *National Water Strategy (2016-2025)*. [http://www.mwi.gov.jo/sites/en-us/Hot%20Issues/Strategic%20Documents%20of%20The%20Water%20Sector/National%20Water%20Strategy\(%202016-2025\)-25.2.2016.pdf](http://www.mwi.gov.jo/sites/en-us/Hot%20Issues/Strategic%20Documents%20of%20The%20Water%20Sector/National%20Water%20Strategy(%202016-2025)-25.2.2016.pdf) (accessed 8.23.19).
- Phillips, D.J.H., Jägerskog, A., Turton, A. 2009.** The Jordan River basin: 3. Options for satisfying the current and future water demand of the five riparians. *Water International*. 34, 170–188. <https://doi.org/10.1080/02508060902832701>

[org/10.1080/02508060902847075](https://doi.org/10.1080/02508060902847075)

- Salameh, E., Alraggad, M., Tarawneh, A. 2014.** Disi Water Use for Irrigation – a False Decision and Its Consequences. *CLEAN – Soil Air Water*. 42, 1681–1686. <https://doi.org/10.1002/clen.201300647>
- Salameh, E., El Naser, H. 2000.** Changes in the Dead Sea Level and their Impacts on the Surrounding Groundwater Bodies. *Acta hydrochimica et hydrobiologica*. 28, 24–33. [https://doi.org/10.1002/\(SICI\)1521-401X\(200001\)28:1<24::AID-AHEH24>3.0.CO;2-6](https://doi.org/10.1002/(SICI)1521-401X(200001)28:1<24::AID-AHEH24>3.0.CO;2-6)
- Shuval, H.I. 2000.** Are the Conflicts Between Israel and Her Neighbors Over the Waters of the Jordan River Basin an Obstacle to Peace? Israel-Syria as a Case Study, in: Belkin, S. (Ed.), *Environmental Challenges*. Springer Netherlands, Dordrecht, pp. 605–630. [https://doi.org/10.1007/978-94-011-4369-1\\_47](https://doi.org/10.1007/978-94-011-4369-1_47)
- UNEP-WCMC. 2019a.** Protected Area Profile for Jordan from the World Database of Protected Areas, August 2019. Prot. Planet. <https://www.protectedplanet.net/country/JO> (accessed 8.23.19).
- UNEP-WCMC. 2019b.** *Protected Area Profile for Syrian Arab Republic* from the World Database of Protected Areas, August 2019. Prot. Planet. <https://www.protectedplanet.net/country/SY> (accessed 8.23.19).
- UNEP-WCMC. 2019c.** *Protected Area Profile for Egypt* from the World Database of Protected Areas, August 2019. Prot. Planet. <https://www.protectedplanet.net/country/EG> (accessed 8.23.19).
- UNEP-WCMC. 2019d.** *Protected Area Profile for Israel* from the World Database of Protected Areas, August 2019. Prot. Planet. <https://www.protectedplanet.net/country/IL> (accessed 8.23.19).
- UN-ESCWA, BGR. 2013.** *Inventory of Shared Water Resources in Western Asia*. United Nations Economic and Social Commission for Western Asia and Bundesanstalt für Geowissenschaften und Rohstoffe, Beirut.
- Wolf, A.T. 1995.** *Hydropolitics Along the Jordan River: Scarce Water and Its Impact on the Arab-Israeli Conflict*. United Nations University Press.
- Yang, Y., Donohue, R.J., McVicar, T.R. 2016.** Global estimation of effective plant rooting depth: Implications for hydrological modeling. *Water Resources Research*. 52, 8260–8276. <https://doi.org/10.1002/2016WR019392>

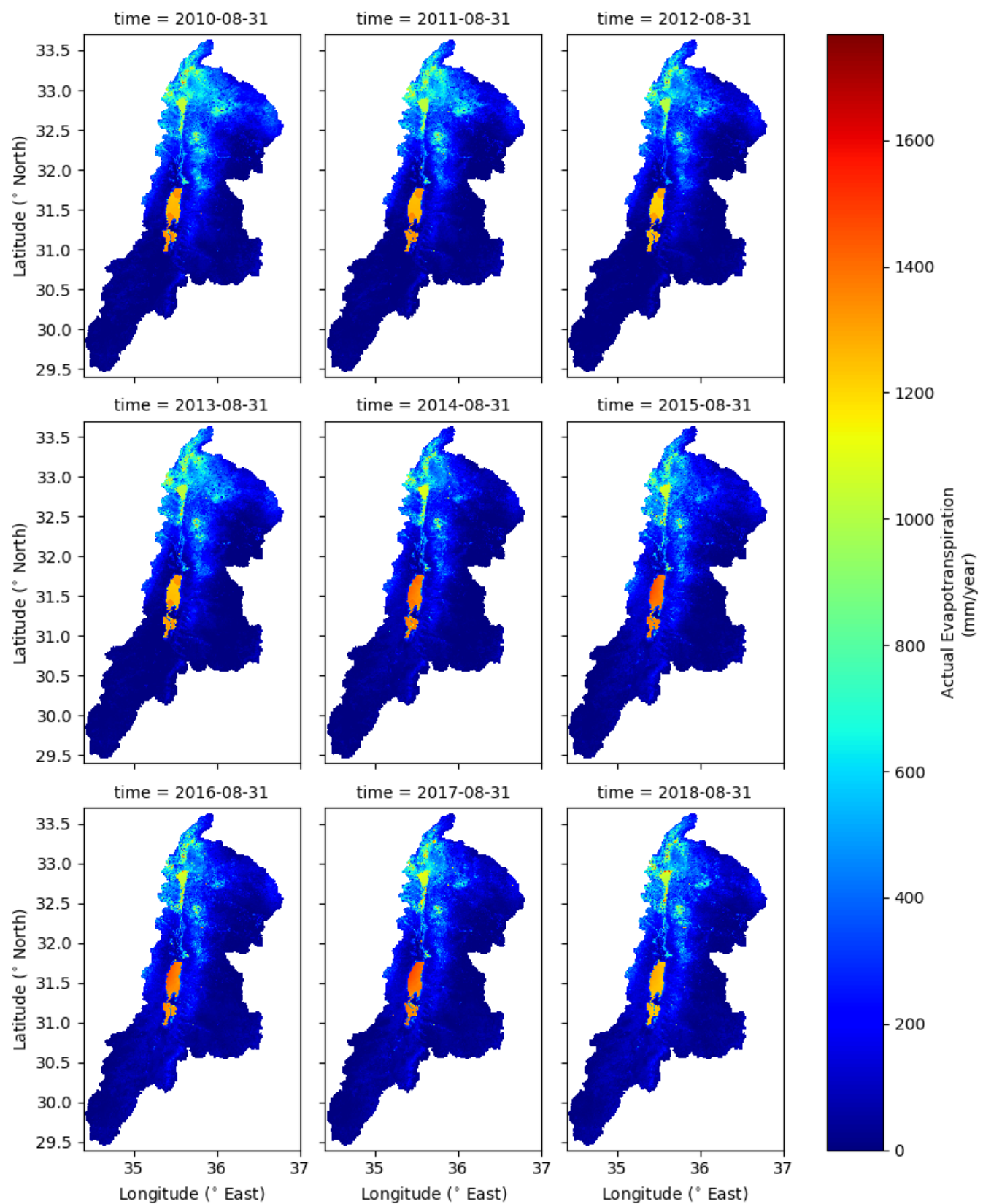
## Annex I. Total annual Precipitation (P) of hydrological years

'Time' value is the ending date of the hydrological year



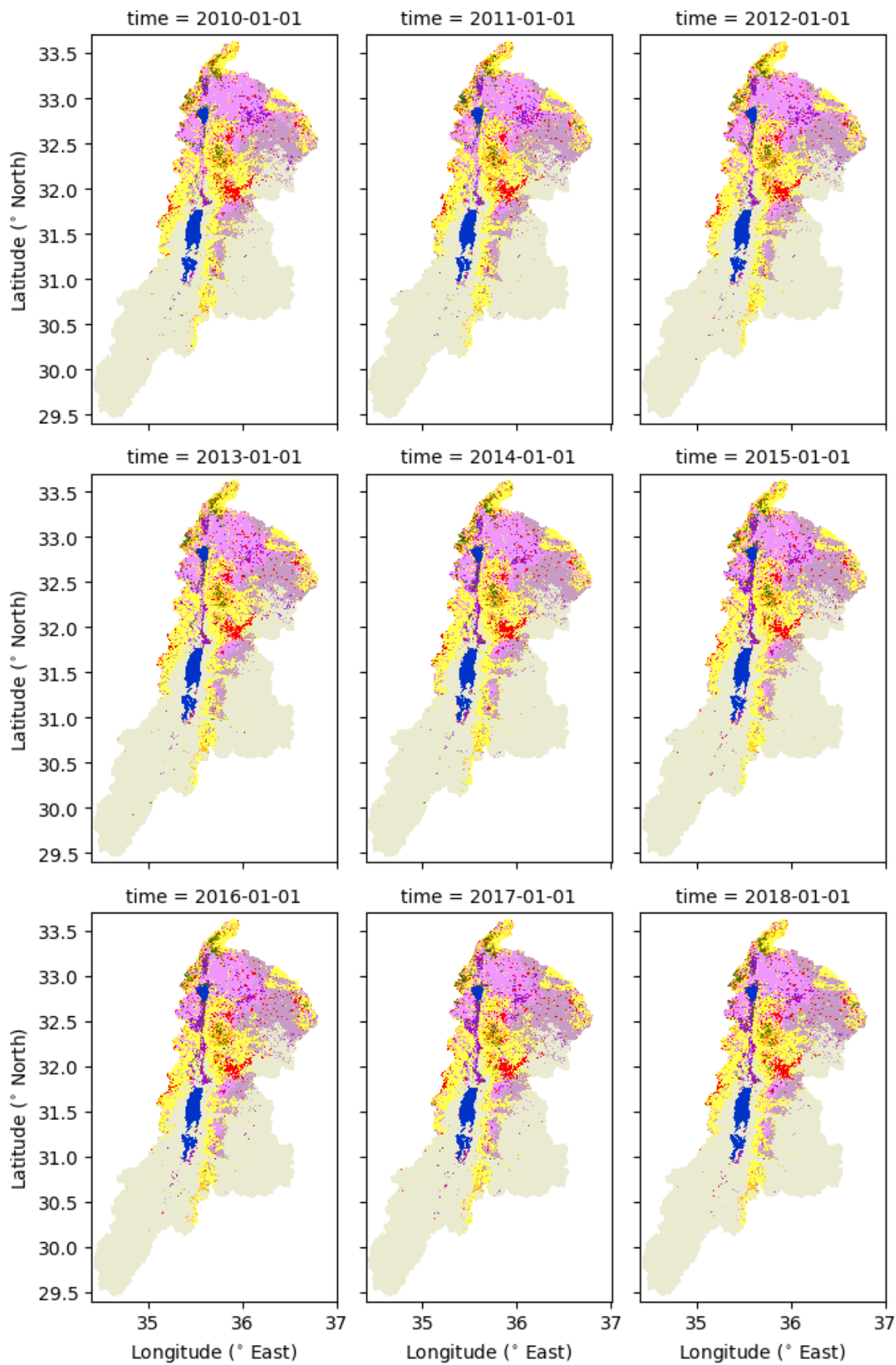
## Annex II. Total annual actual evapotranspiration ( $ET_a$ ) of hydrological years

'Time' value is the ending date of the hydrological year



### Annex III. Yearly WaPOR Land cover classification maps

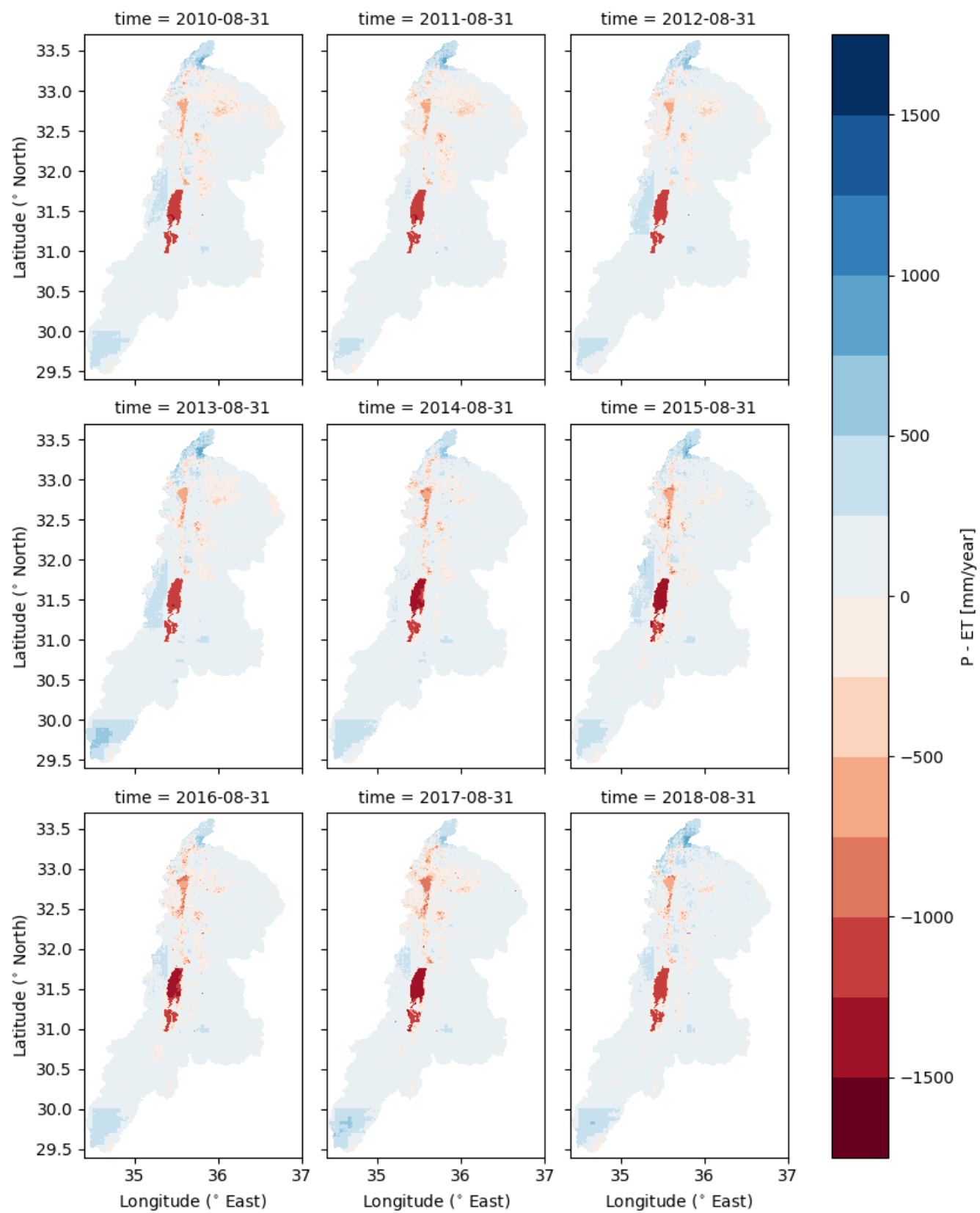
'Time' value is the starting date of the calendar year.





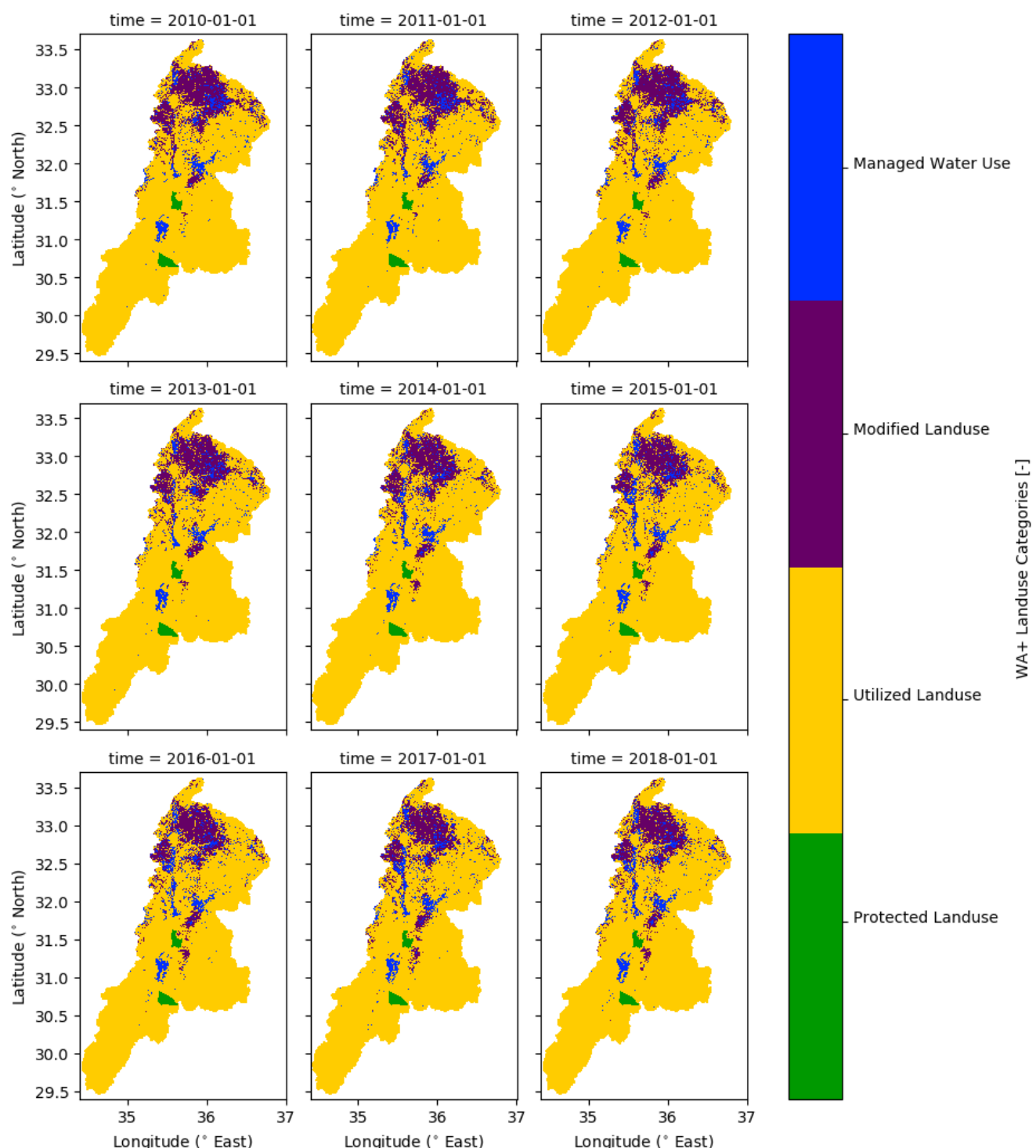
## Annex IV. Total annual P - ET<sub>a</sub> of hydrological years

'Time' value is the ending date of the hydrological year.



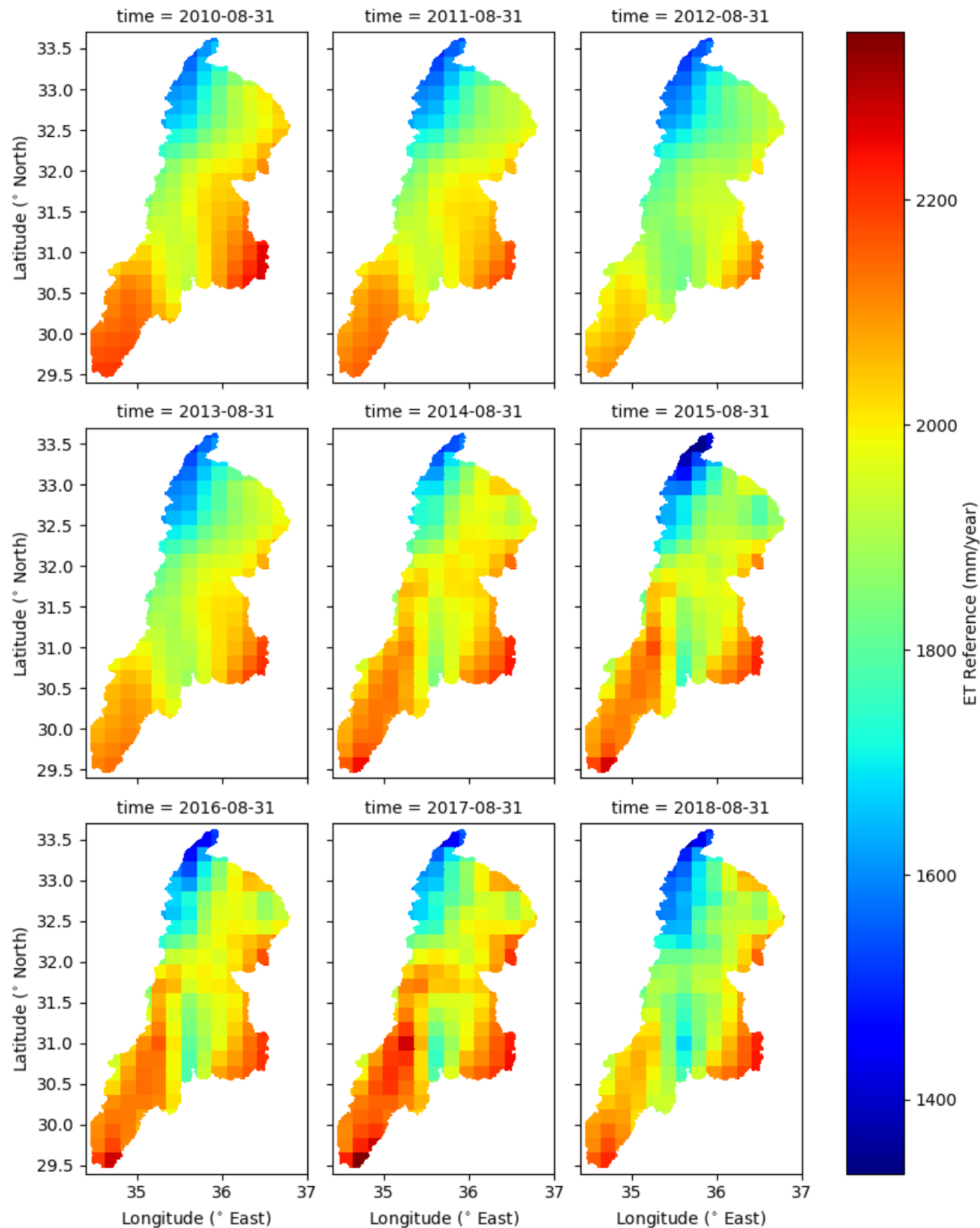
## Annex V. Yearly WA+ Land use classification maps

'Time' value is the starting date of the calendar year.



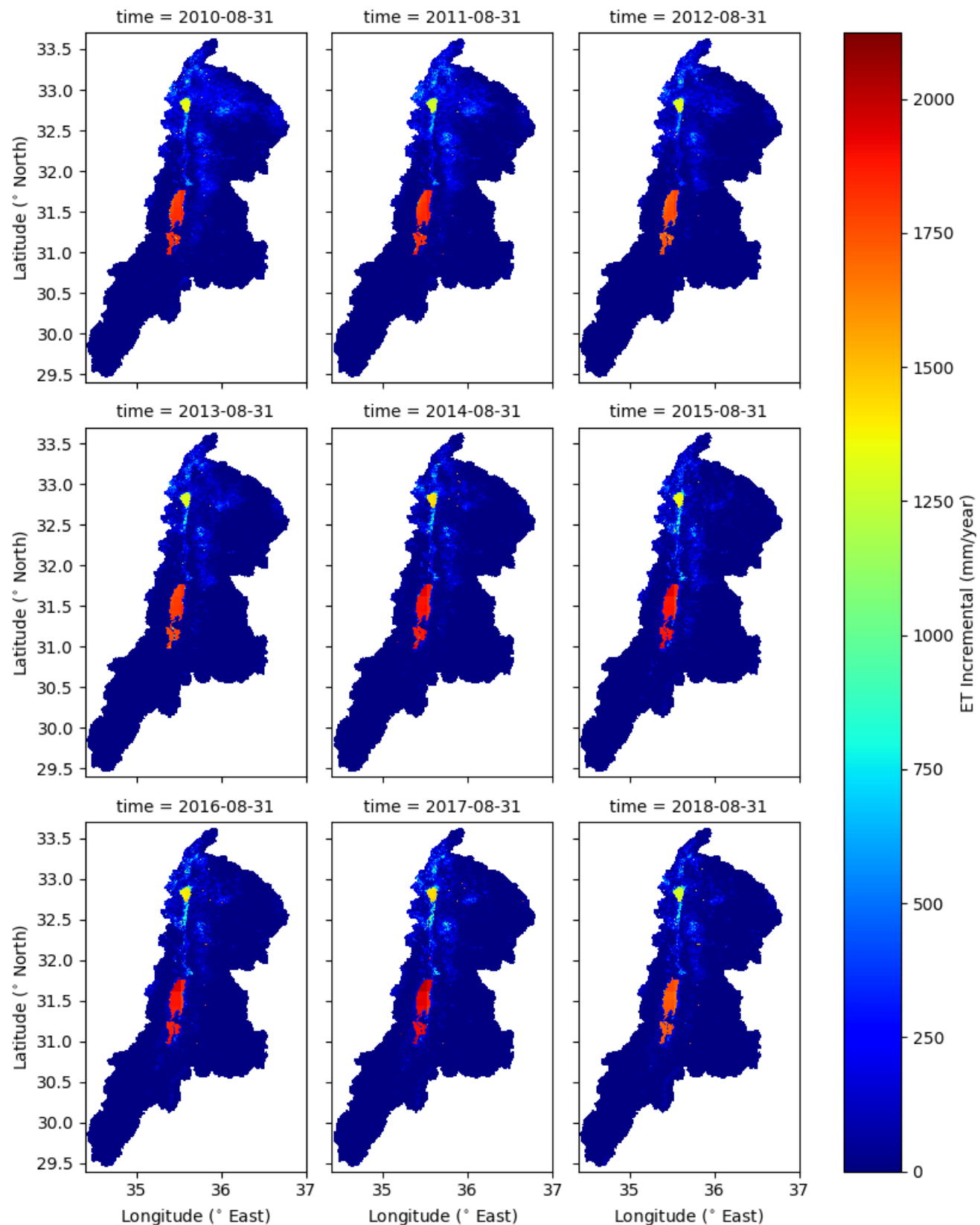
## Annex VI. Total annual reference evapotranspiration ( $ET_{ref}$ ) of hydrological years

'Time' value is the ending date of the hydrological year.



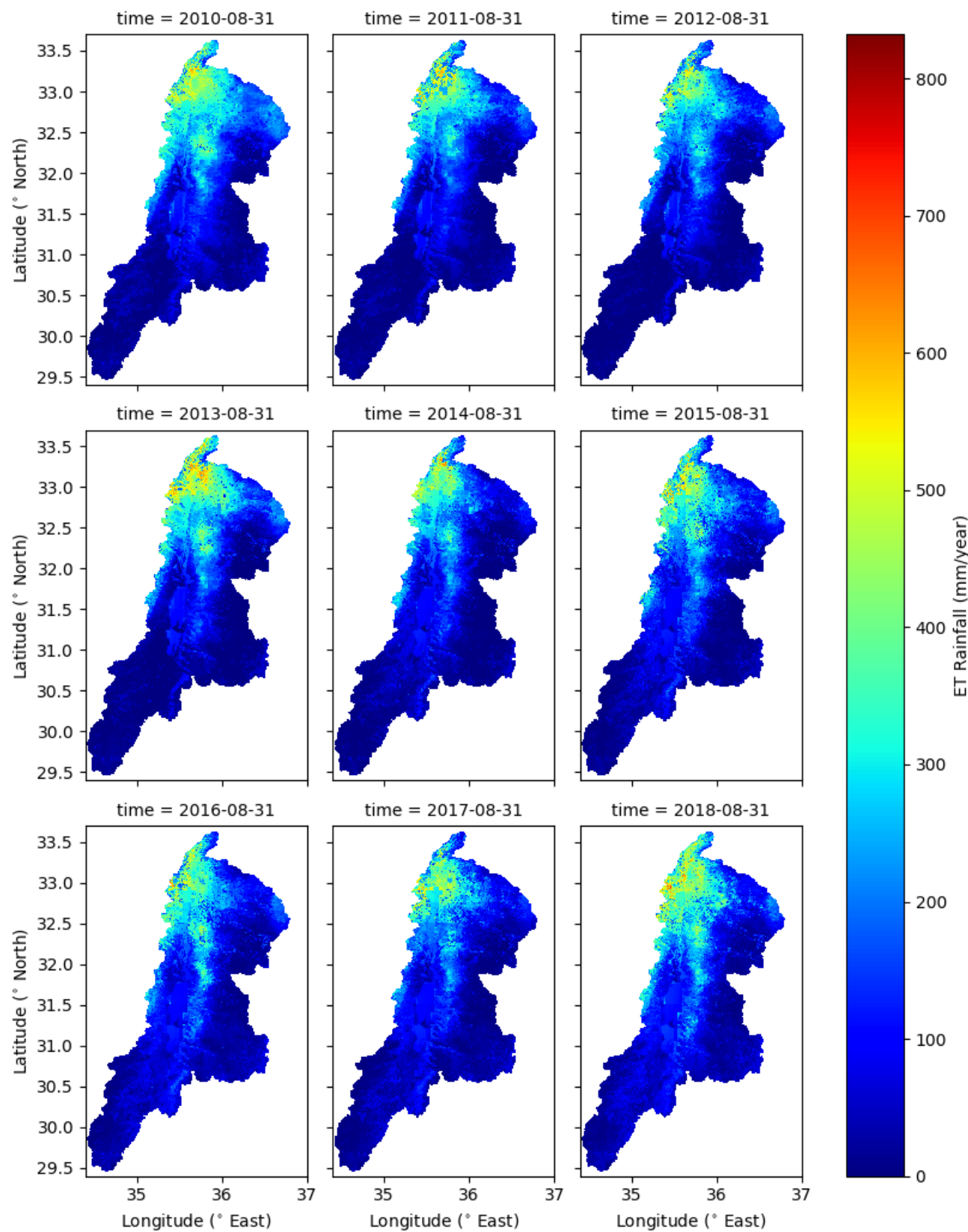
## Annex VII. Total annual estimated Incremental ET ( $ET_{incr}$ ) of hydrological years

'Time' value is the ending date of the hydrological year.



## Annex VIII. Total annual estimated Rainfall ET ( $ET_{rain}$ ) of hydrological years

'Time' value is the ending date of the hydrological year



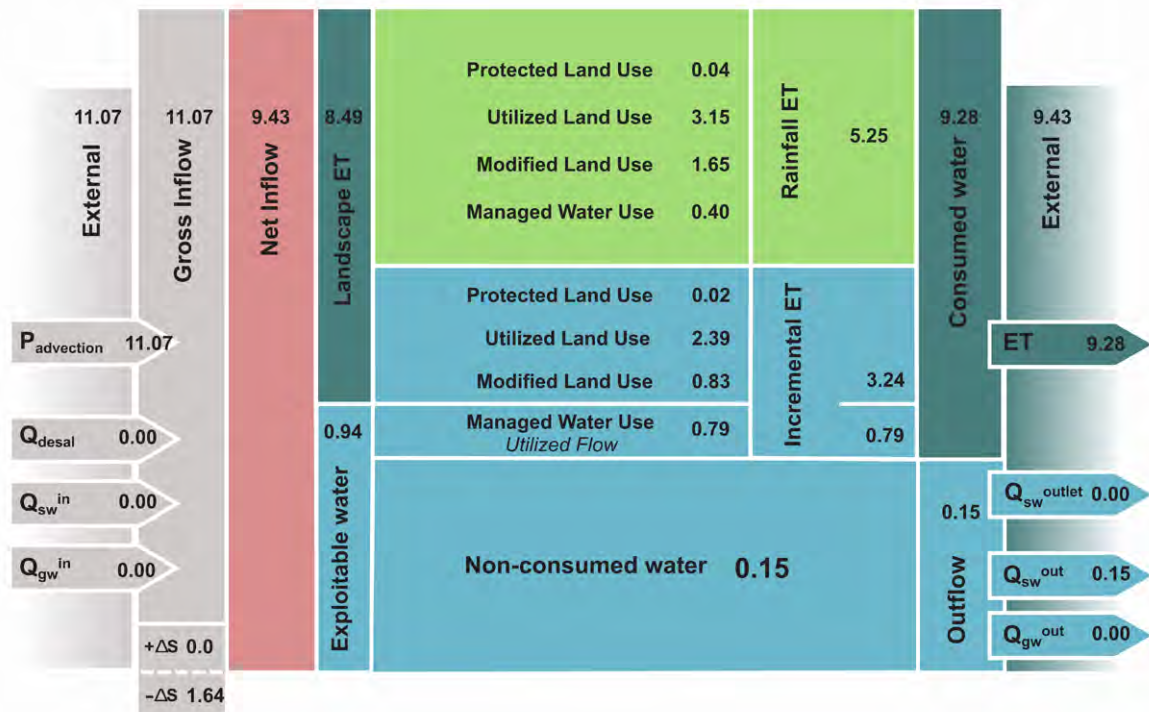
## Annex IX. Yearly WA+ Sheet 1 Resource Base

### Sheet 1: Resource Base

Basin: Jordan

Period: 2010

Unit: km<sup>3</sup>/year (cubic kilometers per year)

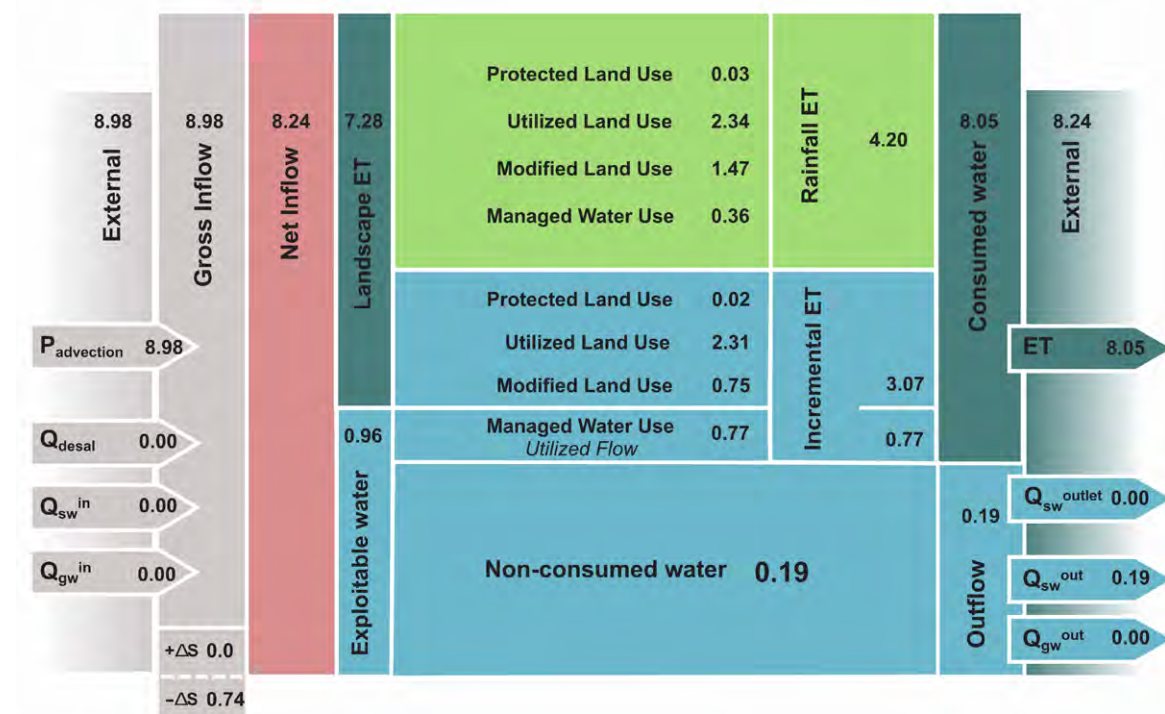


### Sheet 1: Resource Base

Basin: Jordan

Period: 2011

Unit: km<sup>3</sup>/year (cubic kilometers per year)

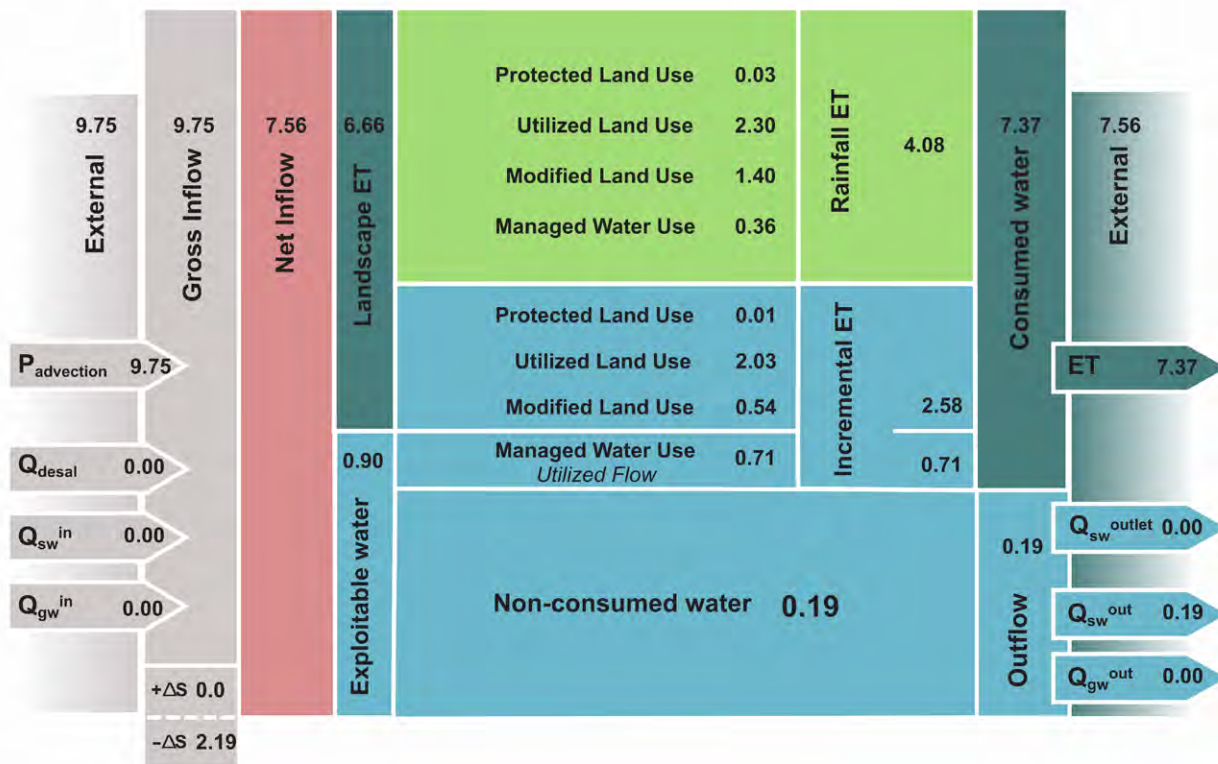


### Sheet 1: Resource Base

Basin: Jordan

Period: 2012

Unit: km<sup>3</sup>/year (cubic kilometers per year)

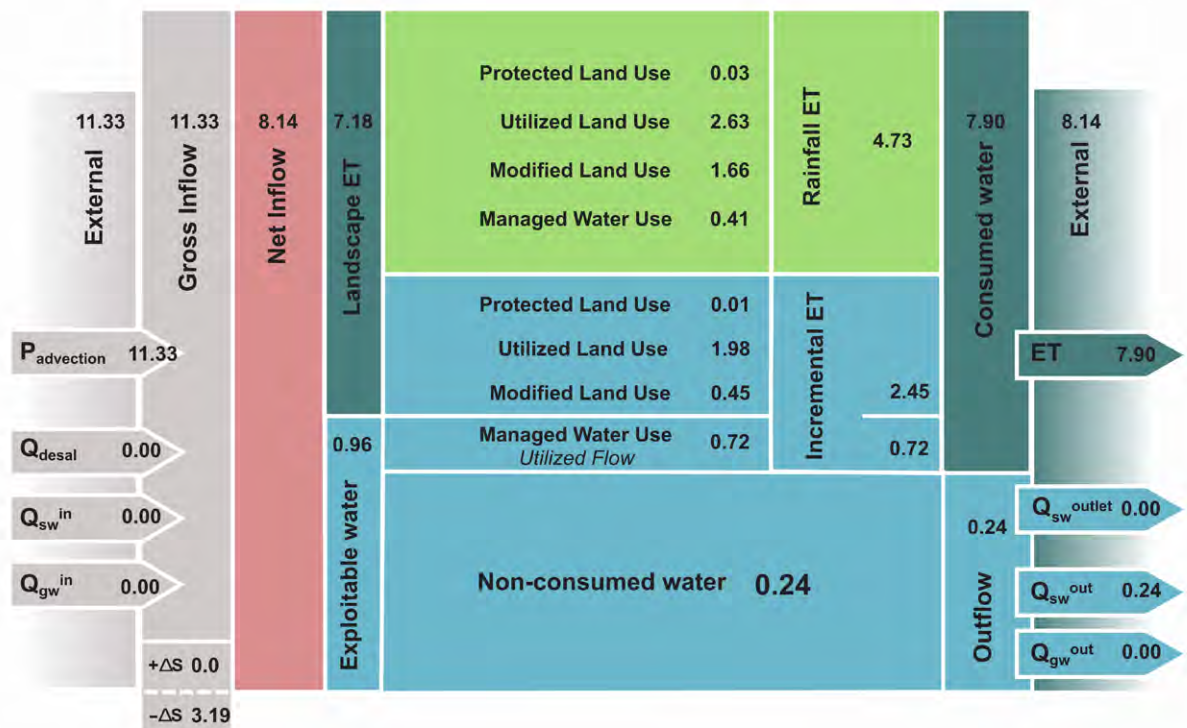


### Sheet 1: Resource Base

Basin: Jordan

Period: 2013

Unit: km<sup>3</sup>/year (cubic kilometers per year)

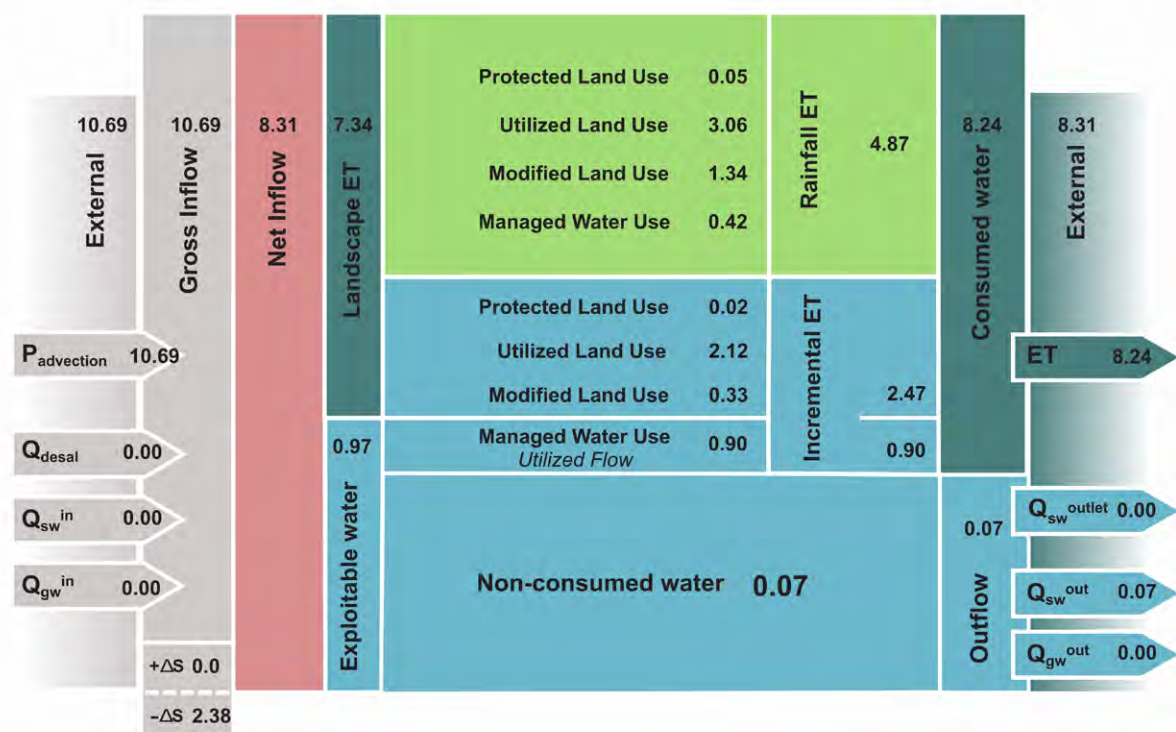


**Sheet 1: Resource Base**

Basin: Jordan

Period: 2015

Unit: km<sup>3</sup>/year (cubic kilometers per year)

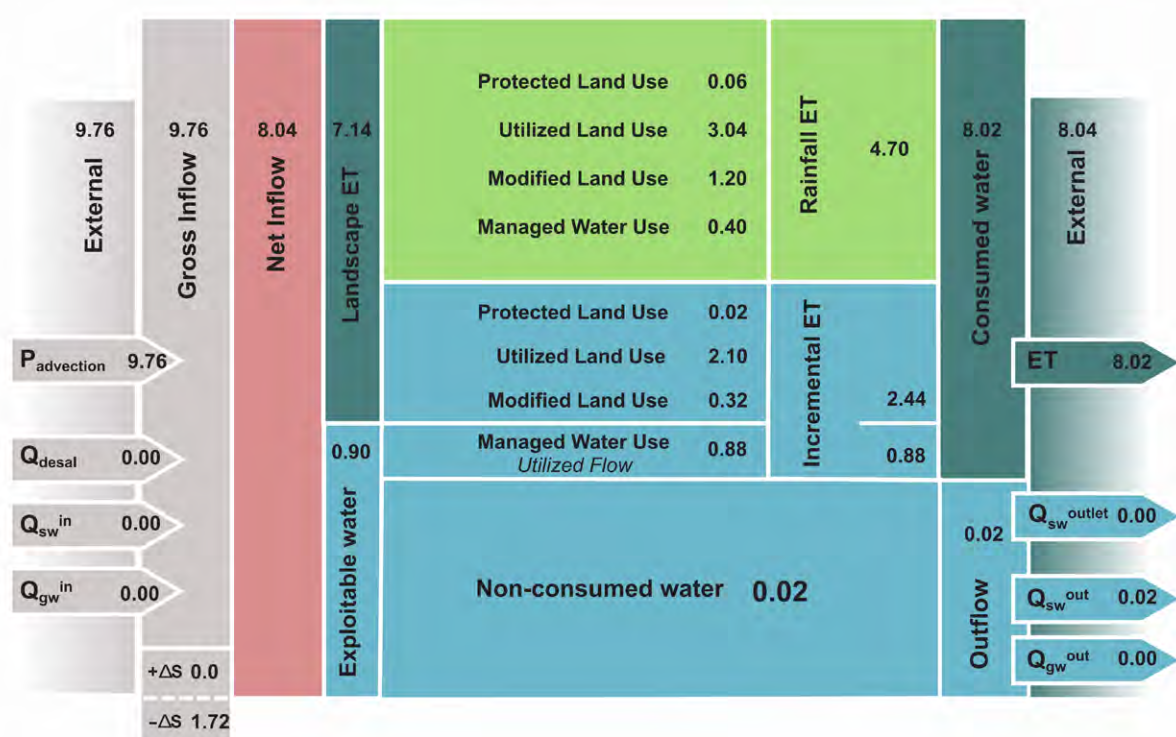


**Sheet 1: Resource Base**

Basin: Jordan

Period: 2016

Unit: km<sup>3</sup>/year (cubic kilometers per year)

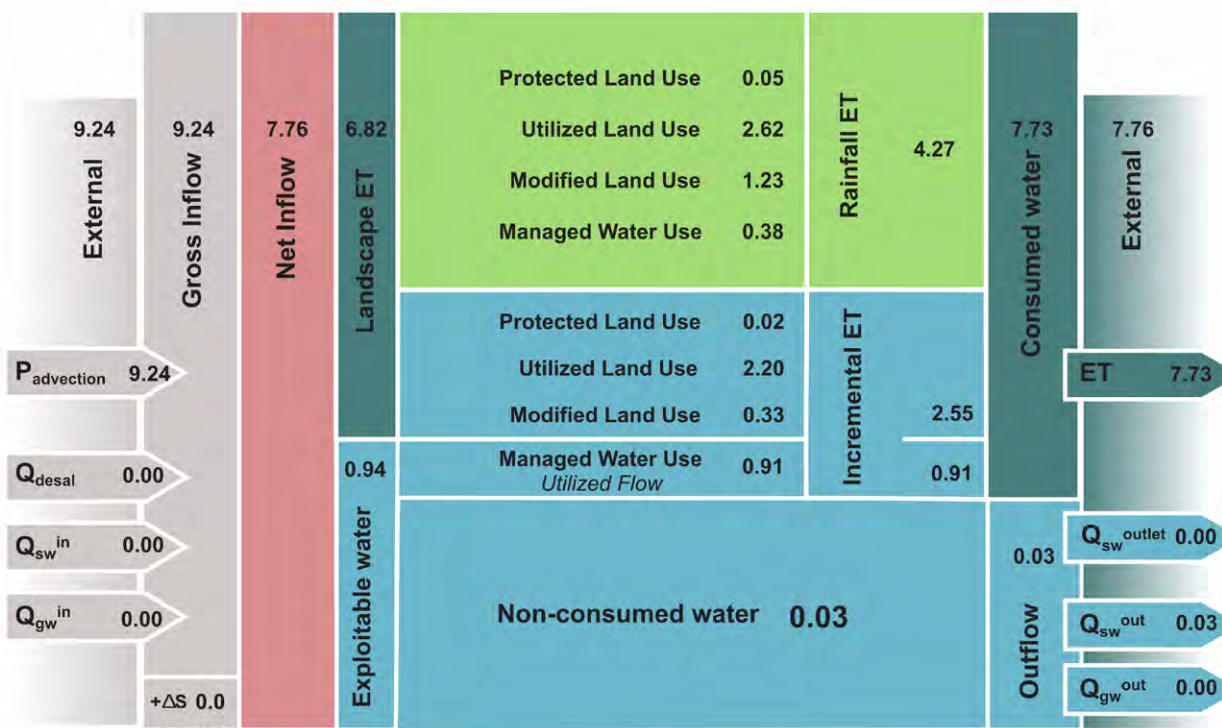


**Sheet 1: Resource Base**

Basin: Jordan

Period: 2017

Unit: km<sup>3</sup>/year (cubic kilometers per year)

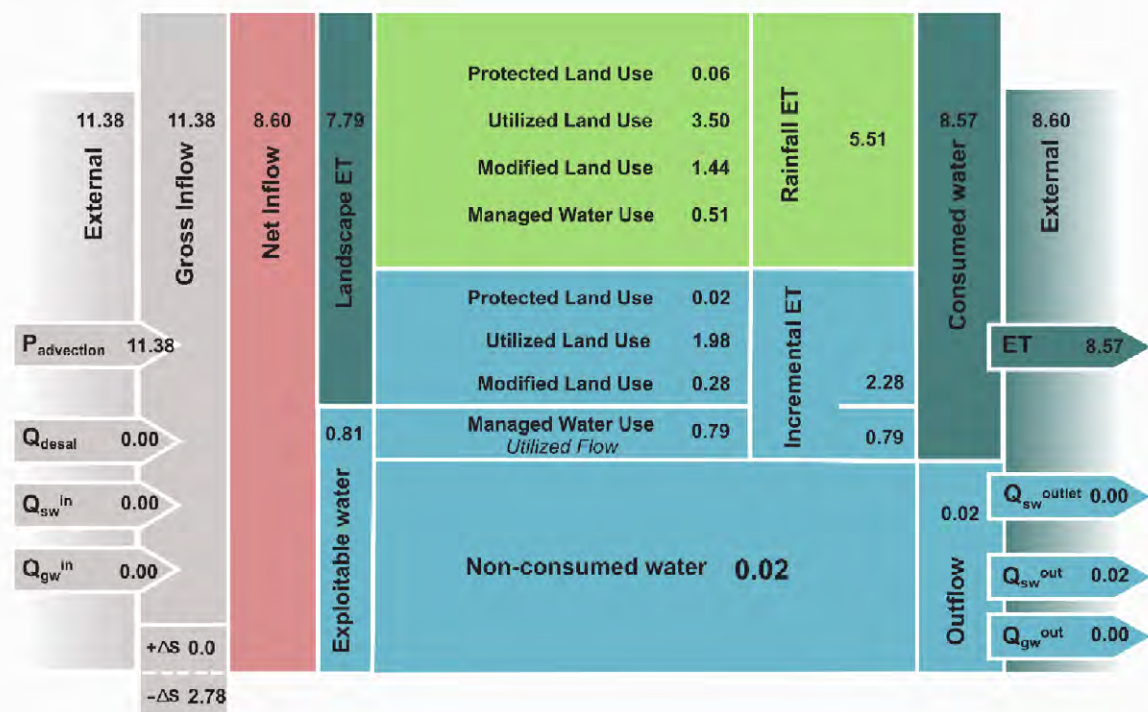


**Sheet 1: Resource Base**

Basin: Jordan

Period: 2018

Unit: km<sup>3</sup>/year (cubic kilometers per year)



## Annex X. Supplementary WA+ Sheet 1 results

This annex is to show the WA+ Sheet 1 key indicators in case water storage change is derived from GRACE TWSA solution instead of WaPOR-based water balance. The difference  $P - ET_a - Q_{sw}^{out} - \Delta S_{GRACE}$  is then considered groundwater outflow ( $Q_{gw}^{out}$ ), where  $Q_{gw}^{out}$  is the surface water outflow through the NWC. Since there is no information on the recommended value of reserved groundwater flow from Jordan Basin, no reserved outflow was deducted from available water which, hereby, remains the same as Table 9. As can be seen in Table X- 1, the stationarity index is -3.2%, which has opposite sign compared to the results from WaPOR-based water balance (Table 9), indicating that water was extracted from the groundwater and/or surface water storage. The basin closure indicator is 75.7%, which is significantly lower than WaPOR-based water balance results (98.8%), as 23% of precipitation is now considered groundwater outflow. If this groundwater outflow is reserved for environmental flow or water uses outside of the Jordan River Basin, the amount available water will be less than 3.03 km<sup>3</sup>/year, which will result in higher managed fraction. As demonstrated here, the state of water resources in the Jordan River Basin will be understood differently due to the uncertainty in the WaPOR data.

**Table X- 1:** WA+ Sheet 1 key indicators of Jordan River Basin for the hydrological years from 2010 to 2018 based on WaPOR Precipitation and Actual evapotranspiration datasets and  $\Delta S$  from GRACE TWSA solution.

	ET fraction	Stationarity index	Basin Closure	Available water (km <sup>3</sup> /year)	Managed water (km <sup>3</sup> /year)	Managed fraction (%)
Year	(%)	(%)	(%)			
2010	83.8	2.8	86.1	2.58	0.79	30.5
2011	89.6	-10.1	80.6	1.70	0.77	45.4
2012	75.6	-15.7	63.7	3.09	0.71	22.9
2013	69.7	0.3	69.9	4.15	0.72	17.3
2014	73.8	3.3	76.2	3.29	0.79	24.0
2015	77.1	0.4	77.4	3.35	0.90	26.7
<b>Average</b>	<b>78.3</b>	<b>-3.2</b>	<b>75.7</b>	<b>3.03</b>	<b>0.78</b>	<b>27.8</b>

## Annex XI. Comparison of Remote Sensing products

### Annex XI.1 Introduction

This annex shows the results of the comparisons of different open access remote sensing products for precipitation and evapotranspiration and GRACE solutions. Table XI - 1 shows the details of the products considered for the analyses. These data sets were resampled to the same spatial resolution of  $0.05^{\circ} \times 0.05^{\circ}$  and monthly temporal resolution and aggregated to annual values using the hydrological year from September to August. Then the data was clipped to the Jordan River Basin shapefile. The period from 2009 to 2018 was used for this analysis, consistent with the period used in the main report.

**Table XI - 1** Data sets considered for Water Balance Computation

Product	Duration	Spatial Res.	Temporal Res.	Coverage	URL
<b>P</b>					
CHIRPS	2009 - 2018	$0.05^{\circ}$	Sub-daily	$50^{\circ}\text{S}-50^{\circ}\text{N}$	<a href="https://www.chc.ucsb.edu/data/chirps">https://www.chc.ucsb.edu/data/chirps</a>
TRMM	2009 - 2018	$0.25^{\circ}$	daily	$50^{\circ}\text{S}-50^{\circ}\text{N}$	<a href="https://pmm.nasa.gov/data-access/downloads/trmm">https://pmm.nasa.gov/data-access/downloads/trmm</a>
GPM	2009 - 2018	$0.1^{\circ}$	monthly	$90^{\circ}\text{N}-90^{\circ}\text{S}$	<a href="https://pmm.nasa.gov/data-access/downloads/gpm">https://pmm.nasa.gov/data-access/downloads/gpm</a>
<b>ET<sub>a</sub></b>					
WAPOR	2009 - 2018	250m	Dekadal	Africa + Near East	<a href="https://wapor.apps.fao.org/catalog/1/L2_ATEL_D">https://wapor.apps.fao.org/catalog/1/L2_ATEL_D</a>
SSEBop	2009 - 2018	1,000m	Dekadal	Global	<a href="https://earlywarning.usgs.gov/fews/product/461">https://earlywarning.usgs.gov/fews/product/461</a>
GloDET (ALEXI)	2013 - 2017	375m	Daily	Global	<a href="https://glodet.nebraska.edu/#/">https://glodet.nebraska.edu/#/</a>
GLEAM	2009 - 2018	$0.25^{\circ}$	Daily	Global	<a href="https://www.gleam.eu/">https://www.gleam.eu/</a>
MOD16	2009 - 2018	500m	8-Daily	Global	<a href="https://lpdaac.usgs.gov/products/mod16a2v006/">https://lpdaac.usgs.gov/products/mod16a2v006/</a>
CMRSET	2009 - 2012	$0.05^{\circ}$	Monthly	Global	Local database at IHE Delft
SEBS	2009 - 2017	5,000m	Monthly	Global	Local database at IHE Delft
<b>GRACE</b>					
CSR	2009 - 2016	$1.0^{\circ}$	Quasi-monthly	Global	<a href="https://podaac.jpl.nasa.gov/dataset/TELLUS_GRAC_L3_CSR_RLo6_LND?ids=DataFormat&amp;values=NETCDF&amp;search=GRACE&amp;temporalSearch=2003-10-31T23:00:00.000ZTO2019-11-26T23:00:00.000Z">https://podaac.jpl.nasa.gov/dataset/TELLUS_GRAC_L3_CSR_RLo6_LND?ids=DataFormat&amp;values=NETCDF&amp;search=GRACE&amp;temporalSearch=2003-10-31T23:00:00.000ZTO2019-11-26T23:00:00.000Z</a>
GFZ	2009 - 2016	$1.0^{\circ}$	Quasi-monthly	Global	<a href="https://podaac.jpl.nasa.gov/dataset/TELLUS_GRAC_L3_GFZ_RLo6_LND?ids=DataFormat&amp;values=NETCDF&amp;search=GRACE&amp;temporalSearch=2003-10-31T23:00:00.000ZTO2019-11-26T23:00:00.000Z">https://podaac.jpl.nasa.gov/dataset/TELLUS_GRAC_L3_GFZ_RLo6_LND?ids=DataFormat&amp;values=NETCDF&amp;search=GRACE&amp;temporalSearch=2003-10-31T23:00:00.000ZTO2019-11-26T23:00:00.000Z</a>
JPL	2009 - 2016	$1.0^{\circ}$	Quasi-monthly	Global	<a href="https://podaac.jpl.nasa.gov/dataset/TELLUS_GRAC_L3_JPL_RLo6_LND?ids=DataFormat&amp;values=NETCDF&amp;search=GRACE&amp;temporalSearch=2003-10-31T23:00:00.000ZTO2019-11-26T23:00:00.000Z">https://podaac.jpl.nasa.gov/dataset/TELLUS_GRAC_L3_JPL_RLo6_LND?ids=DataFormat&amp;values=NETCDF&amp;search=GRACE&amp;temporalSearch=2003-10-31T23:00:00.000ZTO2019-11-26T23:00:00.000Z</a>
GSFC	2009 - 2016	1 arc	Quasi-monthly	Global	<a href="https://ccar.colorado.edu/grace/">https://ccar.colorado.edu/grace/</a>

The analyses consisted of an inter-comparison of the different  $P$ ,  $ET_a$  and GRACE products (section XI.3). Secondly, comparison of runoff based on the water balance with the observed inter-basin transfer and comparison of storage change based on the water balance with the GRACE storage change (section XI.4). Four evapotranspiration, three precipitation and four GRACE solutions provided 48 different possible combinations to compute the water balance for Jordan River Basin. First, the monthly volume of water pumped to the National Water Carrier (NWC) from Lake Tiberias to Israel between 2009 and 2019 is compared to the runoff estimated using the RS product combinations (see chapter two of this report for methodology) and secondly the change in storage is calculated using the water balance and compared to GRACE solutions and presented as error in percentage of precipitation. Finally the spatial variability of the different products were compared by analysing  $P - ET_a$  for different land use classes (section XI.5).

## Annex XI.2 Datasets

### Precipitation products

Three precipitation products were considered:

**1. CHIRPS** - The Climate Hazards group Infrared Precipitation with Stations (CHIRPS) dataset, developed by the U.S. Geological Survey Earth Resources Observation and Science Center and Santa Barbara Climate Hazards Group at the University of California is a precipitation product based on multiple data sources (Funk et al., 2015). CHIRPS incorporates monthly precipitation climatology (Climate Hazards Group Precipitation Climatology, CHPClim), quasi-global geostationary thermal infrared satellite observations, TRMM product, atmospheric model precipitation fields from the National Oceanic and Atmospheric Administration (NOAA) Climate Forecast System (CFS), and observed precipitation (Funk et al., 2015). The global CHIRPS data is missing values over the Jordan valley. We therefore decided to use the WaPOR precipitation product, which is based on the CHIRPS database but it has the missing values are filled in (FAO, 2018).

**2. TRMM** – The Tropical Rainfall Measuring Mission (TRMM), a joint mission of NASA and the Japan Aerospace Exploration Agency, was launched in 1997 to study rainfall for weather and climate research. TRMM Multi-satellite Precipitation Analysis (TMPA) algorithm merges a variety of existing ground- and satellite-based observations to yield high spatial ( $0.25 \times 0.25$  degree) and temporal resolution (three-hourly instantaneous retrievals) observations with a higher degree of accuracy (Huffman et al., 2007).

**3. GPM** is the NASA/JAXA Global precipitation measurement (GPM) mission in coordination with the Goddard Earth Sciences Data and Information Services Center (GES DISC) is the Integrated Multi-satellite Retrievals for GPM, which merges precipitation estimates from passive microwave (PMW), calibrated infrared (IR) sensors and monthly surface precipitation gauge analysis data to provide half-hourly precipitation estimates on a  $0.1^\circ$  grid over the  $60^\circ$  N-S domain. GPM extend the spatial coverage from its predecessor (TRMM), and also provide improved measurements of precipitation globally (Liu et al., 2017)

### Evapotranspiration products

Seven existing  $ET_a$  products were considered. All of them except WaPOR are global scale products. The ET products used are based on multi-spectral satellite measurements and surface energy balance models (Paca, et al., 2019). These models include;

1. MODIS Global Terrestrial Evapotranspiration Algorithm (MOD16) (Mu et al., 2011),
2. Atmosphere-Land Exchange Inverse Model (ALEXI) (Anderson et al., 2007),

3. Global Land Evaporation Amsterdam Model (**GLEAM**) (Miralles et al., 2011),
4. Surface Energy Balance System (**SEBS**) (Su, 2002),
5. Operational Simplified Surface Energy Balance (**SSEBop**) (Senay et al., 2013) and
6. CSIRO MODIS Reflectance-based Evapotranspiration (**CMRSET**) (Guerschman et al., 2009).
7. FAO's data portal to monitor Water Productivity through Open access of Remotely sensed derived data (**WaPOR**) (FAO, 2018)

## GRACE Solutions

Total Water Storage Anomalies (TWSA) from four global solutions based on the Gravity Recovery And Climate Experiment (GRACE) satellite mission were considered for this analysis. GRACE is a NASA and Deutsches Zentrum für Luft- und Raumfahrt (DLR) satellite mission to map the global Earth gravity field every 30 days (Biancamaria et al., 2019). Variations of earth gravity field as mapped by GRACE at the monthly to inter-annual time scales can be attributed mainly to redistribution of water in its fluid envelope (Wouters et al., 2014). GRACE solutions provided as TWSA at monthly time scale corresponds to the sum of all water mass variations at the continents surface and in the soil (i.e. the sum of snow water equivalent, surface water, soil water and groundwater) (Chen et al., 2016).

Four publicly available monthly global GRACE solutions have been considered in this study. The products used correspond to liquid water equivalent thickness in meters on regular grid for the first three solutions (see Table XI - 1) which are labelled here as CSR, GFZ and JPL, respectively;

1. the GRACE Tellus – Land release RL05 monthly mass  $1^\circ \times 1^\circ$  grids computed by the University of Texas – Center for Space Research (CSR, version DSTvSCS1409);
2. GeoForschungsZentrum (GFZ, version DSTvSCS1409);
3. Jet Propulsion Laboratory (JPL, version DSTvSCS1411) processing centers (Swenson and Wahr, 2006; Landerer and Swenson, 2012; Swenson, 2012);
4. The GRACE global mascon solution uses the NASA Goddard Space Flight Center (GSFC) GEODYN precision orbit determination and geodetic parameter estimation software (Luthcke et al., 2013). This data set is provided as centimetres of liquid water equivalent thickness per mascon. The data then is converted to raster of centimetres of liquid water equivalent thickness on  $0.5^\circ \times 0.5^\circ$  grid.

Grace data is available between January 2003 and July 2016. The data is available in quasi-monthly time steps with windows of observation varies. However, most of the data in is centred around on the 16th of each month. Interpolation was made to get data at every 16th of every month to get monthly values and central difference method is used to calculate the change in storage (Biancamaria et al., 2019).

## Annex XI.3 Data comparison

### Precipitation products

The three precipitation products show similar trends and comparable values (Figure XI - 1). TRMM has missing values in the dry months of 2015 to 2017.

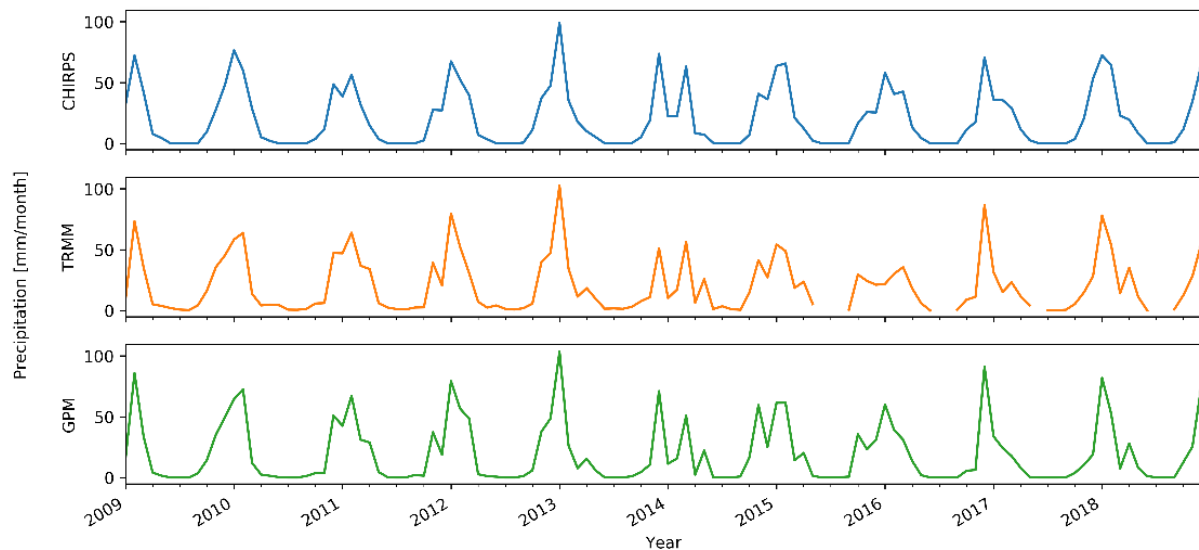


Figure XI - 1 Precipitation values from GPM, TRMM and CHIRPS for Jordan River Basin

The monthly mean and annual precipitation from the three products are shown in the Figure XI - 2 and Figure XI - 3. All products show the same seasonal trend, CHIRPS and GPM show very similar values, whereas TRMM values are slightly lower during the wet winter months (November-March) and slightly higher during the dry months (April-October). The annual precipitation values do not show significant differences either among the different products except for 2017 when CHIRPS showed a significant higher value compared to the other products (up to 75mm/year).

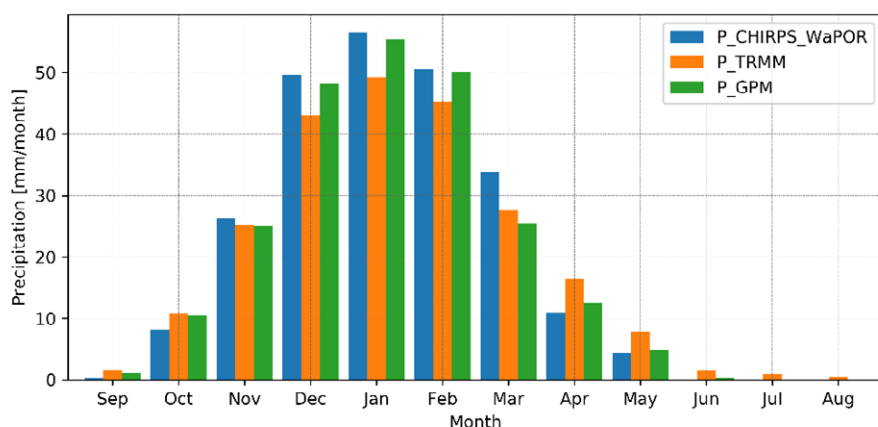


Figure XI - 2 Monthly mean precipitation for Jordan River Basin from CHIRPS, TRMM and GPM

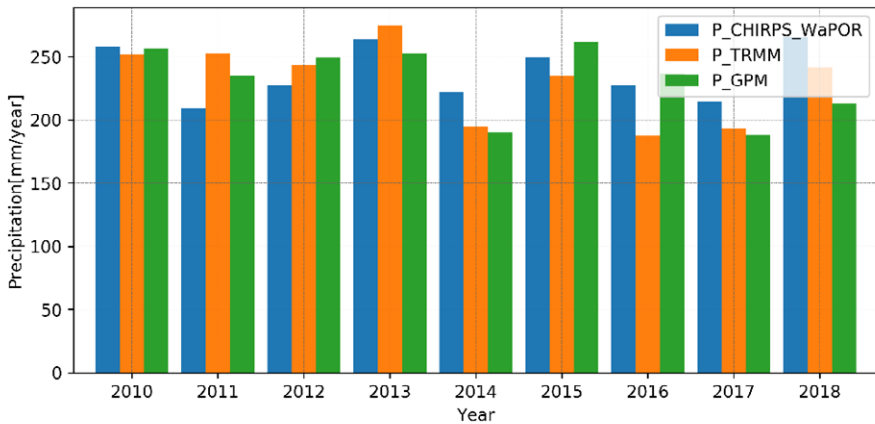


Figure XI - 3 Annual Precipitation for Jordan River Basin from CHIRPS, TRMM and GPM

The correlation between the products (all combinations) show very good correlation (Pearson Correlation Coefficient (PCC) between 0.94 and 0.97) (Figure XI - 4).

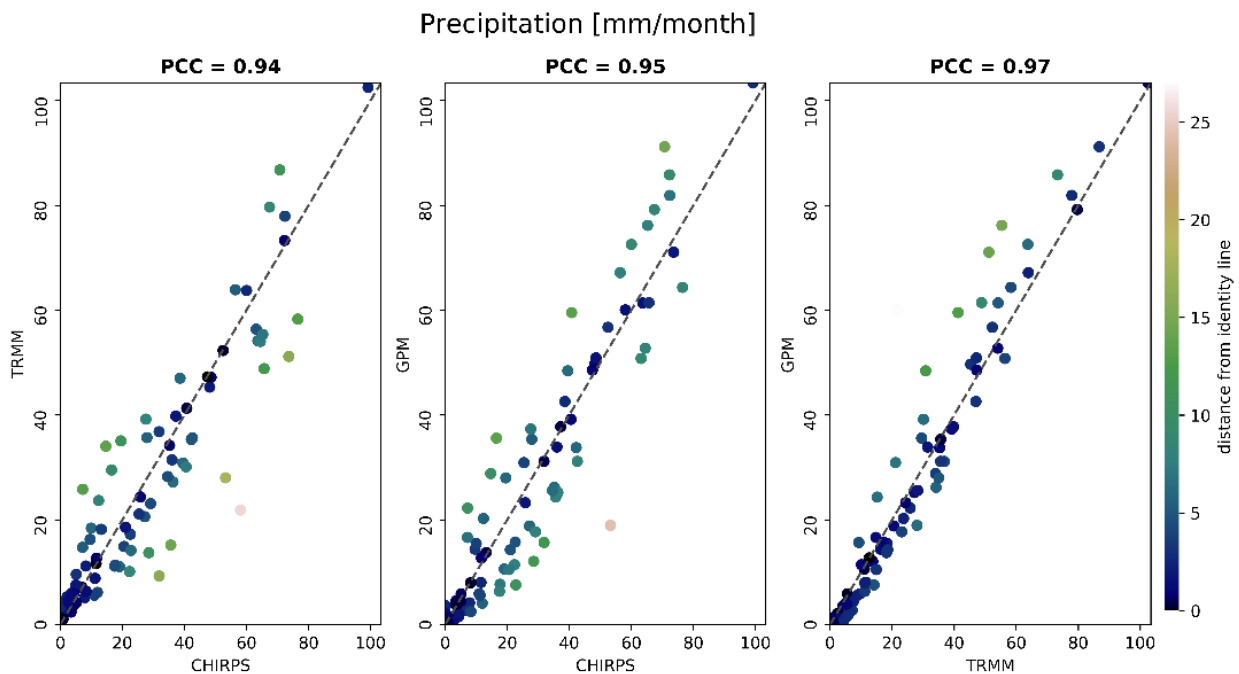


Figure XI - 4 Correlation of the three precipitations data for Jordan River Basin

## ET<sub>a</sub> products

Close investigation of the seven  $ET_a$  products values identified that SEBS and MODIS have significant amount of missing values (31.5% and 68.5% in terms of spatial coverage) for ALEXI we found that water bodies have zero values (Figure XI - 5). Hence these three products are left out from consideration for further analysis.

Of the remaining products, CMRSET has an incomplete dataset ending in 2012 (see Figure XI - 6). The  $ET_a$  values among the four remaining products show significant difference in terms of their magnitude and timing of the peak. CMRSET overall has higher  $ET_a$  values compared to the other products, it ranges between 20 and 50

mm/month while the others show values below 20 mm/month during the dry season and the maximum values do not exceed 40 mm/month.

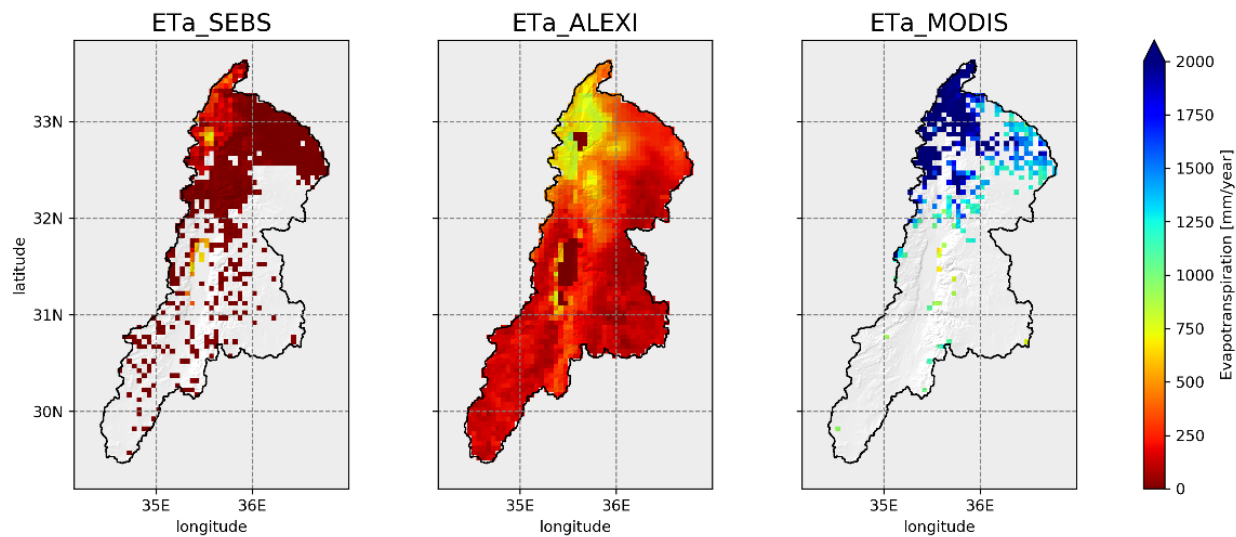


Figure XI - 5 Annual Evapotranspiration for 2009 of Jordan River Basin from SEBS, ALEXI and MODIS

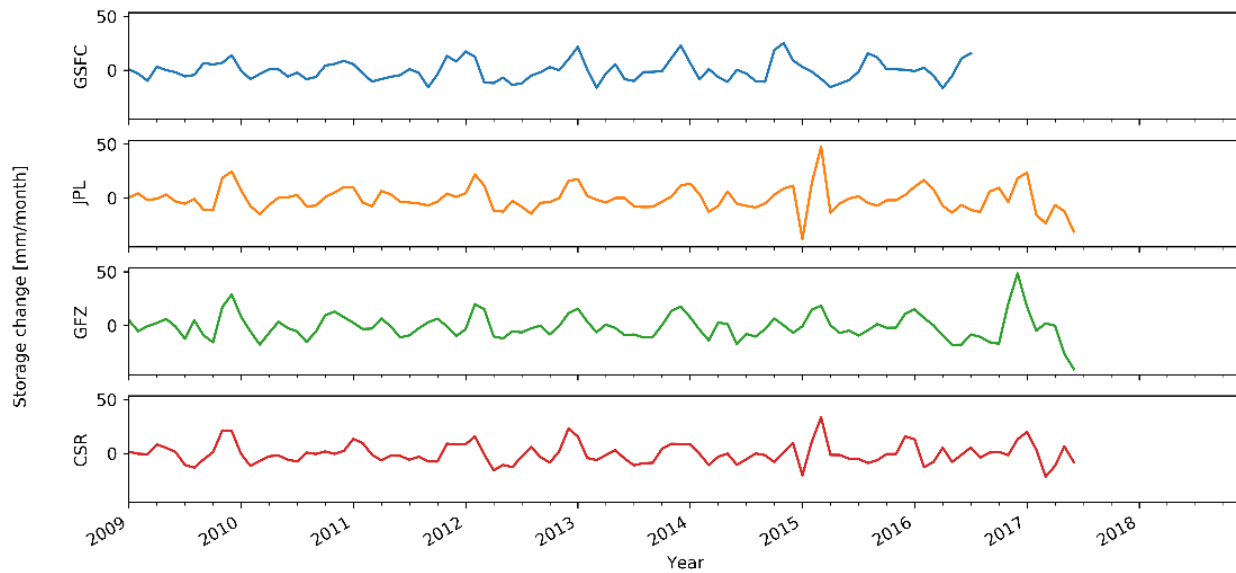


Figure XI - 6 Evapotranspiration values from WaPOR, SSEBop, GLEAM and CMRSET for Jordan River Basin

The monthly mean and annual  $ET_a$  are shown in Figure XI - 7 and Figure XI - 8. CMRSET has the higher monthly mean values in all the months followed by GLEAM, SSEBop and WaPOR. The timing of the peaks also differs, where the peak of SSEBop data occurs in June, the peak observed by CMRSET, GLEAM and WaPOR are in March and April.

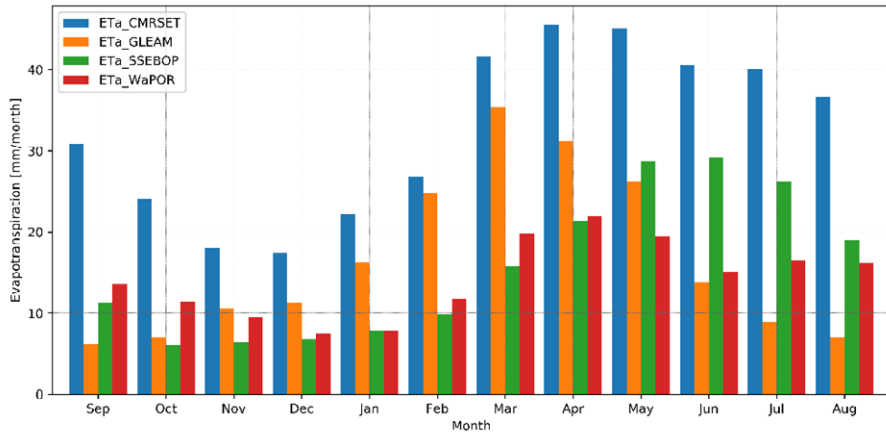


Figure XI - 7 Monthly  $ET_a$  for Jordan River Basin from CMRSET, GLEAM, SSEBop and WaPOR

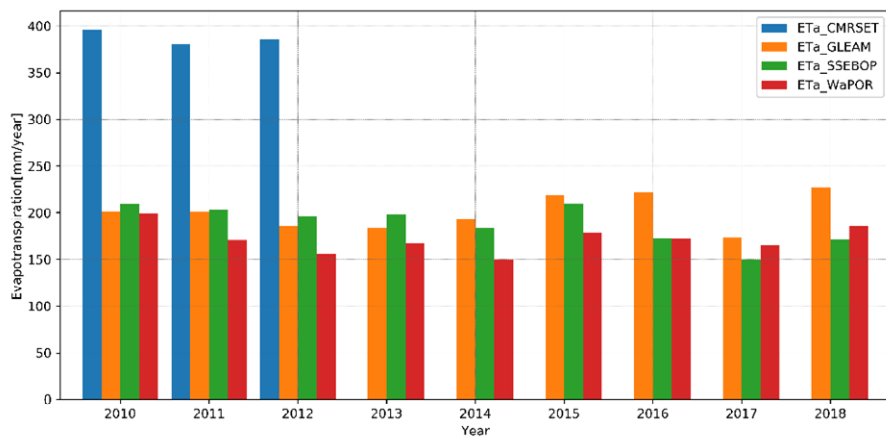


Figure XI - 8 Annual  $ET_a$  for Jordan River Basin from CMRSET, GLEAM, SSEBop and WaPOR

Table XI - 2 Annual  $ET_a$  from CMRSET, GLEAM, SSEBop and WaPOR in mm/year

Year	CMRSET	GLEAM	SSEBop	WaPOR
2010	396	201	209	199
2011	381	200	203	170
2012	385	186	196	156
2013	384	184	198	168
2014	193	193	184	149
2015	218	218	210	178
2016	222	222	173	172
2017	174	174	149	165
2018	227	227	171	186
Average	388	201	188	172

CMRSET annual  $ET_a$  values are close to 400mm/year, which is double the values from the other products, slightly below 200mm/year. Overall annual WaPOR  $ET_a$  is the lowest of all the products (see Table XI - 2).

The map of mean annual  $ET_a$  from the four products are shown in Figure XI - 9. GLEAM has the lowest spatial resolution and does not show the same spatial patterns as the other products. Except for GLEAM, the water bodies in the Jordan valley appear clearly with the highest  $ET_a$ , for CMRSET  $ET_a$  values in the water bodies are more than 1,750 mm/year, compared to 1,250 mm/year for SSEBop and WaPOR.  $ET_a$  in the northern part of the basin also shows variation, with high  $ET_a$  in Syria (1,000 mm/year) estimated by CMRSET compared to 250-500 mm/year estimated by SSEBop and WaPOR.

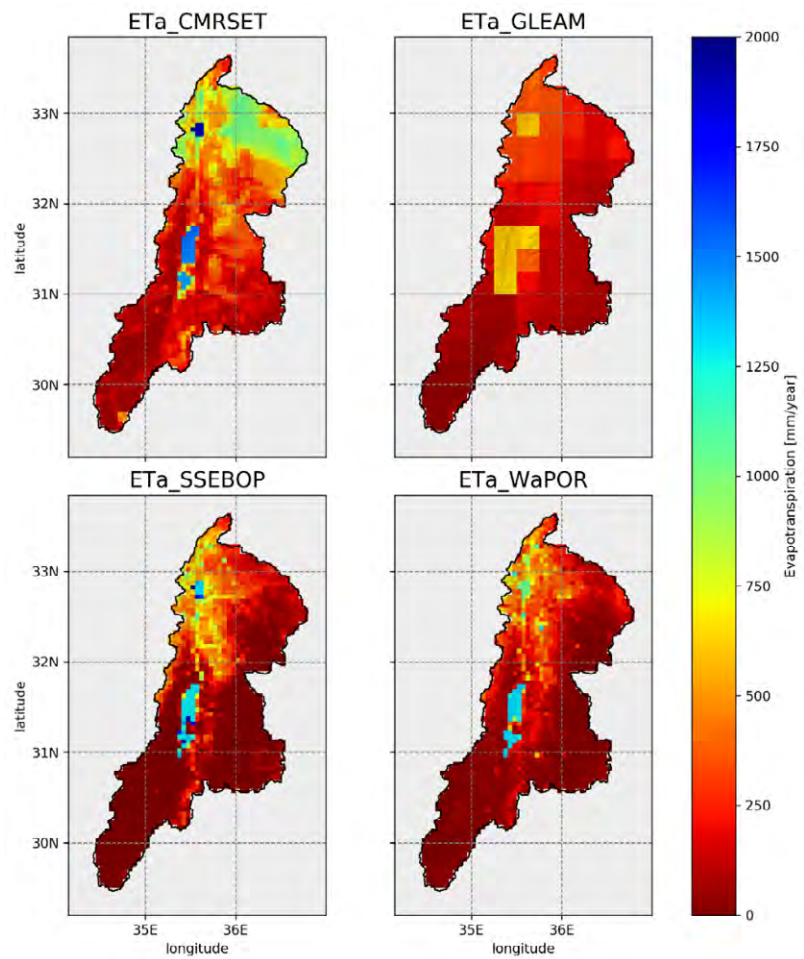


Figure XI - 9 Mean Annual  $ET_a$  of Jordan River Basin from CMRSET, GLEAM, SSEBOP and WaPOR

In terms of correlation, the CMRSET showed good correlation with both SSEBop and WaPOR, however this is based on only four years (see Figure XI - 10). It is also clear that the absolute values differ significantly (variations from the 1:1 line), the correlation only indicates that three data sets exhibit similar trends. When comparing the data sets with similar annual values (SSEBop, GLEAM and WaPOR) for the full period 2009 to 2018, WaPOR versus SSEBop showed the highest correlation.

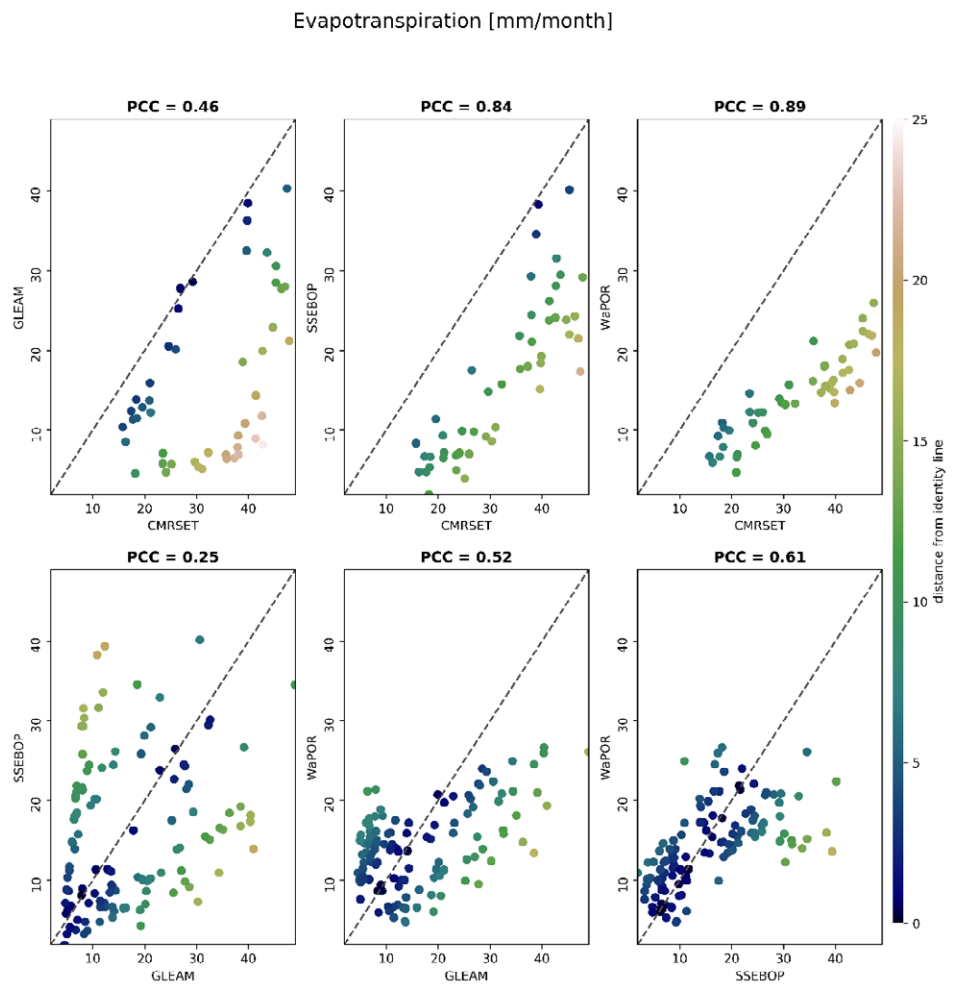


Figure XI - 10 Correlation of CMRSET, GLEAM, SSEBop and WaPOR  $E_T$  for Jordan River Basin

## GRACE solutions

The time series of the storage changes from the GRACE solutions are plotted in Figure XI - 11. All the solutions show a similar trend with some anomalies observed at the beginning of 2015 by CSR and JPL. The GSFC appears to have a slightly smaller amplitude compared to the other products.

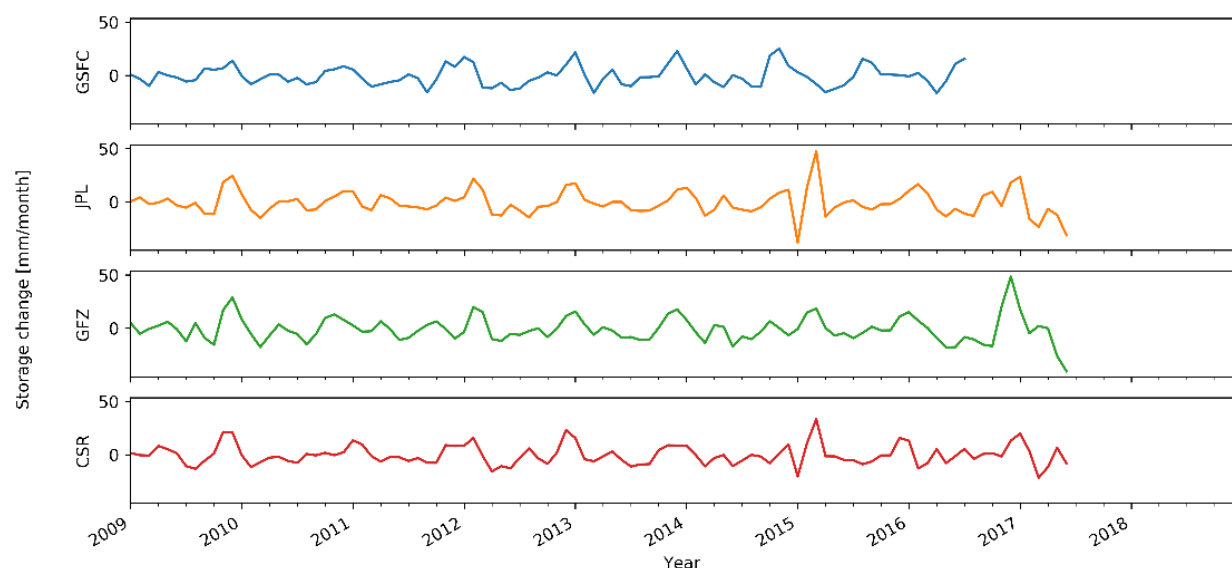


Figure XI - 11 Storage changes from CSR, GFZ, JPL and GSFC for Jordan River Basin

Figure XI - 12 shows the mean monthly change in storage in mm/month for Jordan River basin as derived from the four GRACE solutions. There is significant variation in change in storages among the different GRACE solutions. All solutions show storage gain during the wet winter months (November to January) and storage loss during the dry summer months (April to September). During the transition months (October, February and March), GSFC appears to make the transit earlier than the other products, indicating a storage increase in October and a storage decrease in February, which is an opposite trend to the other products.

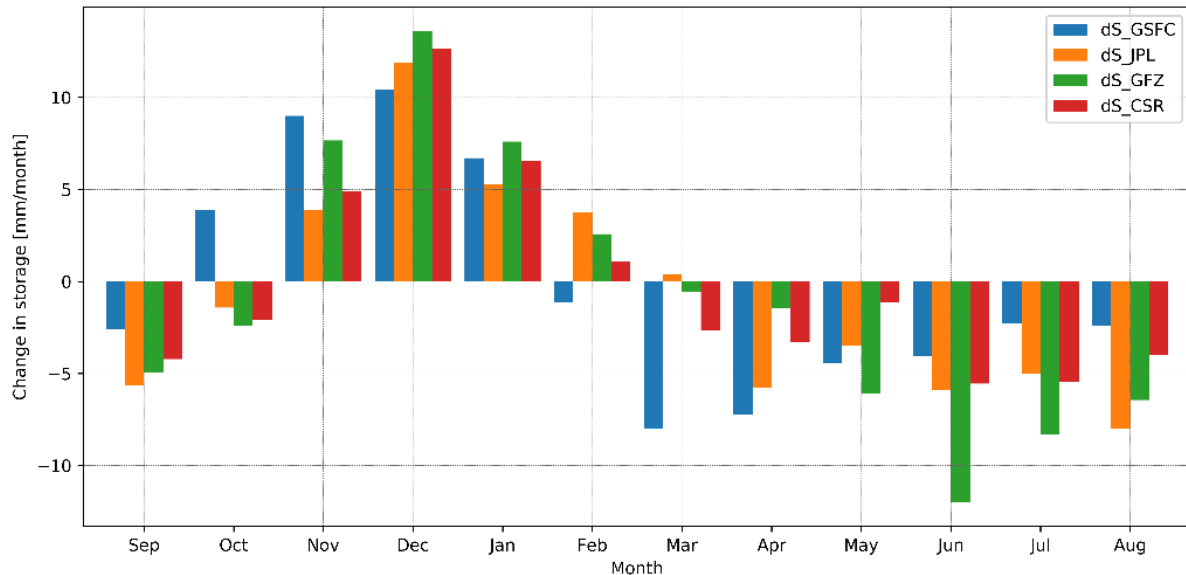


Figure XI - 12 Mean monthly change in storage for Jordan River Basin as computed from four different GRACE solutions

The yearly change in storage plot is shown in Figure XI - 13. The yearly change in storage also show variation among the products, with GSFC most often showing an opposite trend compared to the other products (e.g. 2011, 2014 and 2016). All the products show a decrease in storage during the years 2010 and 2012 and increasing trends in 2015.

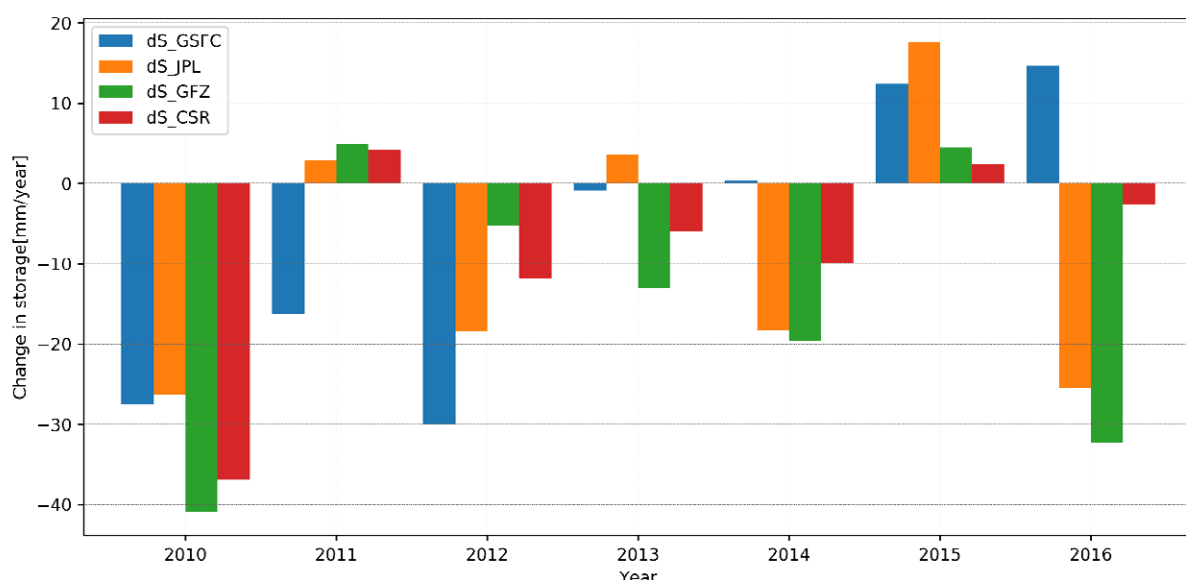


Figure XI - 13 Mean annual change in storage for Jordan River Basin as computed from four different GRACE solutions

The correlation plots (Figure XI -14) show that GSFC has the lowest correlation with the other GRACE solutions (0.30-0.36). The correlation between the other GRACE solutions are better and range between 0.51 and 0.7, which represents the correlation between JPL versus CSR.

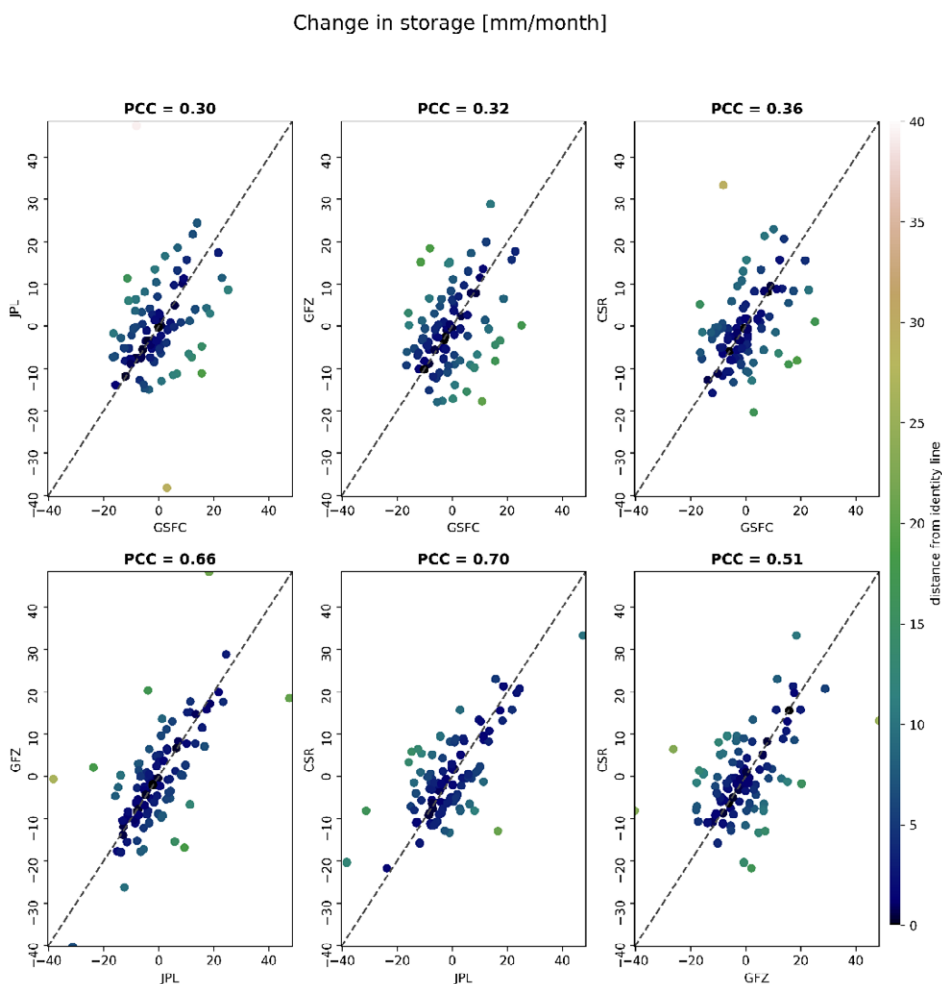


Figure XI-14 Correlation of the four different GRACE solutions for Jordan River Basin

## Annex XI.4 Comparison of runoff and storage change

The comparison in terms of coefficient of determination ( $R^2$ ) and the absolute error as percentage of precipitation between storage change computed from water balance and storage change from GRACE solutions are shown in Figure XI - 15.

$R^2$  for all the combinations varied from 0.0 (no correlation) to 0.79. The best performing combination in terms of  $R^2$  is SSEBop  $ET_a$ , TRMM P and JPL for change in storage. The combination of TRMM with other  $ET_a$  and storage change generally perform better than other precipitation products. CMRSET performs the least of all  $ET_a$  products. In terms of the  $R^2$  values, the  $ET_a$  products ranked from 1<sup>st</sup> to 4<sup>th</sup> are SSEBop, WaPOR, GLEAM and CMRSET respectively. For the GRACE solutions, JPL performs better than the others which showed more or less similar performance. For precipitation, TRMM performs consistently better.

Figure XI - 15 (B) shows the absolute error in change of storage as percentage of precipitation for the different combinations. The combination CHIRPS and CMRSET has the highest error ranging from 32 to 34%. The other combinations with CMRSET and WaPOR also perform much worse (>26% error) than SSEBop and GLEAM with errors ranging from 16-19%. For the error estimations,  $ET_a$  seems to be the most determining factor, whereas for  $R^2$ , precipitation is more important.

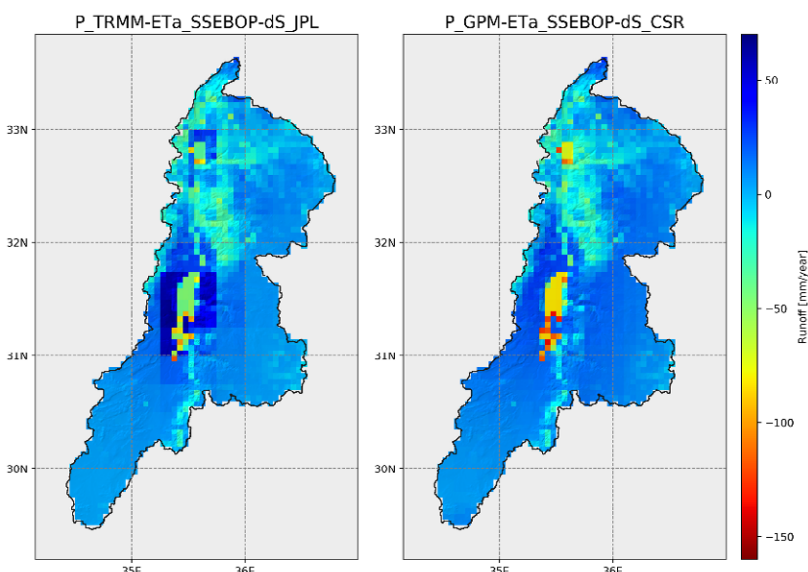


Figure XI - 16 Runoff generation map for the best (left) and worst (right) performer in terms of coefficient of determination

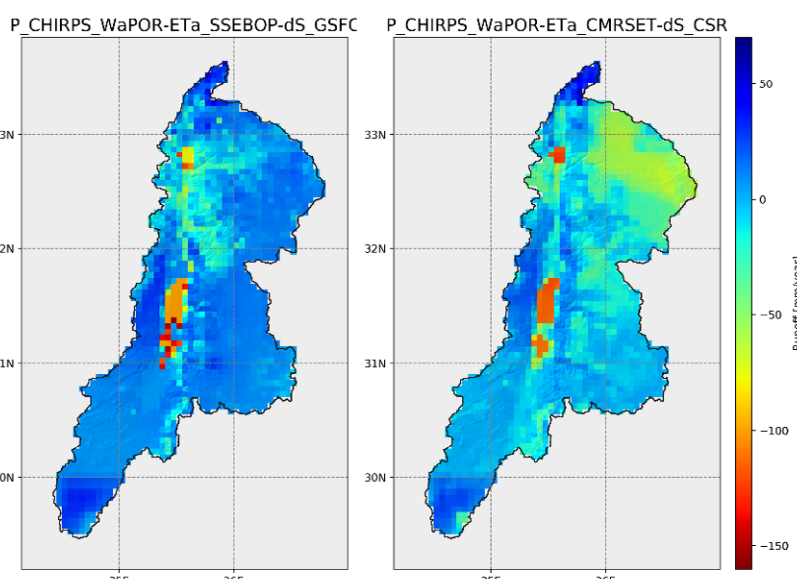


Figure XI - 17 Runoff generation map for the best (left) and worst (right) performer in terms of error in change of storage as percentage of precipitation

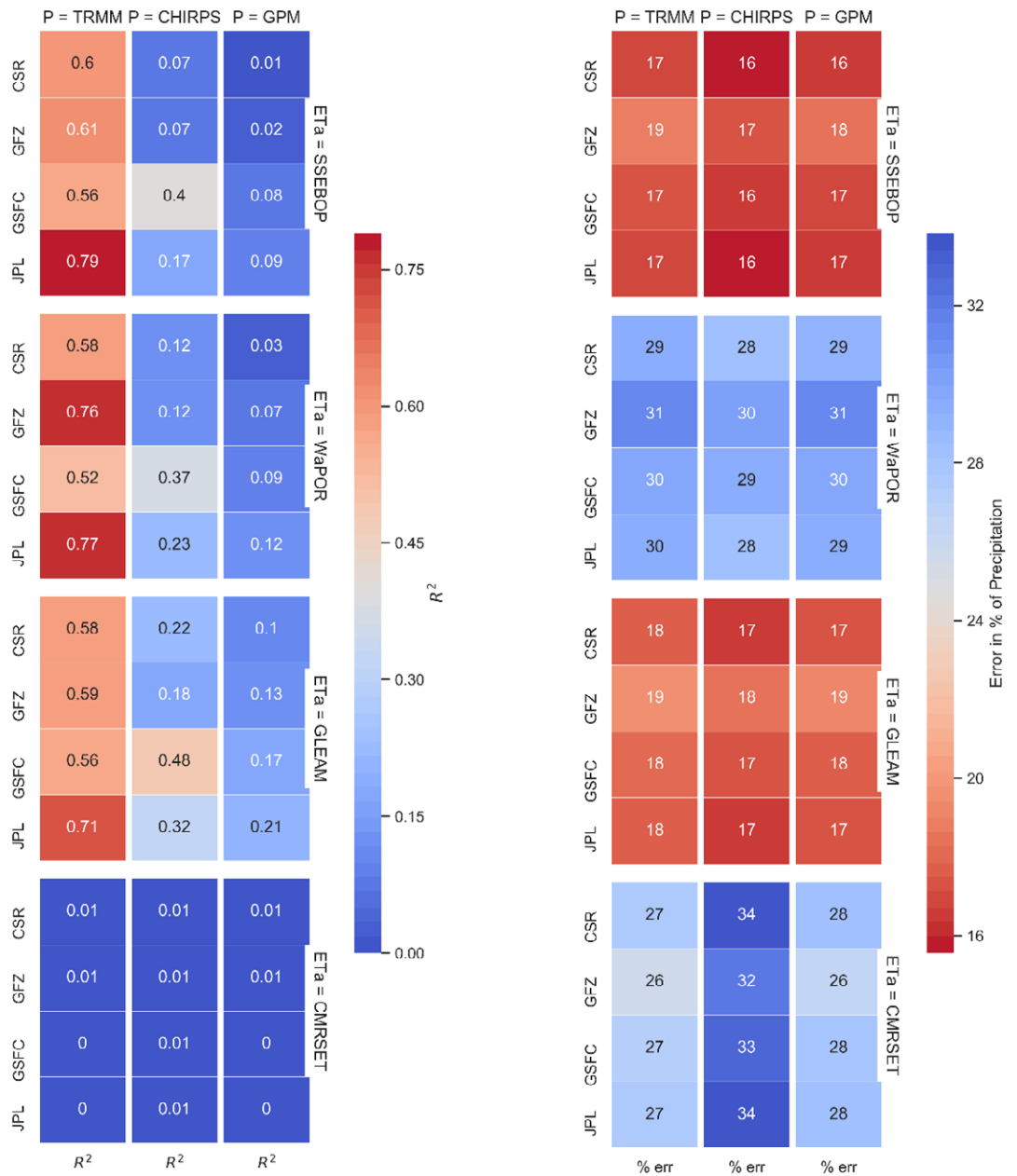


Figure XI - 15 Performance of different combinations of the remote sensing products to calculate the runoff generated from Jordan River Basin. The left figure (A) is the coefficient of determination and the right figure (B) is the absolute error between water balance

Figure XI - 16 shows a comparison of the mean runoff generation for the best performed combination and one of worst in terms of  $R^2$ . The spatial patterns are generally very similar except around Lake Tiberias and the Dead Sea, where TRMM appears to estimate significant precipitation, compared to GPM.

A similar comparison for the best and worst performers combination in terms of error in change in storage as percentage of precipitation (Figure XI - 17), the difference is in that the worst performing combination shows water consumption (negative  $P - ET_a$ ) in the north-western part of the basin.

## Annex XI.5 Spatial comparison of $ET_a$ products

As the indicators used in Figure XI - 15 show a basin average value and Figure XI - 16 and Figure XI - 17 show the spatial variability is equally important, we also compared the  $ET_a$  products by computing  $P - ET_a$  per land cover classes considering one precipitation product (CHIRPS). We expect the products to identify water bodies and irrigated agriculture as water consuming classes and land use classes such as bare / sparse vegetation, grassland and shrubland to be close to zero and built-up areas to be water generating. The results is provided in Table XI - 3. The  $P - ET_a$  for CMRSET show negative values (indicating water consuming) for all type of the land cover classes, which is not realistic. GLEAM showed negative  $P - ET_a$  values for water bodies and irrigated croplands though their amount is very small compared to those of SSEBop and WaPOR (Figure XI - 18). WaPOR and SSEBop showed comparable results, except that SSEBop showed negative values for built-up and shrubland land cover classes.

**Table XI - 3:**  $P - ET_a$  ( $Mm^3/year$ ) per land cover classes for CHIRPS  $P$  compared to CMRSET, GLEAM, SSEBop and WaPOR

Land Cover Class Description	Area ( $km^2$ )	CHIRPS - CMRSET	CHIRPS - GLEAM	CHIRPS - SSEBop	CHIRPS - WaPOR
Bare / sparse vegetation	21,369.2	-764	660	2,513	2,548
Grassland	7,042.6	-125	543	390	900
Cropland, rainfed	5,163.7	-1,827	402	64	123
Cropland, fallow	4,457.4	-1,542	164	606	559
Built-up	1,304.2	-436	109	-82	87
Shrubland	1,197.9	-22	260	-33	99
Water bodies	1,183.3	-1,469	-481	-1,519	-1,164
Cropland, irrigated or under water management	882.4	-392	-4	-195	-145
Tree cover: open, unknown type	572.4	-95	102	-72	-37
Tree cover: closed, unknown type	51.7	-6	17	-8	-11

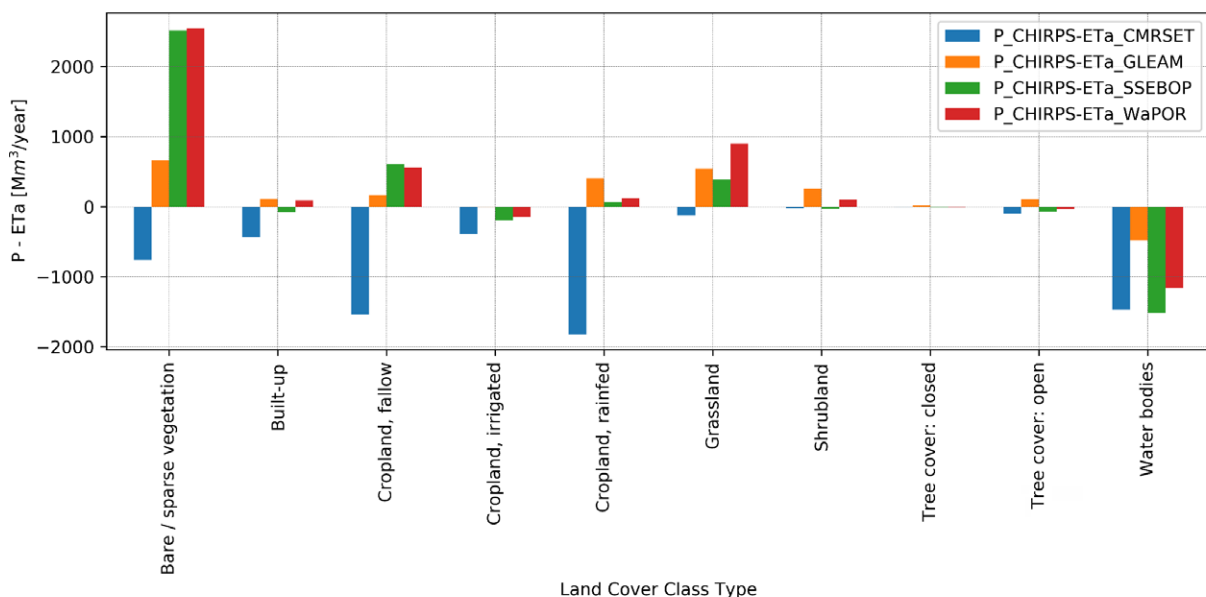


Figure XI - 18  $P - ET_a$  per land cover classes for CHIRPS  $P$  compared to CMRSET, GLEAM, SSEBop and WaPOR

## Annex XI.6 Conclusion

The comparison of the 48 product combinations showed that the  $ET_a$  products have the highest impact on the error of the water balance and precipitation showed the highest impact on the  $R^2$  of the runoff comparison. SSEBop performs better in terms of coefficient of determination followed by WaPOR, GLEAM and CMRSET. While in terms of error in change of storage SSEBop and GLEAM performs better while WaPOR and CMRSET showed high percentage of errors.

Even though GLEAM showed the comparable performance with SSEBop in terms of error in change of storage, it has the lowest resolution of the  $ET_a$  products. This is reflected in the spatial assessment as the  $ET_a$  estimation per land cover class is affected by this resolution, estimating lower consumption over water bodies and irrigated land cover classes compared to SSEBop and WaPOR. This indicates that the performance indices consider the basin water balance as a whole cannot fully determine the performance of the  $ET_a$  products.

The error in change of storage varied from 16 to 34% depending on which combination is used to calculate the change in storage. However, 16% error is still significant to conclude the water balance of the basin is closed. From this it is safe to say that the problem of the water balance not closing for the basin is not inherent only to WaPOR data but with other remote sensing products as well. Before attributing the problem of the water balance to the use of remote sensing products, it is recommended to check the reliability of the observed outflow from the basin. There could be other outflows either not reported or under reported which may help in closing the gap in the water balance.

## Annex XI.7 Additional references

**Anderson MC, Norman JM, Mecikalski JR, Otkin JA, Kustas WP.** 2007. A climatological study of evapotranspiration and moisture stress across the continental United States based on thermal remote sensing: 1. Model formulation. *Journal of Geophysical Research Atmospheres* 112(10):1–17

**Chen, J., Famiglietti, J.S., Scanlon, B.R. et al.** 2016. Groundwater Storage Changes: Present Status from GRACE Observations. *Surveys in Geophysics*. 37, 397–417. <https://doi.org/10.1007/s10712-015-9332-4>

**Guerschman JP, Van Dijk AIJM, Mattersdorf G, Beringer J, Hutley LB, Leuning R, Pipunic RC & Sherman 2009.** Scaling of potential evapotranspiration with MODIS data reproduces flux observations and catchment water balance observations across Australia. *Journal of Hydrology*. 369(1–2):107–119

**Huffman, G. J., Bolvin, D. T., Nelkin, E. J., Wolff, D. B., Adler, R. F., Gu, G., & Stocker, E. F.** 2007. The TRMM multisatellite precipitation analysis (TMPA): Quasi-global, multiyear, combined-sensor precipitation estimates at fine scales. *Journal of Hydrometeorology*, 8(1), 38–55.

**Landerer F.W. and S. C. Swenson.** 2012. Accuracy of scaled GRACE terrestrial water storage estimates. *Water Resources Research*, Vol 48, W04531, 11 PP, doi: 10.1029/2011WR011453.

**Liu, Z., Ostrenga, D., Vollmer, B., Deshong, B., Macritchie, K., Greene, M., & Kempler, S.** 2017. Global precipitation measurement mission products and services at the NASA GES DISC. *Bulletin of the American Meteorological Society*, 98(3), 437–444.

**Miralles DG, Holmes TRH, De Jeu RAM, Gash JH, Meesters AGCA, Dolman AJ.** 2011. Global land-surface evaporation estimated from satellite-based observations. *Hydrology and Earth System Sciences*. 15(2):453–469

**Mu Q, Zhao M, Running SW.** 2011. Improvements to a MODIS global terrestrial evapotranspiration algorithm. *Remote Sensing of Environment*, 115(8):1781–1800

**Paca, V., Espinoza-Dávalos, G.E., Hessels, T.M. et al.** 2019. The spatial variability of actual evapotranspiration across the Amazon River Basin based on remote sensing products validated with flux towers. *Ecological Processes*, 8, 6. <https://doi.org/10.1186/s13717-019-0158-8>

**Swenson S.C.** 2012. GRACE monthly land water massgrids NETCDF RELEASE 5.0. Ver. 5.0. PO.DAAC, CA, USA. <http://dx.doi.org/10.5067/TELND-NC005>.

**Senay GB, Bohms S, Singh RK, Gowda PH, Velpuri NM, Alemu H, Verdin JP.** 2013. Operational evapotranspiration mapping using remote sensing and weather datasets: a new parameterization for the SSEB approach. *Journal of the American Water Resources Association*, 49(3):577–591

**Su Z.** 2002. The surface energy balance system (SEBS) for estimation of turbulent heat fluxes. *Hydrology and Earth System Sciences*, 6(1):85–100.

**Swenson, S. C. and J. Wahr.** 2006. Post-processing removal of correlated errors in GRACE data. *Geophysical Research Letters*, 33, L08402, doi: 10.1029/2005GL025285

**Wouters, B., Bonin, J.A., Chambers, D.P., Riva, R.E.M., Sasgen, I., Wahr, J.** 2014. GRACE, time-varying gravity, Earth system dynamics and climate change. *Reports on Progress in Physics*, 77 (11), 116801. <https://doi.org/10.1088/0034-4885/77/11/116801>.

# Water Accounting in the Jordan River Basin

This report provides the water accounting study for the Jordan River Basin carried out by IHE-Delft using the Water Productivity (WaPOR) data portal of the Food and Agricultural Organization (FAO). The Jordan River Basin is the most important water resource shared between the Middle East countries: Israel, Lebanon, Syria, and Jordan. Its surface water and groundwater have been highly exploited and fought over throughout history. The diverse climate over its area results in spatially variable precipitation and evapotranspiration, thus, variability of water generation and consumption.

To be able to manage the water resources in a sustainable manner, it is important to understand the current state of the water resources. However with limited up-to-date ground observations, in terms of duration, completeness and quality of the hydro-meteorological records it is difficult to draw an appropriate picture of the water resources conditions. The Water Accounting Plus (WA+) system designed by IHE Delft with its partners FAO and IWMI has been applied to gain full insights into the state of the water resources in the basin.



## Funded by:



Ministry of Foreign Affairs of the  
Netherlands

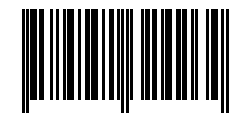
## Frame consortium:



UNIVERSITY  
OF TWENTE.



ISBN 978-92-5-132426-4



9 789251 324264  
CA8668EN/1/04.20